

***Evaluation Of Role Of Virtual Cystoscopy  
In Diagnosis Of Urinary Bladder Carcinoma***

*An essay submitted for the partial fulfillment of  
M.Sc. degree in Radiodiagnosis*

By

***MOHAMED GAMEEL ANWER KISHTAH  
M.B.B.Ch***

Under supervision of

***Prof. Dr. Gannat Aly Mutawe***

*Professor of Radiodiagnosis  
Faculty of Medicine - Al-Azhar University*

***Prof. Dr. Salah Eldin Mohamed Korayem***

*Professor of Radiodiagnosis  
Faculty of Medicine - Al-Azhar University*

***Ass. Prof. Dr. Mohamed Aly Abboud***

*Assistant Professor of Radiodiagnosis  
Faculty of Medicine - Al-Azhar University*

*Department of Radiodiagnosis  
Faculty of Medicine – Al-Azhar University  
2006*

## Acknowledgment

First and foremost, thanks to **ALLAH** the most kind and the most merciful who gave me the ability to complete this work.

I would like to express my sincere and deep gratitude to **Prof. Dr. Gannet Aly Mutawe** Prof. of Radiodiagnosis, faculty of medicine, Al-Azhar university for her kind help, cooperation and valuable suggestions. It is a great honor to work under her guidance and supervision.

I would like to express my deepest thanks to **Ass. Prof. Dr. Salah Eldin Mohamed Korayem**, Ass. Prof. of Radiodiagnosis, faculty of medicine, Al-Azhar university and **Ass. Prof. Dr. Mohamed Aly Abboud**, Ass. Prof. of Radiodiagnosis, faculty of medicine, Al-Azhar university for their great kind support, valuable help, constructive criticism and keen interest in the progress and accomplishment of this work.

I wish also to express my sincere appreciation to my **parents, family and friends**, for their patience, cooperation and helpful assistance through this work.

*Mohamed Gameel*



## CONTENTS

	<i>Page</i>
<i>Introduction and aim of the work</i> .....	1
<i>1. Anatomy of the urinary bladder</i> .....	3
<i>2. Pathology of the urinary bladder carcinoma</i> .....	19
<i>3. Technique of helical CT with post processing virtual cystoscopy</i> .....	53
<i>a. Different imaging modalities in diagnosis and staging of bladder cancer</i> .....	54
<i>b. Types and practical importance of computed tomography scanners</i> ...	63
<i>c. Role of computed tomography in bladder carcinoma</i> .....	68
<i>e. Post processing techniques</i> .....	73
<i>f. Technique of virtual cystoscopy by helical CT</i> .....	77
<i>(i) Virtual cystoscopy of the air-filled bladder</i> .....	77
<i>(ii) Virtual cystoscopy of the contrast material filled bladder</i> .....	80
<i>(iii) Virtual cystoscopy of combined air-distension with intravenous contrast injection</i> .....	84
<i>(iv) Virtual cystoscopy with color mapping of bladder wall thickness</i> .....	87
<i>4. Manifestation of the urinary bladder carcinoma</i> .....	91
<i>5. Treatment of urinary bladder carcinoma</i> .....	114
<i>a. Treatment planning</i> .....	114
<i>b. Post treatment imaging</i> .....	118
<i>6. Summary and conclusion</i> .....	125
<i>7. References</i> .....	132
<i>8. Arabic summary</i>	

### *List of Abbreviations*

<b>BCG</b>	<b>Bacille Calmette-Guerin</b>
<b>BPH</b>	<b>Benign Prostatic Hyperplasia</b>
<b>B-Naphthylamine</b>	<b>Beta Naphthylamine</b>
<b>CT</b>	<b>Computed Tomography</b>
<b>CTA</b>	<b>Computed Tomography Angiography</b>
<b>CTU</b>	<b>Computed Tomography Urography</b>
<b>CTVC</b>	<b>Computed Tomography Virtual Cystoscopy</b>
<b>DNA</b>	<b>Deoxy-ribo Nuclease Acid</b>
<b>HU</b>	<b>Housefield Unit</b>
<b>IVP</b>	<b>Intra-Venous Pyelogram</b>
<b>IVU</b>	<b>Intra-Venous Urography</b>
<b>IVU VC</b>	<b>Intra-Venous Urography Virtual Cystoscopy</b>
<b>MRA</b>	<b>Magnetic Resonance Angiography</b>
<b>MRI</b>	<b>Magnetic Resonance Imaging</b>
<b>MRL</b>	<b>Magnetic Resonance Lymphography</b>
<b>MIP</b>	<b>Maximum Intensity Projection</b>
<b>MDCT</b>	<b>Multi Detector Computed Tomography</b>

<b>MPR</b>	<b>Multi Planar Reformat</b>
<b>MSCT</b>	<b>Multi Slice Computed Tomography</b>
<b>PET</b>	<b>Positron Emission Tomography</b>
<b>SPECT</b>	<b>Single Photon Emission Computed Tomography</b>
<b>SSD</b>	<b>Shaded Surface Display</b>
<b>SCC</b>	<b>Squamous Cell Carcinoma</b>
<b>TCC</b>	<b>Transitional Cell Carcinoma</b>
<b>TIPS</b>	<b>Transjugular Intrahepatic Portosystemic Shunt</b>
<b>TURB</b>	<b>Trans Urethral Resection of Bladder</b>
<b>TURBT</b>	<b>Trans Urethral Resection of Bladder Tumour</b>
<b>3D</b>	<b>Three Dimensional</b>
<b>2D</b>	<b>Two Dimensional</b>
<b>US</b>	<b>Ultra Sonography</b>
<b>UICC</b>	<b>Union International Contre Le Cancer</b>
<b>UVJ</b>	<b>UreteroVesical Junction</b>
<b>URO-Trainer</b>	<b>Urological Trainer</b>
<b>VC</b>	<b>Virtual Cystoscopy</b>
<b>VR-based endoscopy</b>	<b>Virtual Reality Based Endoscopy</b>
<b>VRT</b>	<b>Volume Rendering Technique</b>

## List of Figures

No.	Title	Page
<b>Fig. 1</b>	Male pelvic organs seen from right side	3
<b>Fig. 2</b>	Median section of male pelvis	4
<b>Fig. 3</b>	Median section in female pelvis	4
<b>Fig. 4</b>	Sagittal section of the pelvis of a newborn male infant	6
<b>Fig. 5</b>	Sagittal section of the pelvis of a newborn female infant	6
<b>Fig. 6</b>	Vertical section of the bladder wall	7
<b>Fig. 7</b>	The interior of the urinary bladder	8
<b>Fig. 8</b>	The urinary bladder opened anteriorly, and male urethra	9
<b>Fig. 9</b>	Male pelvis sagittal section	10
<b>Fig. 10</b>	CT anatomy of the male pelvis	14
<b>Fig. 11</b>	Female pelvis sagittal section	18
<b>Fig. 12</b>	Histologic findings of noninvasive carcinoma	29
<b>Fig. 13</b>	Carcinoma in situ (basement membrane is still intact)	30
<b>Fig. 14</b>	Carcinoma in situ of bladder urothelium infiltrating the lamina propria	30
<b>Fig. 15</b>	Invasive transitional cell carcinoma in urinary bladder	31
<b>Fig. 16</b>	Transitional cell carcinoma gross & microscopic pathology	31
<b>Fig. 17</b>	Squamous cell carcinoma gross & microscopic pathology	33
<b>Fig. 18</b>	Squamous cell carcinoma (stage T2b)	33
<b>Fig. 19</b>	Adenocarcinoma of urinary bladder (stage T4a)	35
<b>Fig. 20</b>	Adenocarcinoma of bladder with transitional and small cell components	36
<b>Fig. 21</b>	Small cell carcinoma of urinary bladder	37
<b>Fig. 22</b>	Carcinosarcoma of urinary bladder	38
<b>Fig. 23</b>	Plasmacytoma of bladder	41
<b>Fig. 24</b>	Papillary transitional cell carcinoma, in the bladder neck CTVC & not seen in source CT image	91
<b>Fig. 25</b>	Soft-tissue mass (low-grade papillary carcinoma with punctate calcifications) CTVC	91
<b>Fig. 26</b>	Calcified polypoid lesion arising from the anterior wall of the bladder VC, transverse CT image & conventional cystoscopy	92
<b>Fig. 27</b>	Pseudolesion that mimics a polypoid lesion (calcified phlebolith) VC & source CT image	93
<b>Fig. 28</b>	Enlarged median lobe of the prostate gland VC & source CT image	94
<b>Fig. 29</b>	Bladder trabeculation VC	94
<b>Fig. 30</b>	Sessile Bladder carcinoma VC	95
<b>Fig. 31</b>	Bladder carcinoma sessile mass and three adjacent polyps VC	95
<b>Fig. 32</b>	Recurrent bladder carcinoma VC	95
<b>Fig. 33</b>	Chronic mucosal ulceration VC	95

***List of Figures (Continue)***

No.	Title	Page
<b>Fig. 34</b>	Virtual renderings of urinary bladder showing bladder mass with Prostatic impression and urethral origin	<b>96</b>
<b>Fig. 35</b>	Reconstructed two-dimensional CT (transverse image) from air VC & Air VC images of a bladder tumour	<b>96</b>
<b>Fig. 36</b>	Cystogram, conventional cystoscopy & IVU VC images of bladder tumour	<b>97</b>
<b>Fig. 37</b>	Late excretory Small transitional cell carcinoma seen in VC not seen in coronal MPR nor in trasverse CT images	<b>98</b>
<b>Fig. 38</b>	Transitional cell carcinoma at anterior site of bladder seen in VC not seen in both transverse or sagittal reformatted image	<b>99</b>
<b>Fig. 39</b>	Transitional cell carcinoma at inferior site of bladder VC, sagittal, coronal reformatted & transverse CT	<b>100</b>
<b>Fig. 40</b>	Inadequate mixing of contrast material and urine. Fluid—fluid level in source CT image	<b>101</b>
<b>Fig. 41</b>	Parenchymal phase CTU image, Excretory phase image & Repeated excretory phase image in the prone position	<b>101</b>
<b>Fig. 42</b>	Early parenchymal phase CTU image, Excretory phase CTU image & Coronal thin MIP image from excretory phase CTU images	<b>102</b>
<b>Fig. 43</b>	Metastatic bladder cancer with anterior perivesical soft tissue invasion	<b>103</b>
<b>Fig. 44</b>	Urinary bladder papillary lesion in coupled contrast enhanced pneumo-CT-cystography	<b>104</b>
<b>Fig. 45</b>	Bladder cancer extending to the distal ureter in Unenhanced CT scans, curved MPR reconstructions and Virtual endoscopy	<b>105</b>
<b>Fig. 46</b>	Multiple papillary bladder lesions with vessel feeding lesion	<b>106</b>
<b>Fig. 47</b>	Comparison of transitional cell carcinoma in coronal MPR, VC and conventional cystoscopy	<b>107</b>
<b>Fig. 48</b>	Primary urinary bladder cancer near urethral orifice, transverse, VC & conventiona cystoscopy	<b>107</b>
<b>Fig. 49</b>	Trabeculation because of the prostate hypertrophy in VC images	<b>108</b>
<b>Fig. 50</b>	Virtual CT cystoscopic images of bladder wall diverticulum	<b>108</b>
<b>Fig. 51</b>	Polypoid mass arising from the anterior surface of bladder wall in axial CT image & color mapped VC	<b>109</b>
<b>Fig. 52</b>	Subtle thickening of the left bladder wall axial CT image & Color mapped virtual endoscopy	<b>109</b>
<b>Fig. 53</b>	Air distended bladder in axial CT image & 3-D rendering of external bladder surface with color wall thickness mapping	<b>110</b>
<b>Fig. 54</b>	Large mass at bladder base in axial CT image & 3-D colour mapped wall thickness with dome removed	<b>110</b>

**List of Figures (Continue)**

No.	Title	Page
Fig. 55	Anterior wall polyp by axial CT & color mapped 3-D images	111
Fig. 56	Spots of abnormal wall thickness in 3-D color mapped images	111
Fig. 57	False-positive lesion on virtual cystoscopy (shine through)	112
Fig. 58	Motion artifact in virtual cystoscopy image	113
Fig. 59	Bladder leak after subtotal cystectomy and neobladder formation CT images	116
Fig. 60	Perivesical inflammatory change after recent transurethral resection of noninvasive bladder tumor (Contrast-enhanced CT image)	118
Fig. 61	Parenchymal phase CTU images after cystectomy and ileal neobladder reconstruction for bladder cancer	119
Fig. 62	Contrast-enhanced CT image of the pelvis after resection of stage T1 high-grade bladder TCC	120
Fig. 63	Contrast-enhanced CT image of the abdomen demonstrated large hypoattenuating mass after intravesical BCG therapy for bladder cancer	121
Fig. 64	Axial T2 weighted endorectal MR image of the prostate after intravesical BCG treatment of bladder cancer	121

**List of Diagrams**

No.	Title	Page
Diagram 1	TNM staging system for cancer of urinary bladder	46

**List of Tables**

No.	Title	Page
Table 1	Comparison between TNM classification and Jewett-Strong-Marshall staging system for bladder cancer	47

*Introduction*

*&*

*Aim of the work*

## Introduction

Cancer of the urinary bladder is predominantly a disease of older men. This disease represents 6% of all malignancies in men, making it the fourth most common tumor. In women, bladder carcinoma represents 2% of malignancies, making it the seventh most common tumor (*Kundra and Silverman 2003*).

Cancer is a frequently occurring malignancy with a high rate of recurrence and multifocal manifestations, and therefore it requires reliable diagnostic techniques (*Lämmle 2002*).

Recent advances in CT including software developments have led to the use of three-dimensional (3D) imaging reconstruction techniques and allow CT urography and virtual endoscopy to be used in daily practice (*Kim and Cho 2003*).

Virtual cystoscopy has emerged as a promising diagnostic tool for the detection of bladder cancer, the sensitivity of virtual cystoscopy for detecting bladder tumor was greater than 90% , Virtual cystoscopy is more accurate than multiplanar reconstruction and source CT images for the detection of lesions in the bladder (*Kim et al., 2005*).

CT virtual cystoscopy is a minimally invasive technique that can provide comprehensive information about bladder tumours (*Tsili et al., 2003*).

Virtual multidetector CT cystoscopy is an accurate tool for detection and evaluation of bladder lesions. With multidetector row CT, the detection of lesions <5 mm is possible with high sensitivity (*Mang et al., 2003*).

Virtual Cystoscopy revealed to be a technique which completes morphologic axial images in CT and MRI, which represents the primary methods in diagnosis of bladder tumors (*Panebianco et al., 2003*).

Value of color mapping of bladder wall thickness for detection of tumor as a component of virtual cystoscopy Compared with conventional cystoscopy, the analysis of axial image yielded a sensitivity of 0.80, specificity 0.90, positive predictive value 0.80 and negative predictive value 0.90 for the presence of tumor.



Examination of color mapped 3-D renderings resulted in 0.83, 0.36, 0.42 and 0.71, respectively (*Fielding et al., 2002*).

Virtual cystoscopy is a developing technique for bladder cancer screening. Compared with an expert observer reading the CT achieves 89% sensitivity, 88% specificity, 48% positive predictive value, and 98% negative predictive value (*Jaume et al., 2003*).

### *Aim of the Work*

Aim of this work is to highlight & evaluate the role of virtual cystoscopy CT using three-dimensional imaging reconstruction techniques in diagnosis of urinary bladder carcinoma.

## *Anatomy of the urinary bladder*

The urinary bladder is solely a reservoir and varies in size, shape, position and relations according to its content and the state of the neighboring viscera (*Dyson, 1999*). The position of the bladder varies with the condition of the rectum, being pushed upward and forward when the rectum is distended (Fig.1) (*Williams et al., 1995*).

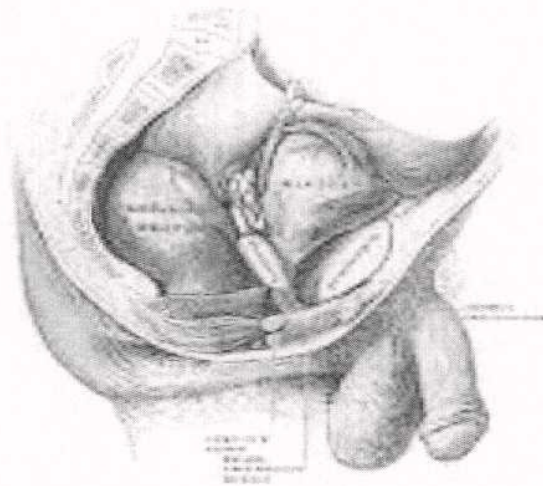


**Fig.1:** *Male pelvic organs seen from right side. Bladder and rectum distended; relations of peritoneum to the bladder and rectum shown in blue.*

*(Quoted from Williams et al., 1995).*

The Empty Bladder is a three-sided pyramid, with an apex pointing forward to the top of the symphysis pubis and a triangular base (trigone) facing backwards. It has two infero-lateral surfaces, a neck where the urethra opens and a superior surface (dome). The **apex** has the remains of the urachus attached to it, the latter forming the median umbilical ligament, which runs up in the median umbilical fold of peritoneum (*Sinnatamby, 1999*).

The **triangular superior surface** is bounded by lateral borders twin the apex to the ureteric entrances and by a posterior border joining them. In males

---

the superior surface is completely covered by peritoneum, extending slightly on to the base and continued posteriorly into the rectovesical pouch, laterally into the paravesical fossa and anteriorly into the median umbilical fold. It is in contact with the sigmoid colon and the terminal coils of the ileum (*Dyson, 1999*).

In females, the superior surface of the bladder is covered by peritoneum and is in relation with the uterus, but it is separated from it by the utero-vesical pouch which may contain coils of ileum (Fig. 2,3).

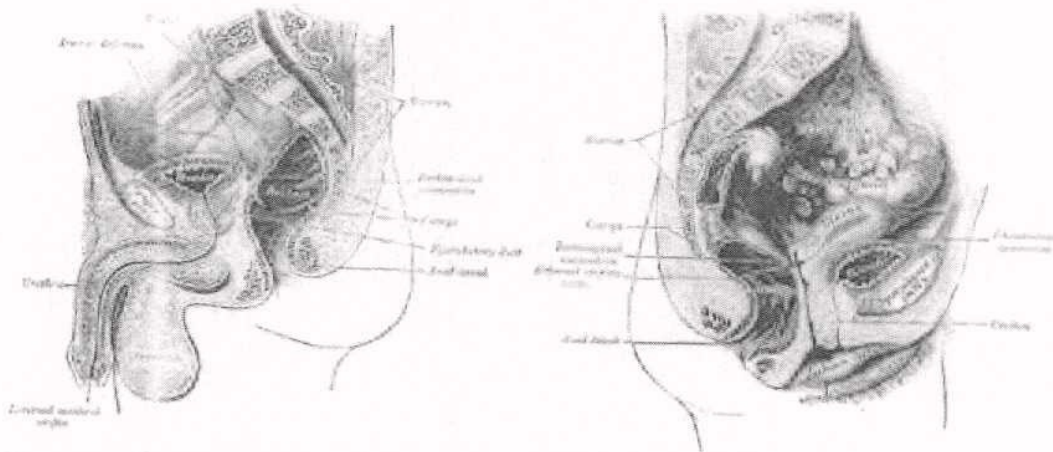


Fig. 2: Median section of male pelvis shows relations of the urinary bladder.      Fig. 3: Median section in female pelvis shows relations of the urinary bladder.

(Quoted from Williams et al., 1995)

The **fundus** or base is triangular and postero-inferior, separated from the rectum by the vasa deferentia, seminal vesicles in males, and by the uterine cervix and vagina in females. The trigone is a triangular area at the base of the bladder lying between the two ureteral orifices (above and laterally) and the internal urethral orifice (centrally and below). (*Tanagho, 1992*).

Each **inferolateral surface** slopes downwards and medially to meet its fellow, lying against the pelvic surface of the levator ani muscles and obturator internus, where the surfaces meet below the apex, there is a retroperitoneal



space behind the pubic bones and symphysis, the retropubic space of Ritzius, containing loose fatty tissue and pubovesical ligaments in females replaced by puboprostatic ligaments in males. (*Sinnatamby, 1999*). Between the bladder and these muscles run the obturator nerve and vessels and the superior vesical vessels (*Weiss et al., 2001*). The infero-lateral surfaces are not covered by peritoneum (*Dyson, 1999*).

The inferior angle of the bladder in the female lies at a lower level than in the male and is closely related to the lower levator ani muscles (*Weiss et al., 2001*).

The **neck** is the lowest and most fixed part of the bladder where the base and the inferolateral surfaces meet and which is pierced by the urethra and internal urethral orifice. In the male, it lies against the upper surface of the prostate; In the female, the neck is above the urethra in the connective tissue of the anterior vaginal wall (*Sinnatamby, 1999*).

Although the vesical fundus should be, by definition, the lowest region, the **neck** is in fact the lowest and also the most fixed; it is 3-4 cm behind the lower part of the symphysis pubis (*Dyson, 1999*).

The bladder is connected to the pelvic fascia by a condensation of fibro-areolar tissue termed the **lateral true ligament** of the bladder. Anteriorly the **lateral and medial puboprostatic ligament** in males, **pubovesical ligament** in females. The apex of the bladder is joined to the umbilicus by the **median umbilical ligament**. As the vesical venous plexus stream backward to join the Internal iliac veins, they are enveloped on each side in a band of fibro-areolar tissue termed the **posterior ligaments** of the bladder. The lateral true ligaments have a supportive function. From the superior surface of the bladder, the peritoneum is carried off in a series of folds, which are termed the false

ligaments of the bladder and do not share in the supportive function. (*Williams et al., 1995*).

As the bladder fills it becomes ovoid. In front it displaces the parietal peritoneum from the suprapubic region of the abdominal wall, so that the infero-lateral surfaces become anterior and rest against the abdominal wall without intervening peritoneum for a distance above the symphysis pubis, varying with the degree of distension but commonly about 5cm (*Dyson, 1999*).

The full bladder's summit points up and forwards above the attachment of the median umbilical ligament, so that the peritoneum forms a supravescical recess of varying depth between the summit and the anterior abdominal wall; this recess often contain coils of small intestine (*Dyson, 1999*).

At birth (Fig 4,5) the bladder is relatively higher than in the adult, the internal urethral orifice being level with the upper symphyseal border; the bladder is abdominal rather than pelvic, extending about two-thirds of the distance towards the umbilicus. It progressively descends, reaching the adult position shortly after puberty (*Dyson, 1999*).



Fig. 4: Sagittal section of the pelvis of a newborn male infant.

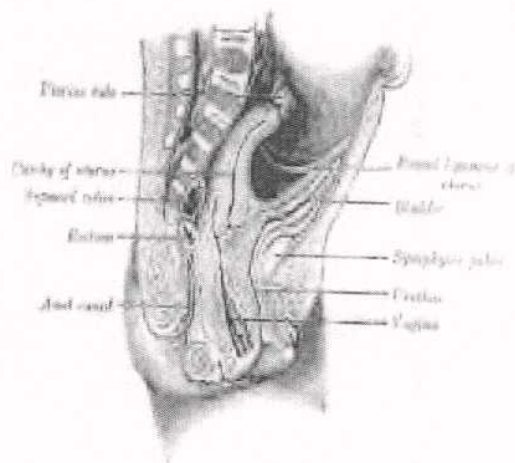


Fig. 5: Sagittal section of the pelvis of newborn female infant.

Note the abdominal position of the urinary bladder (*Quoted from Dyson 1999*).



**Normal Bladder Urothelium:**

The urothelium of the normal bladder is a transitional cell epithelium three to seven cell layers thick. There is a basement cell layer upon which rests one or more layers of intermediate cells. The most superficial layer is composed of the large flat umbrella cells. The cells of the urothelium are oriented with the long axis of the oval nuclei being perpendicular to the basement membrane, giving the urothelium its normal appearance of cellular polarity. The urothelium rests upon a lamina propria basement membrane. In the lamina propria, there is a tunica muscularis mucosa containing scattered muscle fibers, which are irregularly arranged (Fig.6) (Zuk et al., 1989).

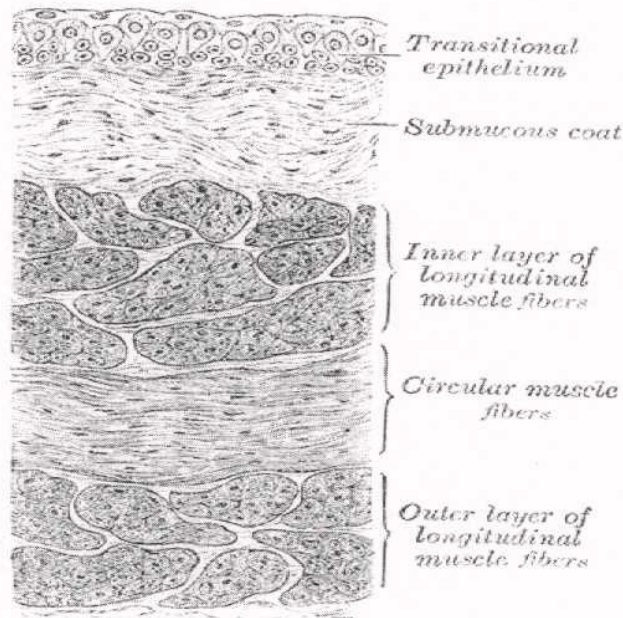
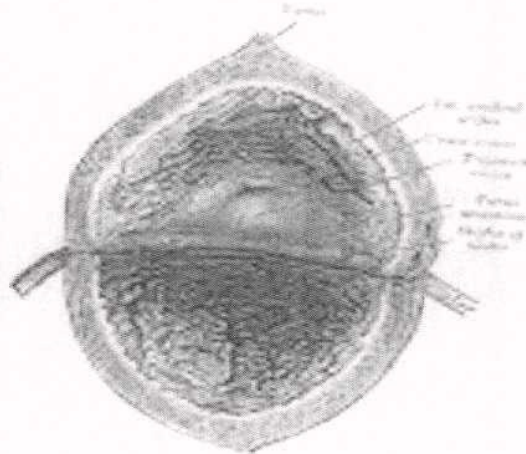


Fig. 6: Vertical section of the bladder wall (Quoted from Williams et al., 1995).

The interior of the bladder is completely covered by transitional epithelium several layers deep. There is a loose underlying connective tissue that permits considerable stretching of the mucosa; for that reason, the mucosal lining is wrinkled when the bladder is empty but quite smooth and flat when the bladder

is distended. This arrangement exists throughout except over the trigonal area, where the mucous membrane is firmly adherent to the underlying trigonal musculature; this is why the trigone is always smooth, whether the bladder is full or empty (Fig. 7) (Tanagho, 1992).

Fig. 7: The interior of the urinary bladder. (Quoted from Williams et al., 1995).

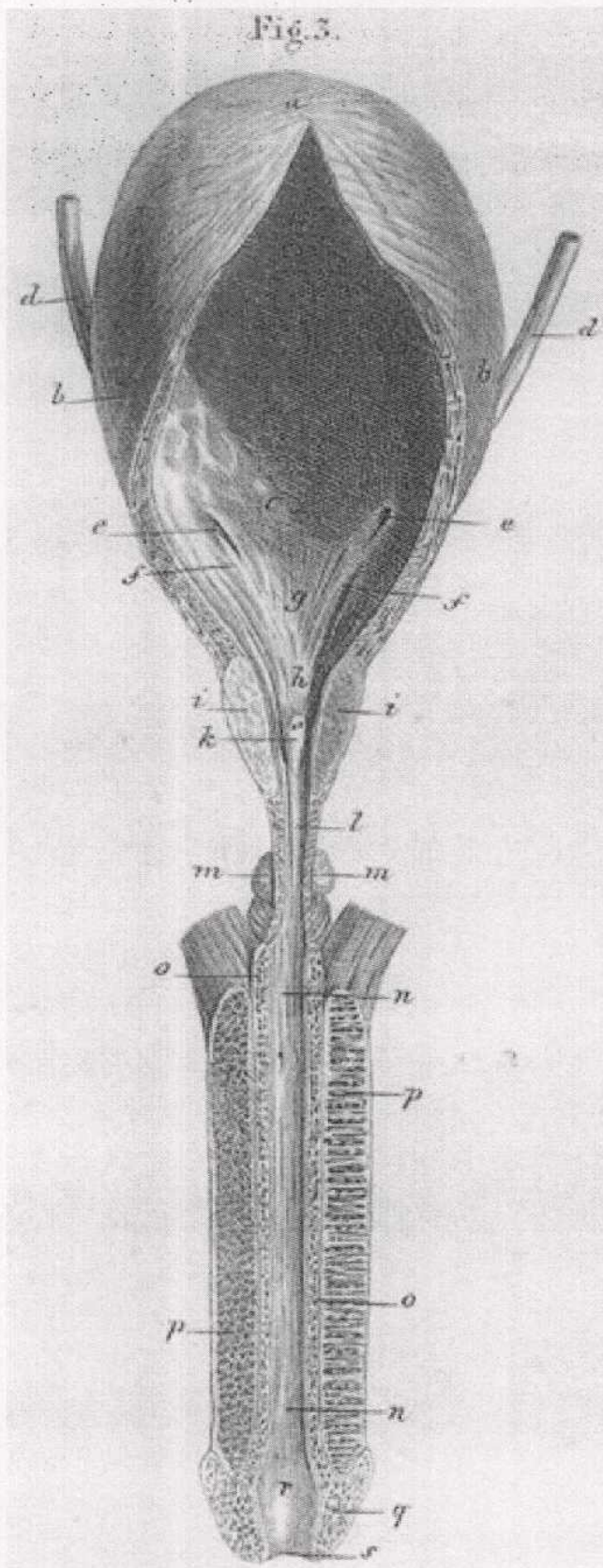


The superior trigonal boundary is a slightly curved **interureteric crest**, connecting the two ureteric orifices and produced by the continuation into the vesical wall of the ureteric, internal longitudinal muscle. At cystoscopy the interureteric crest appears as a pale band and it is a guide to the ureteric orifices in catheterization (Dyson, 1999).

**Ureteric orifices.** Placed at the postero-lateral trigonal angles (Fig 8), they are usually slit like. In empty bladders they are about 2.5 cm apart and about the same from the internal urethral orifice; in distension these measurements may be doubled (Dyson, 1999).

**Internal urethral orifice.** Sited at the trigonal apex, the lowest part of the bladder, this is usually somewhat crescentic in section. In adult males, particularly past middle age, immediately behind it is a slight elevation caused by the median prostatic lobe **the uvula** of the bladder (Dyson, 1999).





- Fig. 3.
- a) Bladder, top (vertex).
  - b) Bladder body.
  - c) Bladder, fundus.
  - d) Ureter.
  - e) Orifice of ureters.
  - f) Ureteric fold.
  - g) Trigone vesicae.
  - h) Bladder neck (with bladder sphincter and ostium of urethra).
  - i) Prostate.
  - k) Prostatic urethra with colliculus seminalis (and opening of ejaculatory duct and prostate duct openings).
  - l) Membranous urethra (isthmus).
  - m) Bulbourethral glands (s. glandula Cowperi).
  - n) Urethra, cavernous portion.
  - o) Corpus cavernosus urethrae.
  - p) Corpus cavernosus penis.
  - q) Glans penis.
  - r) Urethrae, fossa terminalis (s. navicular fossa or fossa of Morgagnii).
  - s) Urethral cutaneous ostium.

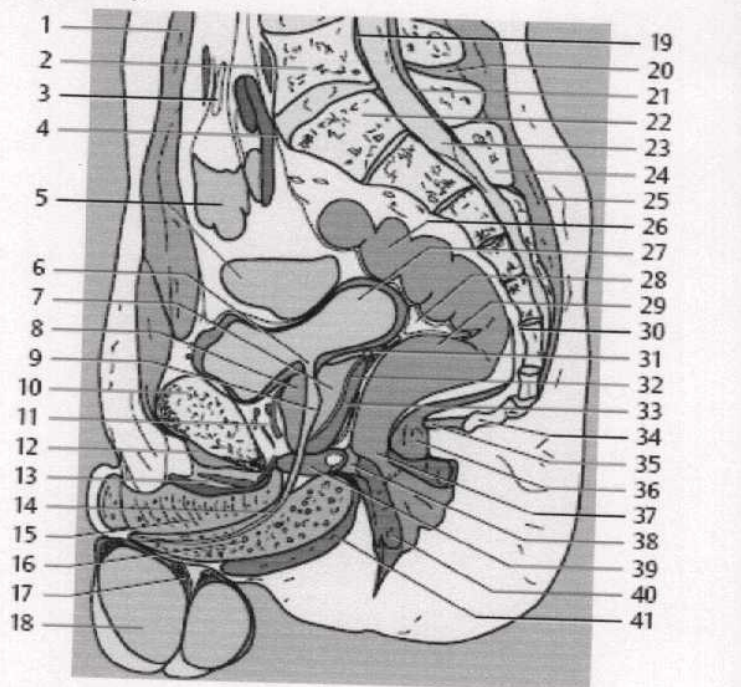
**Fig. 8: The urinary bladder opened anteriorly, and male urethra.**

(Quoted from Bock et al., 2007).



## BLOOD SUPPLY OF THE URINARY BLADDER

In both sexes the arterial supply to the bladder is provided by branches of the internal iliac arteries. The largest branches are usually the superior vesical arteries (Weiss et al, 2001).



- |   |  |
|---|--|
| 1. Rectus abdominis muscle                                    | 24. Spinous process                                |
| 2. Lumbar vertebra (L5)                                       | 25. Erector spinae muscle                          |
| 3. Mesentery  | 26. Sigmoid colon                                  |
| 4. Promontorium   | 27. Urinary bladder                                |
| 5. Small intestine  | 28. Rectovesical pouch                             |
| 6. Urinary bladder (internal urethra orifice)                 | 29. Rectum   |
| 7. Prostate (central zone)                                    | 30. Presacral space                                |
| 8. Prostate (anterior fibromuscular stroma)                   | 31. Seminal gland                                  |
| 9. Seminal colliculus   | 32. Ejaculatory duct                               |
| 10. Pubis   | 33. Prostate, peripheral zone                      |
| 11. Retropubic space with vesical and prostatic venous plexus | 34. Coccyx   |
| 12. Arcuate pubic ligament                                    | 35. Anococcygeal ligament                          |
| 13. Suspensory ligament of penis                              | 36. Levator ani muscle                             |
| 14. Urethra   | 37. Anus   |
| 15. Corpus cavernosum   | 38. Perineal body                                  |
| 16. Corpus spongiosum   | 39. Urogenital diaphragm with bulbo-urethral gland |
| 17. Epididymis  | 40. External anal sphincter muscle                 |
| 18. Testis  | 41. Bulbospongiosus muscle                         |
| 19. Posterior longitudinal ligament                           | 42. Juxta-intestinal mesenteric lymph nodes        |
| 20. Interspinal ligaments                                     | 43. Prevertebral lymph nodes                       |
| 21. Ligamenta flava   | 44. Promontorial lymph nodes                       |
| 22. Sacrum (S1)   | 45. Presacral lymph nodes                          |
| 23. Vertebral canal   | 46. Postvesical lymph nodes                        |
|   | 47. Prevesical lymph nodes                         |

Fig. 9: Male pelvis sagittal section (Quoted from Moeller 2001).

Additional branches arise from the internal iliac arteries and all of these are involved in the supply of blood to the inferior aspects of the bladder wall. These vessels include the inferior vesical, the obturator, and the inferior gluteal arteries (*Weiss et al., 2001*).

In the female the uterine and vaginal arteries also contribute to the vascular supply of the bladder (*Weiss et at, 2001*).

### **Venous drainage:**

Venous blood from the bladder passes into the extensive plexuses of veins that lie within the pelvis in both sexes. The vesical venous plexus lies in the fascia close to the neck of the bladder and communicates with the prostatic or vaginal plexus of veins. Blood from these plexuses drains directly into the internal iliac veins, although anastomoses with the ovarian, superior rectal, and sacral veins provide alternative routes to the inferior vena cava (*Weiss et al, 2001*).

### **Lymphatic drainage:**

Lymphatics from most pelvic viscera pass first to regional nodes largely related to the iliac arteries and their branches before reaching the lateral aortic group. These include common, external, internal, obturator, inferior epigastric, circumflex iliac and sacral groups (*Williams et al., 1995*).

#### **1) Common iliac nodes:**

They are grouped around the common iliac artery inferior to the aortic bifurcation (*Williams et aL.1995*).

#### **2) External iliac lymph nodes:**

These are encased in the fatty areolar tissue surrounding the external iliac vessels from the bifurcation of the common iliac vessels, anterior to the

---



sacroiliac joint, to the inguinal vessels 2 cm above the acetabulum. (*Amendola et al., 1990*).

**3) Obturator lymph nodes:**

This group carries special importance as it is the first site in the lymphatic system to which urinary bladder carcinoma spreads. (*Smith, 1988*).

**4) Internal iliac lymph nodes:**

Lie along the course of the internal iliac artery and its branches. They lie below the bifurcation of the common iliac artery situated posteriorly within the true pelvis. The most cephalic nodes of this group is called the hypogastric lymph nodes, just below the sacroiliac joint and dorsal to the external iliac vessels (*Amendola et al., 1990*).

**5) Inferior epigastric & circumflex iliac nodes:**

They are associated with their vessels and drain the corresponding areas being outline members of the external iliac groups (*Williams et al., 1995*)

Lymphatic drainage can go directly from the anterior bladder wall to the external iliac nodes, from the lateral bladder wall to the obturator nodes and from the posterior bladder wall to the internal iliac nodes. (*Friedman et al., 1990*)

### **CT Anatomy of the Urinary Bladder**

Urinary bladder (Figs 8&9) is a hollow muscle which functions to hold urine. In adults it is located posterior and superior to the pubic bones. In infants the bladder is located in the abdomen. It starts entering the pelvis at about 6 years of age. Until then it is located in the abdomen. An adult bladder is located in the pelvis but it extends into the abdomen when it is full of urine. The bladder is a very distensible organ that has folds called rugae, except in the trigone where it is smooth. The trigone is the triangular shaped area in the base of the bladder (*Wayne State University, 2007*).

---

On unenhanced computed tomography, the urine within the bladder is of water density. The bladder wall on CT appears as a rim of soft tissue, the inner margins of which are best seen if the bladder is distended with urine, air, oil or carbon dioxide. The outer margin of the bladder wall is smooth and generally well delineated by perivesical fat (*Hricak and White, 1999*).

Following the intravenous injection of contrast medium, urine within the bladder will be opacified and, since contrast-laden urine is heavier than non-opacified urine, urine-contrast demarcation is often seen on transverse images. While contrast enhancement is helpful for the evaluation of intraluminal filling defects, demonstration of the bladder wall is indistinct (*Hricak and White, 1999*).

Intravenous administration of contrast material facilitates opacification of the major vascular structures in addition to the ureters and urinary bladder. Oral contrast, rectal contrast, and a vaginal tampon aid in defining the anatomy within the pelvis (*Scoutt et al., 1992*).

The seminal vesicles appear as tubular structures related to the superior aspect of the prostate, posterior to the lower bladder and anterior to the rectum. There is a fat plane between the seminal vesicle and the bladder (*Kabala et al., 2003a*). Tumor invasion of the seminal vesicles should be suspected if a soft tissue mass obliterates the seminal vesicle-fat angle. This sign should be interpreted with caution because the normal seminal vesicle angle may be lost if the rectum is over-distended or if the patient is scanned in the prone position. When no distinct fat planes are present between the bladder and the rectum, uterus, prostate, or vagina, early tumor invasion into these neighboring structures may be difficult to exclude (*Kim et al., 1994*).



.....  
**Lower sacral level-in male:**

The bladder has a rather square shape when it contains urine. It extends anteriorly to the anterior abdominal wall. Posteriorly are the seminal vesicles. The rectum is just behind the seminal vesicles, separated from them by the perirectal fascia and is surrounded by perirectal fat. Outside the perirectal fascia is the pararectal fat. This is continuous with the fat lining the pelvis above the levator ani muscle (*Ryan and McNicholas, 1998*).



*Fig. 10 (a, b) : CT anatomy of the male pelvis (Quoted from Kim et al., 2005).*

**Lower sacral level-in female:**

The uterus is seen closely applied to the posterior surface of the bladder. The position of the ovaries is variable and they may be found lateral to the uterus or behind it. The ureters are close to the posterolateral aspect of the bladder at this level. They hook medially in the broad ligament of the uterus (which can not be identified as a separate structure), passing under the uterine artery and above the lateral vaginal fornix before entering the bladder. Immediately behind is the anorectal junction in the posterior (anal) triangle, the ischiorectal fossa is seen on either side of and behind the anal canal. The puborectalis fibers of levator ani surround the external anal sphincter (*Ryan and McNicholas, 1998*)

The bladder neck surrounds the internal urethral orifice. In females the bladder neck has a direct inferior relationship to the urogenital and pelvic diaphragm. In males, it is separated from the pubis by a moderate amount of connective tissue and fat called the retropubic space of Ritzius. Since the superior aspect of the prostate base slopes obliquely downwards, the lower bladder can project anterior to the prostate base on transverse image. (*Friedman et al., 1990*).

The distended bladder creates **supravesical** and **perivesical** peritoneal pouches between the parietal peritoneum inside the anterior abdominal wall and visceral peritoneum over the bladder dome. These are divided as follows:

**Intraperitoneal paravesical spaces:**

As the urinary bladder protrudes posteriorly into the anterior peritoneal space of the pelvis, recesses are formed between its peritoneal covering and the more lateral portions of the peritoneum along the anterior abdominal wall. (*Friedman et al., 1990*).

**These recesses include:**

**A) Anterior intraperitoneal paravesical space:**

The peritoneum in this space is raised into five ridges converging upwards. A median umbilical fold extends from the apex of the bladder to the umbilicus containing the urachus. On each side of it, the obliterated umbilical artery raises a medial umbilical fold ascending from the pelvis to the umbilicus. Further laterally, each inferior epigastric artery raises a lateral umbilical fold below its entry into the rectus sheath (*Williams et al., 1995*).

---



These folds further subdivide the anterior intraperitoneal paravesical space into:

**1-Supravesical space:**

This space extends along the bladder and then above it, between the medial umbilical folds. It is usually occupied by bowel loops and by the fundus of the distended urinary bladder.

**2-Medial inguinal fossae:**

These lie between the medial and lateral umbilical folds. They are usually occupied at least partially by caecum and ileum on the right and sigmoid colon on the left.

**3-Lateral inguinal fossae:**

These lie between the lateral umbilical folds and the lateral parietal peritoneum as it is reflected over the vas deferens or round ligaments. They are occupied at least posteriorly by caecum or sigmoid colon respectively (*Kazam, 1986*).

**B) Posterior intraperitoneal paravesical spaces:**

These are formed by reflection of the peritoneum from the surfaces of the pelvic viscera with differences in both sexes (*Williams et al., 1995*).

In **males**, peritoneum is reflected from the sides and front of the rectum continuing over the upper poles of the seminal vesicles to the bladder leading to formation of:

•**Pararectal fossae:** on either side of the rectum.

•**Rectovesical pouch:** located anterior to the rectum limited laterally by peritoneal folds from the sides of the bladder reaching posteriorly to the anterior aspect of the sacrum, the sacrogenital folds (**Fig. 9**) (*Williams et al., 1995*).

---

.....  
In **females**, pararectal fossae also appear, but the rectovesical pouch is, of course, divided by the uterus and vagina into:

**•Vesico-uterine space:**

This space is considerably smaller than the more posterior Cul-de-sac and is continuous anterosuperiorly with the supravesical space. Peritoneally disseminated metastasis to this space can extend inferiorly to the level of the upper vagina; displacing the bladder anteriorly and mimicking wall mass (Fig.11) (Kazam, 1986)

**•Recto-uterine pouch or Cul-de-sac:**

It is located posterior to the uterus and broad ligaments bounded laterally by recto-uterine folds corresponding to the sacrogenital folds in males and passing back to the sacrum from the sides of the cervix lateral to the rectum (William et al, 1995).

**Extraperitoneal paravesical spaces:**

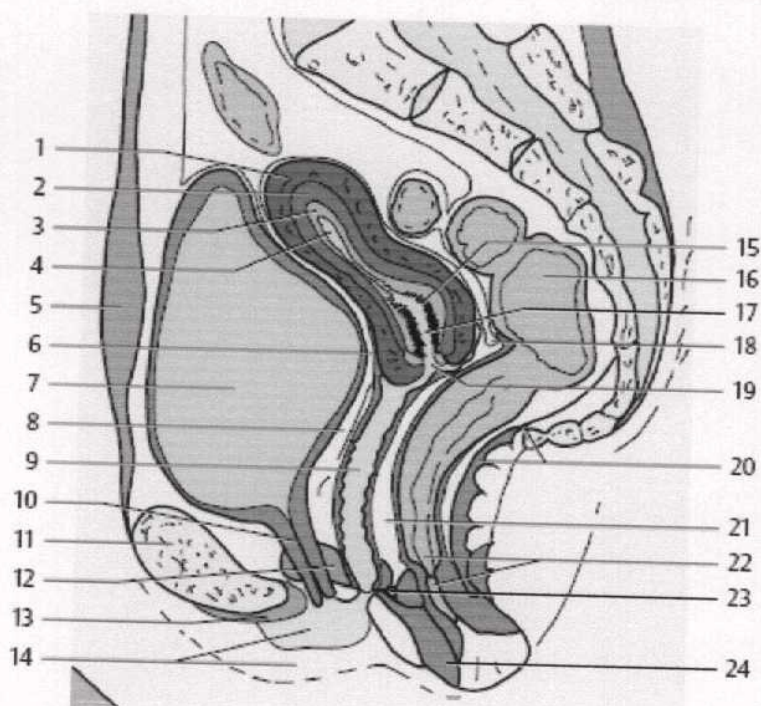
Anterior to the peritoneum and posterior to the transversalis fascia, the umbilicovesical fascia spreads inferiorly from the umbilicus to surround the urachus, obliterated umbilical arteries and urinary bladder. (Kazam, 1986).

The umbilicovesical fascia divides the anterior extraperitoneal fat into **perivesical** and **prevesical** spaces. (Spring et al., 1983).

The prevesical space lies anterior and lateral to the umbilicovesical fascia (Kazam, 1986).

.....





- |   |  |
|---|--|
| 1. Body of uterus (myometrium)                              | 14. Labium minus and majus                       |
| 2. Uterus (junctional zone)                                 | 15. Palmate folds (of cervix of uterus)          |
| 3. Uterus (endometrium)                                     | 16. Rectum                                       |
| 4. Uterus (cavity)  | 17. Cervical canal                               |
| 5. Rectus abdominis muscle                                  | 18. Rectouterine pouch (of Douglas)              |
| 6. Vesicouterine pouch                                      | 19. Portio                                       |
| 7. Urinary bladder  | 20. Anococcygeal ligament and levator ani muscle |
| 8. Fatty layer between urinary bladder, urethra, and vagina | 21. Fatty layer between vagina and rectum        |
| 9. Vagina (wall)  | 22. Anal canal and anus                          |
| 10. Urethra   | 23. Perineal body                                |
| 11. Pubis   | 24. External anal sphincter muscle               |
| 12. Deep transverse perineal muscle                         |  |
| 13. Arcuate pubic ligament                                  |  |

Fig. 11: Female pelvis sagittal section. (Moeller 2001).

The clinical significance of the smaller perivesical spaces lies in the fact that perivesical collections, which tend to be confined around the urinary bladder by the umbilicovesical fascia may be confused with bladder thickening or perivesical tumor extension. Hence, care must be taken during interpretation of CT following biopsy of the bladder due to possibility of mistaking perivesical fluid extravasation for perivesical tumor extension (Spring et al, 1983).

## *Pathology Of Urinary Bladder Carcinoma*

Bladder cancer is the commonest malignancy of the urinary tract and represents roughly 4% of all malignancies; 95% originate from the urothelium and 4% are of non-epithelial origin (leiomyosarcoma, rhabdomyosarcoma below the age of 6, and lymphoma): The remaining 1% includes rarities such as carcinoid and metastases. Direct involvement of the bladder by cancer in adjacent pelvic organs (especially rectum, cervix and prostate) is not uncommon (*Kabala et al., 2003b*).

### *Epidemiology Of Urinary Bladder Carcinoma*

#### **Natural history:**

Approximately 70% of bladder cancers are low-grade, superficial tumours. The majority of patients develop tumour recurrence following endoscopic resection. Usually, tumours that are well- differentiated and superficial at the time of initial diagnosis remain so throughout the life of the patient. Of these, about 25% recur with higher-grade. Most recurrences are probably new tumours arising from other areas of dysplastic urothelium, but a significant proportion may be true recurrences resulting from inadequate treatment or from tumour cell implantation. (*Malmstrom et al., 1987*).

About 10 to 15% of patients with superficial tumours subsequently develop invasive or metastatic cancer (*Lutzeyer et al., 1982*). Most patients (80 to 90%) with invasive bladder cancer already have invasive disease at the time of initial diagnosis. About 50% of patients with muscle-invading bladder cancer already have occult distant metastases. Only 10 to 35% of patients with limited regional lymph node metastases survive 5 years or more without evidence of metastases



following radical cystectomy and pelvic lymphadenectomy (*Skinner et al., 1982*).

### **Incidence**

The bladder is the most common site of cancer in the urinary tract. Cancer bladder is 2.7 times more common among men than women. In men it is the fourth most common cancer after prostate, lung and colorectal cancer, accounting for 10% of all cancer cases. In women, it is the eighth most common cause of cancers, accounting for 4% of all cancers, the incidence of bladder cancer among whites is higher than among blacks (*Silverberg et al., 1990*). In Egypt, Bilharzial induced carcinoma of the urinary bladder is the most common cancer (*El Bolkainy et al., 1981*).

### **Age:**

Although bladder cancer can occur at any age-even in children-it is generally a disease of the elderly with median age of diagnosis being approximately 67 to 70 years old. Younger patients appear to have a more favorable prognosis because they present more frequently with superficial low grade tumours, however, the risk for disease progression is the same grade for grade in young patients as in older patients (*Silverberg et al., 1990*).

### **Mortality:**

The mortality rate of a cancer is the number of deaths occurring per 100,000 persons per year. In 1990, there was 10,200 bladder cancer deaths in the USA,

including 6900 men and 3300 women. This makes bladder cancer the fourth most common cause of cancer deaths in men in the USA (after prostate, lung, and colorectal cancer), accounting for 5% of all cancer deaths in men. In women it accounts for about 3% of all cancer deaths (*Silverberg et al., 1990*).

### **Aetiology Of Urinary Bladder Carcinoma:**

A number of factors have been implicated in the causation of bladder cancer. Some of the more important contributors include the followings (*Cotran et al., 1999*).

#### **Cigarette Smoking**

Smoking is not only the most important risk factor for transitional cell carcinoma of the urinary bladder, but is also associated with higher grades of the tumor. There is significant association between the smoking history and stage, grade, and the number of recurrences of transitional cell carcinoma of the bladder. Cigarette smoking correlates with higher rates of progression, invasion, and lethality in patients. (*Mohseni et al., 2005*).

Smoking increases the risk of urothelial atypia. Discontinuing smoking decreases the risk, although a higher risk than non-smokers remains for up to 10 years of smoking cessation (*De Vita et al., 2001*).

Many epidemiologists implicate cigarette smoking as the primary environmental risk factor for bladder cancer in the United States. Tobacco smoke contains various aromatic hydrocarbons including B-naphthylamine as well as other possible carcinogens such as nitrosamines (*Murphy, 1997*).



The specific chemical carcinogen responsible for cancer in cigarette smoke has not been identified. However, increased urinary tryptophan metabolites have been demonstrated in cigarette smokers (*Hoffman et al., 1989*).

### **Occupational Exposure:**

Aniline dyes, introduced in the mid-1800s to colour fabrics, are urothelial carcinogens. Other chemicals that have been shown to be carcinogens as combustion gases and soot from coal; and possibly, chlorinated aliphatic hydrocarbons (*Silverberg et al., 1990*).

It is estimated that occupational exposure accounts for 1/4 to 1/3 of bladder cancer cases in the United States. The latent period may be as long as 40 to 50 years, but more intensive exposure to the carcinogen may shorten the latent period. Most bladder carcinogens are aromatic amines. Occupations reported to be associated with an increased risk of bladder cancer include those of, painters, truck drivers, drill press operators, leather workers, dry cleaners and paper manufactures (*Silverman et al., 1989*).

### **Chronic Cystitis:**

Chronic cystitis, indwelling catheters, congenital anomalies or calculi are associated with an increased risk for squamous cell carcinoma of the bladder. Between 2 and 10% of paraplegics with long-term indwelling catheters develop bladder cancer. Approximately 30% of these are squamous cell carcinomas (*Locke, et al., 1985*). These rates can be further augmented by associated urinary tract infection and dietary factors (*Murphy, 1997*).

---

Similarly, *Schistosoma Haematobium* cystitis is causally related to the development of squamous cell cancer. In Egypt, where Schistosomiasis is endemic; squamous cell carcinoma of the bladder (Bilharzial bladder cancer) is the most common cancer. Cystitis -induced bladder cancer from all causes is usually associated with severe, long term infections (*Tricker and Spiegelhalder, 1989*).

N-nitroso compounds produced by chronic inflammation appear to be of particular importance as a suggested causative agent since they were found at high levels in the urine of these patients (*Mostafa et al., 1999*).

The worm itself probably has no important carcinogenic properties, but the combination of long term urothelial irritation by calcified eggs, chronic infection and perhaps dietary factors peculiar to these endemic areas creates conditions leading to carcinogenesis (*Murphy, 1997*).

### **Coffee and Tea Drinking:**

Coffee and tea drinking has been implicated in some -but not all- studies in the aetiology of bladder cancer. This association is complicated because of the widespread consumption of coffee & tea, and The fact that coffee and tea drinking, artificial sweeteners and cigarette smoking are often associated (*Silverman et al., 1989*).

### **Artificial Sweeteners:**

Large doses of artificial sweeteners, including saccharin and cyclamate, have been shown to be bladder carcinogens in experimental studies in rodents (*Sontag, 1980*). In contrast, case-control epidemiological studies in humans show little

---



evidence of increased risk of bladder cancer in consumers of artificial sweeteners (*Risch et al., 1997*).

### **Analgesic Abuse:**

Consumption of large quantities (5 to 15 kg over a 10 year period) of the analgesic “phenacetin”, which has a chemical structure similar to that of the aniline dyes, is associated with an increased risk for transitional cell carcinoma of the renal pelvis and urinary bladder (*Piper et al., 1985*).

### **Pelvic Irradiation:**

Women treated with radiation therapy for carcinoma of the uterine cervix have a two to four fold increased risk of developing transitional cell carcinoma of the bladder (*Sella et al., 1989*).

### **Cyclophosphamide:**

Patients treated with cyclophosphamide (which is used in the treatment of rheumatoid arthritis or as a chemotherapeutic agent) have increased risk of developing bladder cancer (usually high grade). Most of these tumours are muscle-infiltrating at the time of diagnosis (*Durkee and Benson, 1980*). Most likely the pathogenic mechanism is related to the formation of cyclophosphamide metabolites that are capable of DNA alterations (*Damjanov& Linder, 1996*).

### **Dietary components:**

---

Dietary components consumed in high quantities such as fried meat and fat are associated with bladder cancer while vitamin A supplements appear to be protective (*De Vita et al., 2001*).

### **Hereditary:**

Little evidence exists for a hereditary cause of most cases of bladder cancer. An explanation for familial clusters may be due to similar exposure to the same environmental factors (*Arce et al., 1983*). Most bladder tumors occur more frequently in whites than in blacks (*Olsen et al., 1995*).

Although no chromosomal abnormalities specific for bladder neoplasm have been found, aberrations in chromosomes 1,3,5,9,11,17&Y are most common. Two different patterns have been suggested, an autosomal dominant and multifactorial polygenic patterns. Alterations in both the number of chromosomes and their structure. These abnormalities are ordinarily found in transitional cell carcinoma of high grade and stage (*Kroft & Oyasu, 1994*).

### **Pre-neoplastic Proliferative Abnormalities:**

#### **(I) Epithelial Hyperplasia:**

The term epithelial hyperplasia is used to describe an increase in the number of cell layers without nuclear or architectural abnormalities. A variety of changes can occur in the urothelium in response to inflammation, irritation or carcinogens. These changes may be proliferative, metaplastic or both. (*Damjanov & Linder, 1996*).

**Von Brunn's nests** are proliferative solid invaginations of urothelial cells into the lamina propria retaining a continuity with the surface urothelium. The cells



are devoid of dysplastic features. They are now considered to be a normal component of the urinary tract. They are found in all urinary bladders especially at the trigone and their frequency increases with age (*Damjanov & Linder, 1996*).

**Cystitis Cystica** probably develop from Brunns' nests that acquire a lumen. They also represent a normal variant of urothelium because there is no evidence linking them pathogenically to infection. They are predominantly seen in the trigonal area (*Damjanov & Linder, 1996*).

**Inverted Papilloma** is a benign proliferative lesion caused by chronic inflammation or bladder outlet obstruction. Most commonly, it occurs in the trigone and bladder neck areas in men with prostatism. Inverted papilloma may contain areas of cystitis cystica or squamous metaplasia. Two different types of inverted papilloma occur: trabecular and glandular. Rare cases of malignant transformation of inverted papillomas have been reported (*Kunz et al., 1983*).

## (II) Dysplasia:

The term dysplasia denotes epithelial changes that are intermediate between normal urothelium and carcinoma in situ. There are three categories of dysplasia: mild, moderate and severe. It is difficult to make a sharp distinction between severe dysplasia and carcinoma in situ (*Friedell et al., 1986*).

## (III) Urothelial Metaplasia:

### A. Cystitis glandularis:

Is similar to cystitis cystica except that the transitional cells have undergone glandular metaplasia. Cystitis glandularis may be a precursor of adenocarcinoma. It has been reported to occur frequently in patients with pelvic lipomatosis.

.....

Cystoscopically, cystitis glandularis may appear as a papillary lesion (*Gordon et al., 1990*).

### **B. Squamous Metaplasia:**

It describes the appearance of keratinizing or non-keratinizing squamous epithelium replacing portions of normal urothelium (*Damjanov and Linder, 1996*).

#### **1. Non keratinizing squamous metaplasia:**

It has been found in the trigone and bladder neck in up to 86% of women of reproductive age and in 72% of postmenopausal women (*Damjanov and Linder, 1996*). It is six times more frequent in women than in men and is apparently a benign lesion carrying little risk of future neoplasia (*Murphy, 1997*).

#### **2. Keratinizing squamous metaplasia (Leukoplakia):**

Leukoplakia is defined as cornification of a normally non-cornified membrane. Leukoplakia is believed to be a response of the normal urothelium to noxious stimulants. It is generally considered a pre-malignant lesion or a lesion that heralds the presence of malignant disease elsewhere in the bladder. Vesical leukoplakia may progress to squamous cell carcinoma in up to 20% of patients. Usually, they are confused with leiomyosarcoma (*Huang et al., 1990*).

### **C. Nephrogenic Adenoma :**

Nephrogenic adenoma is a rare lesion that histologically resembles primitive renal collecting tubules. It is a metaplastic response of the urinary bladder urothelium to trauma, infection or radiation therapy. Nephrogenic adenoma is more common in men and is often associated with symptoms of dysuria and urinary frequency.

.....



Nephrogenic adenoma also has been reported in children (*Kay and Lattanzi, 1985*)

#### (IV) Urinary Bladder Neoplasms :

##### **A -Epithelial**

- Carcinoma in situ
- Transitional cell carcinoma
- Squamous cell carcinoma
- Adenocarcinoma
- Small cell carcinoma
- Carcinosarcoma
- Metastatic

##### **B -Non- Epithelial**

- Neurofibroma
- Pheochromocytoma
- Primary lymphoma
- Plasmacytoma
- Sarcoma
- Myoblastoma

#### A – Epithelial neoplasms :

##### **1-Carcinoma in situ :**

Carcinoma in situ appears as a velvet patch of erythematous mucosa on cystoscopic examination. Histologically, it consists of poorly differentiated transitional cell carcinoma confined to the urothelium. Carcinoma in situ may be asymptomatic or may produce severe symptoms of urinary frequency, urgency and dysuria (*Connor and Olsson, 1989*)

Carcinoma in situ occurs more commonly in men. Its symptoms may be



mistaken for prostatism, urinary tract infection or neurogenic bladder. It portends a poor prognosis. Patients with carcinoma in situ have higher tumour recurrence rates (Flamm and Bucher, 1990).

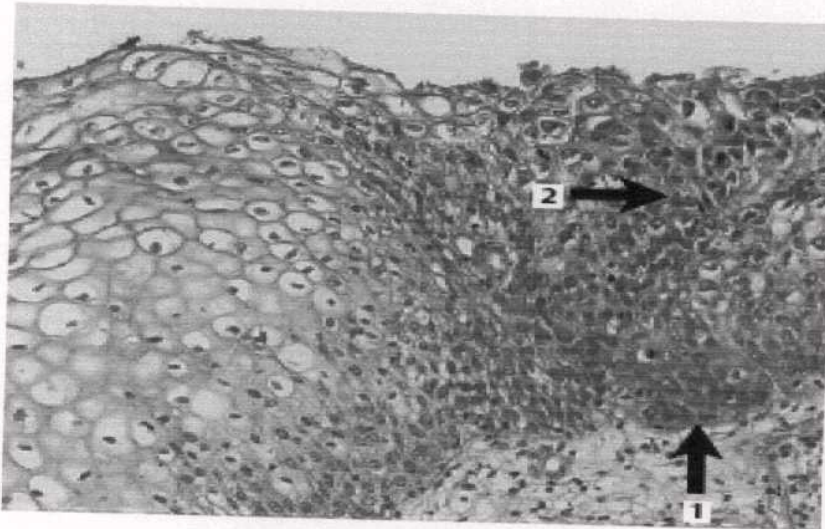


(Fig. 12) Severe epithelial atypia in the squamous epithelium and loss of polarity with an intact basement membrane (E1) and histologic findings of noninvasive carcinoma (E2) (Quoted from Riede and Werner 2004).

Carcinoma in situ is a serious disease that demands clinical attention, as its course is unpredictable. When it appears as the initial neoplasm, the frequency of invasion is low. In contrast, an adverse outcome is likely when carcinoma in situ occurs in association with papillary or invasive carcinomas (Prout et al., 1983).

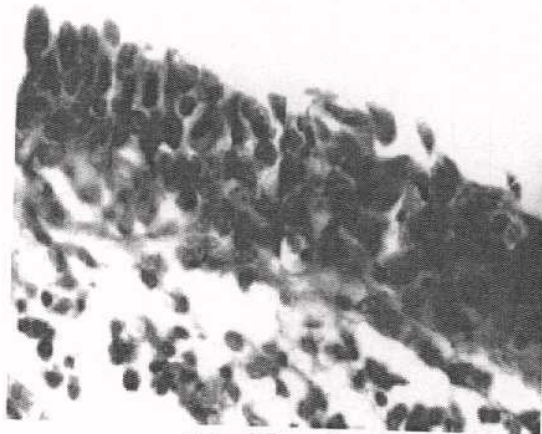


Fig.13

Fig.13. Carcinoma in situ. The cells have hyperchromatic nuclei that vary in size, shape, and orientation. The basement membrane is still intact

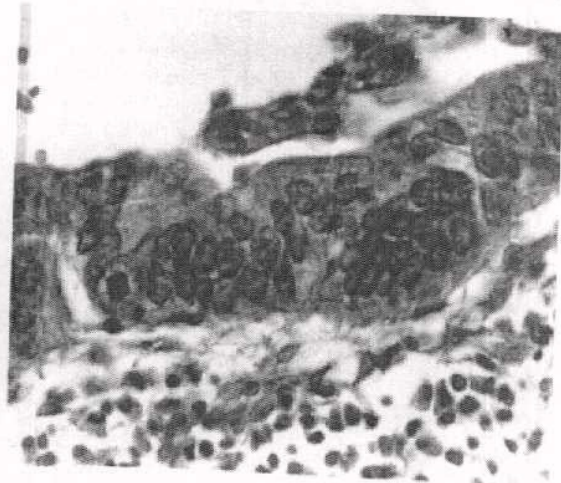


Fig.14

Fig.14 . Carcinoma in situ of bladder urothelium with the dense inflammatory infiltrate in the lamina propria. (Quoted from Veličković et al., 1998)

## 2-Transitional cell carcinoma:

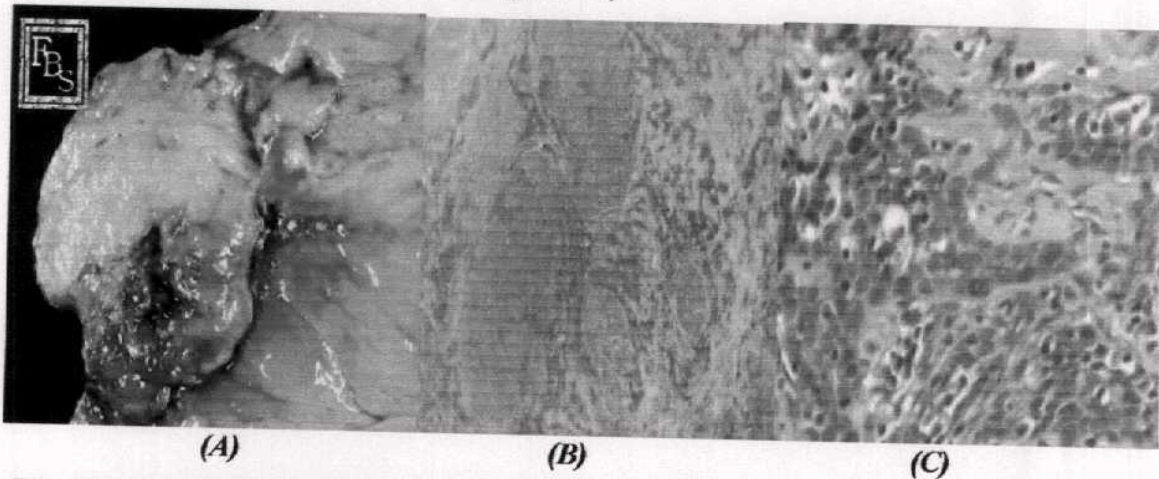
Transitional cell carcinomas can be separated into those of low and high grades. Low-grade Transitional cell carcinomas arise primarily at the bladder base and are usually solitary. High-grade Transitional cell carcinoma is a highly anaplastic tumour that arises at the bladder base and is usually nodular with or without papillary components (Murphy, 1997). More than 90% of bladder cancers are transitional cell carcinomas. Transitional cell carcinomas manifest a variety of patterns of tumour growth including papillary, sessile infiltrating, nodular, mixed and flat intraepithelial growth. Moreover, cancer invasion into the smooth muscle cells of the tunica muscularis mucosa sometimes can be mistaken for invasion into the bladder detruser muscle (Keep et al., 1989).





Fig. (15) *Invasive transitional cell carcinoma in urinary bladder.*  
(Quoted from Sharma 2003).

Transitional cell epithelium has a great metaplastic potential; therefore, transitional cell carcinomas may contain spindle cell, squamous cell or adenocarcinomatous elements. These elements are present in about one third of bladder cancer. Transitional cell carcinomas are most commonly in the trigone of bladder base area and on the lateral bladder walls; however, they may arise anywhere within the bladder (Young, 1987).



(Fig.16): 64 year old female presenting with hematuria,  
(A) Semi-polypoid, yellow-white mass with focal areas of hemorrhage.  
(B) Low power and (C) High power transitional cell carcinoma.  
(Quoted from Bioscience 2007).



### 3- Squamous cell carcinoma:

Squamous cell carcinoma is the most common non-transitional cell bladder tumor, accounting for 3-7% of all bladder tumors in the United States. Approximately 80% of squamous cell carcinomas in Egypt are associated with chronic infection caused by Schistosomiasis (*Messing and Catalona 1998*). These cancers are called Bilharzial bladder cancers. Bilharzial squamous cell cancers are nodular, fungating lesions that usually are well differentiated and have a relatively low incidence of lymph node and distant metastases. Although some investigators have speculated that the low incidence of distant metastases may be due to capillary and lymphatic fibrosis resulting from chronic schistosomal infection, it is most probably related to the fact that, most of these tumours are low-grade (*EI-Bolkainy et al., 1981*).

Non-bilharzial squamous cell carcinomas occur in association with chronic irritation from urinary calculi, long-term indwelling catheters, or chronically infected bladder diverticula. (*Messing and Catalona 1998*). Most of them are invasive, fungating tumours or infiltrative and ulcerative, they often cover large areas of the bladder and are deeply invasive by the time of discovery (*Cotran et al., 1999*).

Squamous cell carcinomas characteristically have keratinised cell that contain concentric aggregates of cells called squamous pearls. Squamous cell cancers shed keratinised cells into the urine that sometimes can be detected cytologically. However, cytology has been of limited usefulness in patients with this tumours (*kantor et al., 1988*)

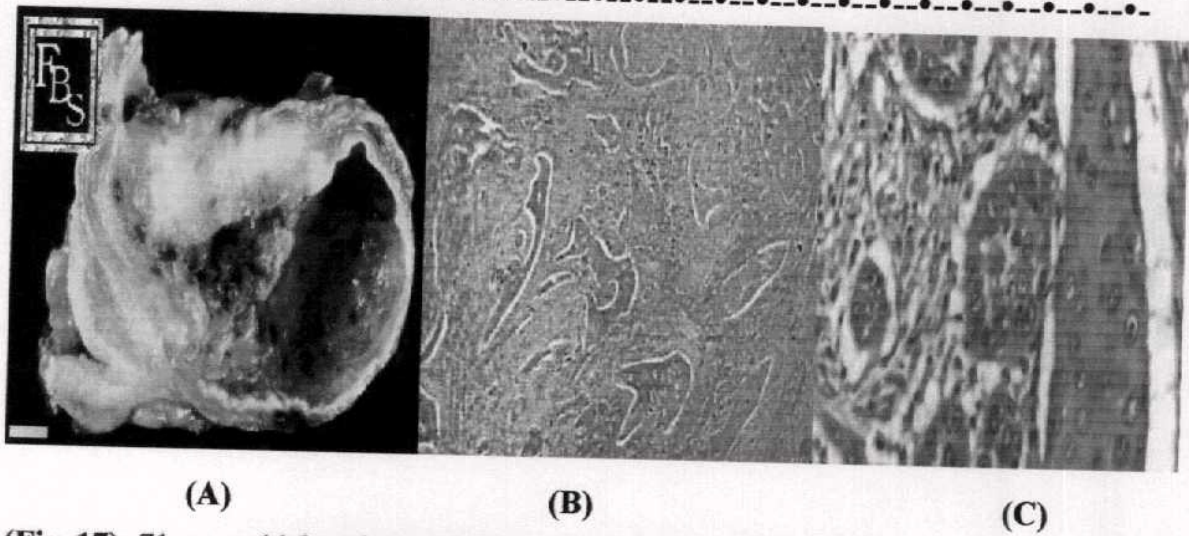


(Fig. 17): 71 year old female presenting with hematuria Fungating,  
(A) tan-white, indurated mass.  
(B) Low power and (C) High power squamous cell carcinoma.  
(Quoted from Bioscience 2007).

Metastases have been identified in at least 10% of patients at the time of diagnosis. Interestingly, metastases from squamous cell carcinomas of the urinary bladder often occur at sites other than the regional lymph nodes. Common metastatic sites include bone, lung, and bowel (Murphy 1997).

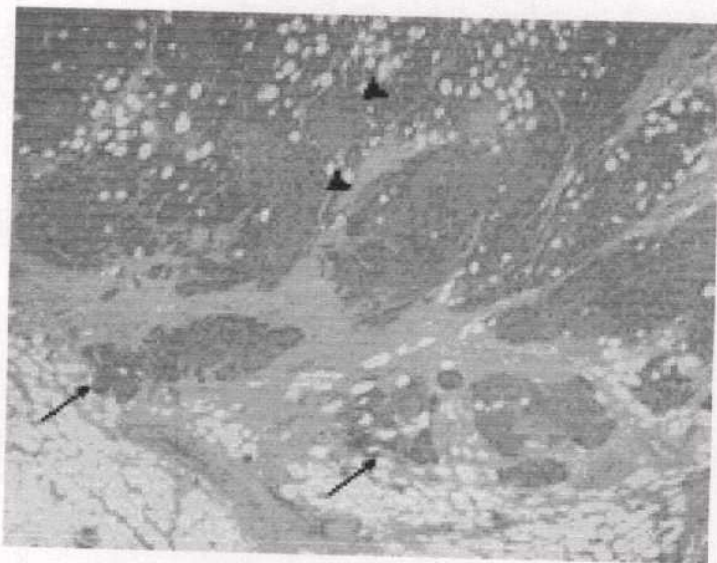


(Fig. 18). Stage T2b squamous cell carcinoma. Photomicrograph of cystectomy specimen shows squamous cell carcinoma with formation of keratin pearls (arrows). (Quoted from Tekes et al., 2003).



#### 4-Adenocarcinoma:

Adenocarcinoma of the urinary bladder is uncommon, accounting for 0.5-2% of all bladder malignancies (*Chan and Epstein 2001*). Adenocarcinomas are classified into three groups: Primary, urachal and metastatic (*Messing and Catalona 1998*).

Adenocarcinoma also occurs in intestinal urinary conduits, pouches, and with uretero-sigmoidostomy (*Kalble et al., 1990*).

##### (i) Primary vesical adenocarcinoma:

Adenocarcinoma arises in two common sites: the base of the bladder, including the trigone, and the dome of the bladder. (*Messing and Catalona 1998*). However, adenocarcinomas can occur anywhere in the bladder. Adenocarcinoma is the most common type of cancer in exotrophic bladder. These tumours develop in response to chronic inflammation and irritation. Adenocarcinoma also has been reported with Schistosomiasis. However, it is less common than squamous cell carcinoma with schistosomiasis (*Bennett et al., 1984*).

Other established risk factors have not been documented except, possibly coffee drinking. Adenocarcinoma may be papillary or solid. Signet-ring adenocarcinomas characteristically produce linitis plastica of the bladder (*Fig.19*) (*Blute et al., 1989*). Signet ring cell cancers are usually diffusely infiltrating and are of advanced stage at the time of diagnosis. Deep muscle invasion is the rule (*Murphy 1997*).

The generally poor prognosis associated with adenocarcinoma is due primarily to the fact that they are diagnosed at an advanced stage (*Blute et al., 1989*).



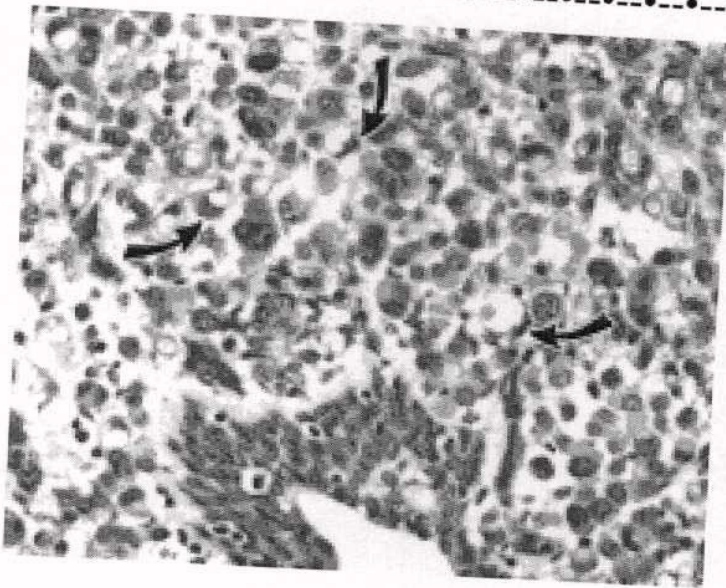


(Fig. 19) Stage T4a adenocarcinoma of urinary bladder. Photomicrograph of adenocarcinoma obtained from cystectomy specimen at high magnification shows cancer cells with signet ring cell features (arrows).

(Quoted from Tekes et al., 2003)

#### (ii)- Urachal carcinoma:

Urachal carcinoma is extremely rare tumours that arise outside the bladder and histologically may be adenocarcinomas, transitional cell carcinomas, squamous cell carcinomas, or rarely sarcomas. For a tumour to be classified as urachal carcinoma, there must be a sharp demarcation between the tumour and the adjacent bladder mucosa, and the tumour must be located within the bladder wall beneath the normal urothelium (Kakizoe et al., 1983).

Many urachal tumours have stippled calcifications on radiographs. Patients with urachal carcinomas have a worse prognosis than those with primary bladder adenocarcinomas (Brick et al., 1988).

#### (iii)- Metastatic adenocarcinoma:

One of the most common forms of adenocarcinoma of the bladder. The primary sites of these tumours include the rectum, stomach, breast, prostate and ovary. Nevertheless, metastases to the bladder from adenocarcinoma is still a relatively rare phenomenon occurring in only 0.26% of cases (Choi et al., 1984).

## 5-Non-urothelial neoplasm:

### I- Small-cell carcinoma:

It is believed that small-cell carcinomas of the bladder are derived from neuro-endocrine stem cells. Small-cell carcinoma may be mixed with elements of transitional cell carcinoma in the same tumour (**Fig.20**) Another possible source of small-cell carcinoma is the dendritic cells in the normal urothelium. (*Swanson et al., 1990*).

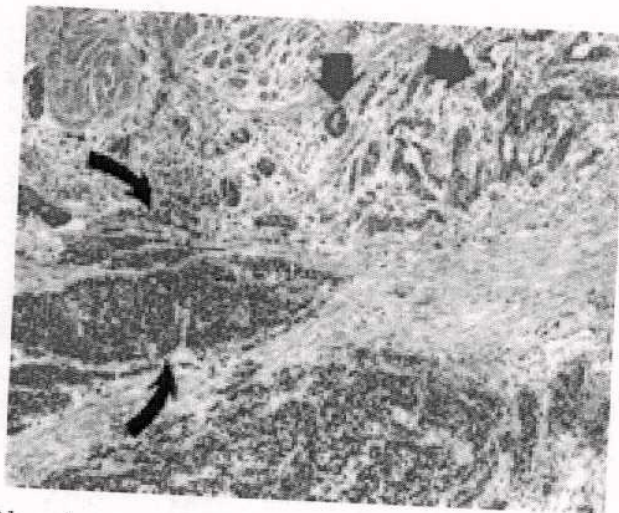


**(Fig. 20)** Stage T3b adenocarcinoma of bladder with transitional and small cell components. Photomicrograph of cystectomy specimen shows infiltrating high-grade urothelial carcinoma consisting of adenocarcinoma and small cell carcinoma. Adenocarcinoma component shows glands with more abundant cytoplasm and more open chromatin (arrows). Small cell component shows cells with hyperchromatic nuclei, little cytoplasm, and nuclear molding (curved arrows).

(Quoted from *Tekes et al., 2003*)

Small cell carcinoma of the urinary bladder accounts for only 0.48-1% of all bladder malignancies. Most patients with this bladder tumor have shown at least muscular invasion at the time of diagnosis and their clinical course has been highly aggressive, with early and widespread metastasis and a poor overall survival rate. Transurethral resection, commonly applied in early-stage transitional cell



carcinoma of the bladder, is known to be ineffective in the treatment of patients with small cell carcinoma of the bladder (*Kim et al., 2003*).

Cystoscopically, small cell carcinomas tend to be polypoid or nodular and often appear as ulcerated masses that cannot be distinguished from other high-grade bladder cancers. Small cell carcinomas can arise from various locations and are not predominantly localized to the base of the bladder. Metastatic spread occurs rapidly, and the most frequent sites are the regional lymph nodes, bones, and peritoneal cavity (*Murphy 1997*).

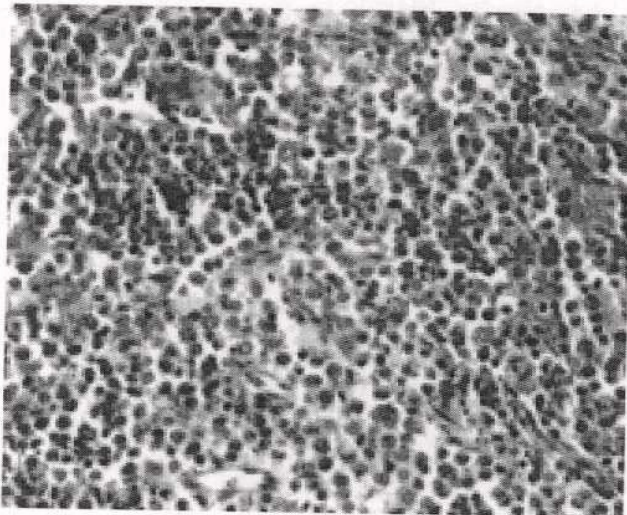


(**Fig. 21**) Stage T4a small cell carcinoma of urinary bladder. Photomicrograph of cystectomy specimen shows small cell carcinoma with sheet of hyperchromatic cells, abundant mitoses, and apoptosis.

(*Quoted from Tekes et al., 2003*)

## II-Carcinosarcoma:

Carcinosarcoma of the urinary bladder is a rare neoplasm; They are most frequently observed in the female genital tract. Neither the etiology nor the pathogenesis of carcinosarcomas is currently known. Bladder carcinosarcomas predominate in men, with a ratio of 3:1. Most patients complain of hematuria, but clinical symptoms are nonspecific. The tumors are most common at the base of the bladder and are polypoid masses. Carcinosarcomas are usually deeply infiltrative at



the time of clinical detection. Most deaths result from complications of local growth rather than distant metastasis. Histologically, the most common epithelial component is transitional cell carcinoma, although glandular, squamous, and even small cell carcinomas have been reported. The sarcomatous component is most commonly poorly differentiated and spindled, but cartilaginous, osseous, and muscle differentiation are also seen (**Fig. 22**) (*Murphy1997*).

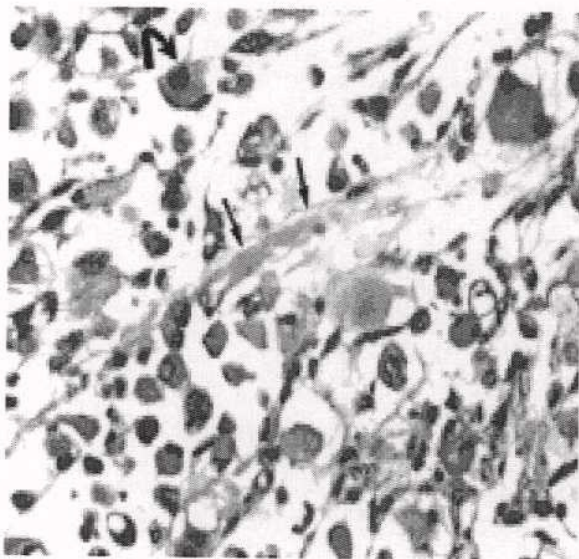


*Fig.22.a*

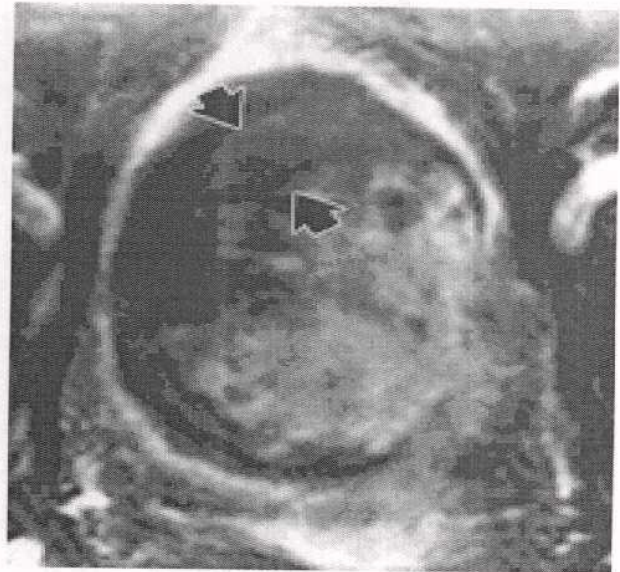


*Fig.22.b*

(*Fig. a.*) Stage T3b carcinosarcoma of urinary bladder. Photomicrograph of cystectomy specimen shows that this mass lesion includes rhabdosarcoma, transitional cell carcinoma, and adenocarcinoma components. High magnification of rhabdomyosarcoma component (curved arrow) of tumor shows cells, spindled to round, with abundant eosinophilic cytoplasm. Strap cell with striations (straight arrows) can be seen in center of field.

(*Fig. b.*) Axial arterial phase contrast-enhanced fast spoiled gradient-echo MR image shows large polypoid fungating mass arising from left lateral wall and protruding into lumen with heterogeneous enhancement.

(*Quoted from Tekes et al., 2003*)

### **III-Metastatic carcinoma:**

Cancers from virtually any other primary site may secondarily involve the bladder. The most common primary sites are prostate, ovary, uterus, colon, lung, breast and stomach as well as primary melanoma, lymphoma and leukemia (*Sen et al., 1985*).

### **B-Non-Epithelial bladder neoplasms**

The three categories of non-epithelial bladder tumours are as follows:

- (i) Primitive connective tissue tumours, including leiomyosarcoma, rhabdomyosarcoma, chondrosarcoma, osteosarcoma, liposarcoma and granular cell myoblastoma
- (ii) tumours of non-connective tissue origin including angiosarcoma, neurosarcoma, neurofibroma, pheochromocytoma and melanoma
- (iii) Secondary non-epithelial tumours including lymphoma, leukaemia, plasmacytoma and melanoma (*Rosi et al., 1983*).

#### **1-Neurofibroma:**

A neurofibroma is a benign tumour of the nerve sheath resulting from overgrowth of the Schwann cells. In the bladder, neurofibromas arise from the ganglia of the bladder wall and may occur as either solitary lesions or plexiform lesions. Vesical neurofibromatosis often becomes clinically manifest in childhood with symptoms of urinary tract obstruction, urinary incontinence, vesical irritability or pelvic mass. Rarely, bladder neurofibromas may undergo malignant

---



degeneration to form neurofibrosarcomas (*Clark et al., 1989*).

## 2-Pheochromocytoma:

Bladder pheochromocytomas account for less than 1% of all bladder tumours. They arise usually in the region of the trigone. There is no sex predilection, and the peak age incidence is from the 2<sup>nd</sup> through the 4<sup>th</sup> decades. About 10% of bladder pheochromocytomas are malignant and have the capacity to metastasis to the regional lymph nodes or distant sites. Most pheochromocytomas in the bladder are metabolically active, causing paroxysmal attacks of hypertension on filling and emptying of bladder in two thirds of patients and haematuria in about one half of patients (*Deklerk and Catalona, 1988*).

## 3-Primary lymphoma:

Primary, bladder lymphoma arises in the submucosal lymphoid follicles and is the second most common type of non-epithelial bladder tumour. The peak age is 40 to 60 years old and women are affected more often than men (*Bullock et al., 1990*).

## 4-Plasmacytoma, granular cell myoblastoma, malignant melanoma, choriocarcinoma and yolk sac tumours:

These rare primary bladder tumours, which exhibit the same characteristics as their counterparts in other sites of the body and are managed in a similar fashion (*Tsakamoto and Lieber, 1990*).



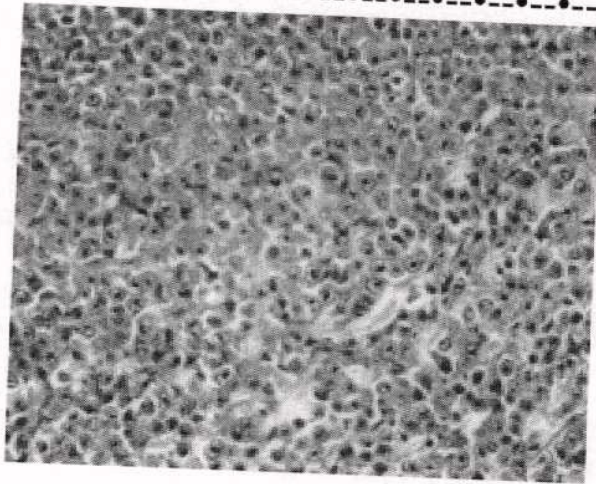


(Fig. 23) Stage T2b plasmacytoma of bladder. Photomicrograph of cystectomy specimen shows plasmacytoma consisting of sheet of discohesive cells with prominent nucleolus and eccentric eosinophilic cytoplasm (Quoted from Tekes et al., 2003).

### 5-Sarcoma:

Malignant connective tissue tumours containing cell types that are normally present in the bladder include angiosarcoma and leiomyosarcoma those that contain tissues not normally present in the bladder include rhabdomyosarcoma, chondrosarcoma and osteosarcoma. Sarcoma of the bladder account for less than 1% of all malignant bladder tumours (Kabalin et al., 1990).

#### *a-Angiosarcoma:*

Angiosarcomas are extremely rare turnouts that arise within the bladder wall. Histologically they contain dilated vascular channels with prominent papillary endothelial proliferation (Tsukamoto and Lieber, 1990).

#### *b-Leiomyosarcoma:*

Leiomyosarcoma is the most common malignant mesenchymal tumour of the bladder occurring in adults. It is twice as common in men as in women. The presence of nuclear abnormalities distinguish a leiomyosarcoma from a benign leiomyoma (Tsukamoto and Lieber, 1990).

**c- Rhabdomyosarcoma:**

Rhabdomyosarcoma may occur at any age but is most common in young children. Embryonal rhabdomyosarcoma in children characteristically produces polypoid lesions in the base of the bladder, giving rise to the descriptive term sarcoma botryoides. Rhabdomyosarcoma is an extremely aggressive tumour that metastasize to lymph nodes in 40% to 50% of patients; it is the sarcoma with the greatest propensity for lymph nodes metastases (*Kabalin et al., 1990*).

**Patterns of spread of urinary bladder carcinoma:**

**I-Direct extension:**

Bladder cancer spreads by invading through the lamina propria into the submucosa and muscularis of the bladder wall. This process may occur either because tumour cells are not able to synthesize components of the basement membrane or because of an increased degradation of basement membrane component by enzymes produced by tumour cells. In the submucosa and muscularis, tumour cell gain access to blood vessels and lymphatics through which they may metastasize to regional lymph nodes and/or distant metastases. A significant correlation exists between muscle invasion and distant metastases (*Zuk et al., 1989*).

Bladder cancer may spread locally to invade adjacent organs, including the prostate, uterus, vagina, ureters, rectum and intestine. More than 40% of men undergoing cystectomy for invasive bladder cancer have involvement of the prostate. In the majority of such cases, the prostatic urethra is the site of



involvement. In such patients there is a high incidence (80%) of subsequent distant metastases. It has been suggested that patients with prostatic involvement should be treated with neoadjuvant chemotherapy (*Hardeman et al. 1990*).

Tumours arising in bladder diverticula pose a special problem; they can invade directly from the mucosa into the perivesical tissues because bladder diverticula do not have a muscular wall (*Montie, 1990*).

## II-Metastatic spread:

About 5% of patients with superficial papillary cancer and approximately 20% with high-grade carcinoma in situ have vascular or lymphatic spread, presumably from invasion of tumour cells into superficial lymphatic and vascular channels just beneath the lamina -propria (*Beahrs et al., 1990*).

### a- Lymphatic spread:

Lymphatic metastases occur earlier and independent of haematogenous metastasis in some patients. The most common sites of lymphatic metastasis in bladder cancer are the pelvic lymph nodes, occurring in about 78% of patients. Among these, the para-vesical nodes are involved in 16% and the external iliac nodes in 65% (*Smith et al., 1990*).

Once the tumour has reached the peri-vesical fat, the disease can be expected to have local spread to local lymph nodes or beyond in 84% of cases. The risk of metastatic disease is proportional to the depth of tumour invasion to the bladder. 20% of patients with cancer invading lamina propria, 30% with superficial muscle invasion and 60% of patients with full muscle thickness invasion will have lymph nodes metastases (*Kent et al., 1990*).

The regional lymph nodes are the nodes of the true pelvis, which essentially are the pelvic nodes below the bifurcation of the common iliac arteries, thus they include the following groups of lymph nodes: hypogastric, obturator, internal and external iliac, perivesical, pelvic, sacral and presacral lymph nodes. The common iliac nodes are considered sites of distant metastases. (*Beahrs et al., 1990*).

***b-Blood borne spread:***

Blood borne spread of urothelial cancer is usually a late event and is generally associated with invasive anaplastic lesions, it may also occur in some patients with well-differentiated tumours. The common sites of vascular metastases from bladder cancer are liver 38%, lung 36%, bone 27%, adrenal gland 21% and intestinal 13%. Any other organ may be involved (*Babaian et al., 1990*).

**III- Implantation:**

Bladder cancer also spreads by implantation in abdominal wound, resected prostatic fossa or traumatized urethra. Implantation occurs more commonly with multiple tumours and high-grade tumours. Tumour implantation into the resected prostatic fossa is an infrequent occurrence (*Van Der Werf-Messing, 1984*).

**Staging systems of urinary bladder carcinoma:**

Urinary bladder carcinoma is distressing for both the patient and the physician. It is the most common malignant tumour of the urinary tract. The disease can take an unpredictable and protracted course. Its treatment and



prognosis are largely determined by the depth of tumour infiltration and the extent of metastases. Therefore, exact staging is mandatory (*Beahrs et al., 1990*).

### Goals of staging:

The first treatment decision based on tumour stage is whether the patient has a superficial or invasive tumour. The second treatment decision made on the basis of staging is to identify patients with invasive tumours who may benefit from aggressive or potentially curative therapy. For this purpose, CT scanning, ultrasonography and magnetic resonance imaging (MRI) have been used to evaluate the local extent of bladder tumours to determine whether the tumour localized, extensive or metastatic (*Barentsz et al., 1996*).

Two staging systems for bladder cancer are currently in widespread use. One proposed initially by Jewett-Strong (1946) modified by Marshall (1952) and the other by The Union International Contre Le Cancer in 1974 (*Smith et al., 1999*).

### I- The T.N.M Staging:

According to Union International Contre Le Cancer (UICC), staging depends on degree of invasion of the tumour to urinary bladder wall (T), size of lymph node (N) and metastases (M) (*Walsh, 1996*).

#### 1- (T) The primary tumour:

- T0: No evidence of primary tumour.
- Tis: Pre-invasive carcinoma (carcinoma in situ).
- Ta: Papillary non-invasive carcinoma.
- T1: The tumour does not invade beyond the lamina propria.
- T2: Invasion of the superficial muscle.
- T3: (a, b) Invasion of deep muscle (T3a) and invasion perivesical fat (T3b).
- T4: (a, b) The tumour is fixed and extended to pelvic organs (T4a) abdominal organs (T4b).

**2-(N) Regional and juxta lymph node:**

- N0: No evidence of regional lymph node involvement.
- N1: Evidence of involvement of a single ipsilateral external or internal iliac lymph node.
- N2: Evidence of involvement of the contralateral or bilateral or multiple regional lymph nodes.
- N3: Evidence of involvement of fixed regional lymph nodes where there is a fixed mass on the pelvic wall with a free space between this mass and the primary tumour.
- N4: Evidence of involvement of the juxta-regional (common iliac, aortic, inguinal) lymph nodes.

**3-(M) Metastases:**

- M0: No evidence of distant metastases.
- M1: Evidence of distant metastases.

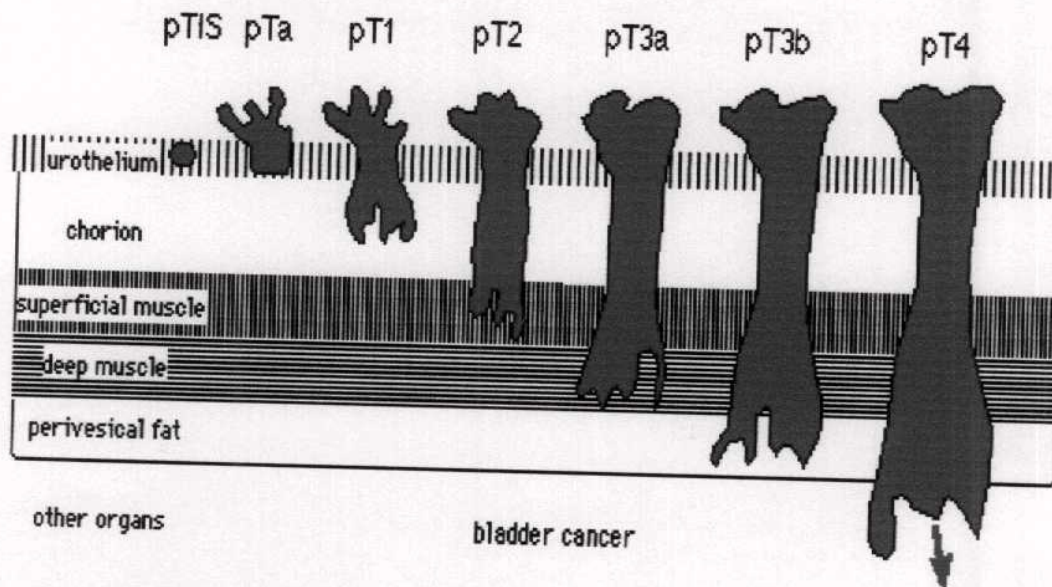


Diagram 1: Drawing shows TNM staging system for cancer of urinary bladder.  
(Quote from Van Tilborg and Van Rhijn 2003).



### **II-Jewett-Strong Marshall Staging:**

Based on the relationship of the depth of tumour penetration into the bladder wall with the incidence of lymph node or metastases.

- 0: Lesion limited to superficial mucosa.
- A: Submucosal invasion.
- B: Muscular layer invasion, subdivided to:
  - (B 1) superficial muscle invasion.
  - (B 2) deep muscle invasion.
- C: Perivesical invasion.
- D: Metastases, subdivided to:
  - (D 1) spread to adjacent organs
  - (D 2) spread to extrapelvic lymph nodes or distant metastases.

**Table (1): STAGING SYSTEM FOR BLADDER CANCER**

Description	TNM Stage	Jewett-Strong-Marshall Stage
No tumor	T0	0
Carcinoma in Situ (CIS)	Tis	0
Papillary Tumor Noninvasive	TA	0
Papillary Tumor Lamina Propria Invasion	T1	A
Muscle Invasion	T2	B1
Tumor invades superficial muscle (inner half)	T2A	
Tumor invades deep muscle (outer half)	T2B	
Perivesical Fat Invasion	T3	
Microscopic	T3A	B2
Macroscopic (extravesical mass)	T3B	C
Invasion of Contiguous Viscera	T4A	D1
Invasion of Pelvic/Abdominal Wall	T4B	D1
Single Ipsilateral Regional Adenopathy To	N1-3	D1
Bilateral Multiple Pelvic Adenopathy		
Distant Metastases	M1	D2

*(Quoted from Zafar et al., 2005).*

## II. Tumor-like lesions and other causes of mural thickening

### A. Chronic inflammation and special forms of cystitis

Chronic cystitis may result in a number of structural and pathological changes. There may be gross wall thickening, reduction in bladder capacity (*Kabala et al, 2003b*). There is more extreme heaping up of the epithelium with the formation of red, friable, granular, sometimes ulcerated surface. When there is ulceration of large areas of the mucosa, or sometimes the entire bladder mucosa, this is known as ulcerative cystitis (*Cotran et al., 1999*).

Several special variants of cystitis are distinctive by either their morphologic appearance or their causation:

#### Malacoplakia

Malacoplakia is clearly related to chronic bacterial infection, mostly by *E. coli* or occasionally *Proteus* species. This designation refers to a peculiar pattern of vesical inflammatory reaction characterized macroscopically by soft, yellow, slightly raised mucosal plaques 3 to 4 cm in diameter. It occurs with increased frequency in immunosuppressed transplant recipients (*Cotran et al, 1999*).

#### Focal cystitis

Focal cystitis may develop in response to chronic irritation, for example by a calculus, catheter or other foreign body or in association with paravesical disease, particularly diverticulitis, pelvic abscess and Crohn's disease. The resultant localized mural swelling may simulate a carcinoma (*Kabala et al., 2003b*).



## Tuberculosis

This usually arises due to hematogenous spread from the lungs, rarely from the gastrointestinal tract or skin. It is virtually always associated with renal tuberculosis. It produces irregular mural thickening which subsequently proceed to fibrosis. Calcification is present in approximately 10%, especially when there is extensive tuberculosis throughout the urinary tract (*Kabala et al., 2003b*).

## Schistosomiasis

The form of schistosomiasis affecting the urinary tract involves **Schistosoma haematobium**. In the bladder wall the eggs provoke odema and granuloma formation. Wall thickening (up to 1 cm or more) and single or multiple polypoidal lesions, which may be sessile or wave-like and may protrude into the lumen, are often shown. Changes are most marked in the region of the bladder base and trigone. Later, fibrosis and calcification develops. The condition predisposes to bladder cancer of any histological sort, particularly squamous cell carcinoma (*Kabala et al., 2003b*).

## B. Mechanical problems of the bladder wall

### 1. Trabeculation

A great variety of intrinsic and extrinsic diseases of the bladder may narrow the urethral orifice and cause partial or complete vesical obstruction. In the male patient, the most important lesion is enlargement of the prostate gland due either to nodular hyperplasia or to carcinoma. Vesical obstruction is somewhat less common in the female patient and is most often caused by cystocele of the bladder (*Cotran et al., 1999*).

In the early stages, there is only some thickening of the bladder wall, presumably due to hypertrophy of the smooth muscle. The mucosal surface at this time may be entirely normal. With progressive hypertrophy of the muscle coat, the individual muscle bundles greatly enlarge and produce trabeculation of the bladder wall (Cotran et al., 1999). The bladder wall often appears thickened and its inner aspect shows an undulating or ridged pattern. In severe outflow obstruction, saccules and later diverticula may develop (Kabala et al., 2003b).

## 2. Diverticula

These are focal herniations of the urothelium and submucosa through weak sites in the bladder wall (Kabala et al., 2003b). Diverticula may arise as congenital defects but more commonly are acquired lesions from persistent urethral obstruction. The increased intravesical pressure causes outpouching of the bladder wall and the formation of diverticula (Cotran et al., 1999).

Acquired diverticula are most often seen with prostatic enlargement producing obstruction to urine outflow and marked muscle thickening of the bladder wall. The congenital form may be due to a focal failure of development of the normal musculature or to some urinary tract obstruction during fetal development (Cotran et al., 1999).

Congenital diverticula usually originate just postero-lateral to the ureteric orifice (paraureteric diverticula) (Kabala et al., 2003b)

They are frequently multiple and have narrow necks located between the intervening hypertrophied muscle bundles. In both the congenital and the acquired forms, the diverticulum usually consists of a round to ovoid, sac-like pouch that varies from less than 1 cm to 5-10 cm in diameter (Cotran et al., 1999). They may become



larger than the bladder itself. They are prone to calculus formation, infection and occasionally malignancy (*Kabala et al., 2003b*).

### C. False bladder masses of prostatic origin

#### 1. Benign prostatic hyperplasia

Benign prostatic hyperplasia (BPH) is the development of nodular hyperplasia within the glandular tissue of the transitional zone of the prostate. It is essentially a disease of age, being present in 8% of males around the age of 40 years, up to 50% by the age of 60 years, and around 90% at the age of 90. Presentation is usually with of bladder outflow obstruction, increased wall thickness and the development of trabeculation and diverticula (*Kabala et al., 2003b*).

#### 2. Malignancy

In males, prostate cancer is the most common malignancy encountered and the second commonest cause of cancer-related deaths. The vast majority of prostate cancer is adenocarcinoma (*Kabala et al., 2003b*).

### D. Endometriosis of the urinary bladder

Endometriosis is a common benign gynecological disease, affecting 15-20% of women with a child-bearing potential, characterized by the presence of ectopic endometrial tissue outside the uterus. Involvement of the urinary tract, however is rare and seen in about 1 % of patients, the vesical location being the most frequent of these presentations (84%) (*Gupta et al., 2001*).

Broadly two different etiologies appear to exist causing vesical endometriosis, one

being spontaneous and the other post-Cesarean, In the former, the bladder lesion is a manifestation of the generalized pelvic disease, whereas after iatrogenic dissemination, growth of ectopic endometrium is usually limited to the bladder wall (*Gupta et al., 2001*).

Endometriosis of urinary bladder rarely occurs in postmenopausal woman without exogenous estrogen replacement (*Chen et al., 1996*).



## Technique of helical CT with post processing virtual cystoscopy

### Conventional cystoscopy:

Conventional cystoscopy was accepted as a gold standard in bladder (*Arslan et al., 2006*). It plays a key role in the diagnosis of urinary bladder tumours due to its capability to detect subtle alteration in mucousal texture and to allow direct resection with or without mucousal biopsy (*Prando, 2002*).

Conventional cystoscopy is a standard diagnostic approach for urinary bladder evaluation, its primary indication is the diagnosis of lower urinary tract disease, signs and symptoms that may be related to the urinary tract are evaluated using cystoscopy to directly visualize lower urinary tract anatomy and macroscopic pathology. However, this procedure has drawbacks, including its high costs and an invasiveness that may lead to iatrogenic bladder injury and urinary sepsis. There are several disadvantages of the conventional cystoscopy. It is often difficult to perform adequately when exploring the anterior bladder wall or a diverticulum cavity, diagnosis is often difficult with conventional method (*Arslan et al., 2006*).

There are some contraindications for the conventional cystoscopy such as bacteriuria, acute cystitis, urethritis, prostatitis, obstructive prostatic hypertrophy, and stricture or rupture of the urethra. Marked hematuria is another factor that limits the technical success of cystoscopy, thereby decreasing its reliability. On the other hand, cystoscopy is performed in general or local anesthesia and it is an invasive and

uncomfortable procedure for patients, and complications such as infections, uretral or bladder perforation, scarring, and stricture of the urethra have been observed (*Arslan et al., 2006*).

Furthermore, endoscopes display only the inner surface of hollow organs and yield no information about the anatomy within or beyond the wall. This limitation prevents evaluation of the transmural extent of tumors and limits the ability to localize the lesion relative to surrounding anatomic structures (*Jolesz et al., 2007*).

### **Different imaging modalities in the diagnosis and staging of bladder cancer:**

Regardless of treatment, correct clinical staging is paramount. It is well known that staging of bladder cancer by clinical methods alone (bimanual examination under general anaesthesia and transurethral resection biopsy) may under or over stage up to 50% of the patients. Thus, through the years, various imaging studies have, been used in an attempt to improve these statistics by providing information regarding wall invasion, extra-vesical spread, ureteric obstruction and extension to regional lymph nodes (*Putman and Ravin 1994*).

#### **1-Plain Radiography:**

Plain radiography may be first study to alert the radiologist to presence of a renal mass or bladder mass, although plain radiographic findings are nonspecific, particularly the presence of calcification, which has a wide differential, and they



usually contribute little to the diagnosis. Uncommonly, radiographically discernible areas of punctate calcification may be seen in TCC. The calcification is on the surface of the tumor and not within the mass duct. Intrinsic calcifications suggest an adenocarcinoma or the unusual cell type, Surface calcification of a bladder tumor may be seen on plain radiographs in 1% of cases. Osseous expansive destruction or lung metastases may be seen (*Khan et al., 2007*).

Preliminary plain radiography can detect bony metastases. Also, in the bilharzial bladder complicated by carcinoma, the plain radiography may suggest the correct diagnosis. The calcification of the wall of the bilharzial bladder usually appears as a continuous curved line of calcification, either smooth or irregular in contour depending on the state of dispensability of the bladder. With the development of cancer in that bladder, the neoplasm interrupts the continuity of the linear calcification. Calcification can occur on the surface of the bladder tumor; it has a stippled appearance or appears as a dense or even a calcified nodule in the bladder region (*Elkin, 1980*).

## **2- Intravenous urography (I.V.U):**

Intravenous urography (IVU) is a common diagnostic test in patients with hematuria, although the early detection of small urothelial tumors may be difficult. A meticulous IVU technique is required (*Khan et al., 2007*).

The IVU should be performed before diagnostic cystoscopy to provide information related to the bladder as well as upper tracts abnormalities referable to the bladder including hydronephrosis, non functioning kidney, lack of bladder

distensibility and filling defects. It should be noted that filling defects or deformities in the underfilled bladder provide little diagnostic information (*Smith et al., 1990*).

Non-function of the renal unit may result from neoplastic obstruction of its uretero-vesical junction. Demonstration of a fungating or polypoid mass protruding into the lumen and causing a filling defect in the opacified bladder is pathognomonic for bladder neoplasms (*Hahn, 1990*).

Bladder TCC shows an irregular filling defect with broad base and fronds. Increased thickness of the bladder wall in the region of the tumor should indicate infiltration, SCC is radiographically indistinguishable from TCC; however, SCC is less likely to be a polypoid tumor. Although a diagnosis may be made on the basis of urograms or cystograms, a small bladder tumor, especially one of the infiltrative types, can remain undetected. Occasionally, contrast material may be trapped within a blood clot formed in the ureter and then extruded into the bladder as a stringy mass that may trap contrast material in an irregular fashion. However, this entrapment is coarser than that seen with neoplastic stippling. Fungus balls or mycetoma may also occasionally entrap contrast material, but the pattern of entrapment is lamellar and frequently associated with gas formation (*Khan et al., 2007*).

Fixation of the bladder wall (lack of distensibility and collapsibility) suggests extension into the muscularis and hence a more advanced stage of bladder neoplasm (*Hahn, 1990*).

Despite of numerous attempts to increase the accuracy of urography and cystography with the use of multiple oblique projections, post-void films and double-contrast studies, only about 60% of bladder tumours are detected. This is due to in



part to the fact that many bladder tumours are small when first coming to clinical attention (due to haematuria and irritative symptoms) and they are frequently located on or near the trigone, which is difficult to visualize radiographically. Cystography, therefore, may also give an inappropriate sense of security because of its high false-negative rate (*Putman and Ravin, 1994*). Furthermore, a dense concentration of contrast material may obscure the intraluminal part of the urothelial tumor (*Khan et al., 2007*).

Traditionally, an excretory urogram (intravenous pyelogram IVP) is performed first to identify the cause of clinical symptoms. If a mass is found and cystoscopic biopsy confirms cancer, a staging workup follows. However, several problems exist with this regimen. Excretory urography may actually fail to detect as many as 75% of bladder lesions smaller than 5 mm (*Sen and Zincke, 1984*).

Retrograde pyelography is useful when the kidney cannot be visualized by means of IVU or when IVU cannot be performed because of renal disease or an adverse response to the contrast agent. Retrograde pyelography also has the advantage that it can be combined with various biopsy techniques (*Khan et al., 2007*).

With the recent introduction of CT urography, the role of excretory urography in evaluating the renal collecting system and ureter has been challenged (*Kawashima et al., 2004*).

### 3- Ultrasonography (U/S):

Bladder US is performed using a transabdominal, endorectal, endovaginal, or endourethral approach (*Skucas 2006*). Non invasive trans-abdominal ultrasound is seldom used today because it is inaccurate in the assessment of tumour spread beyond

the bladder wall and visualization of the tumour is often obscured in obese patients and by air containing bowel loops adjacent to the bladder wall. Further problems related to inaccessibility of tumours arising in the region of the bladder neck and to the evaluation of lymph node metastasis (*Richareds and Jones, 1998*).

Ultrasonography is unable to distinguish malignant tumour from chronic cystitis, local hypertrophy or blood clots (*Dershow and Scher, 1987*). On sonograms, calculi may be confused with high-grade Transitional cell carcinomas, which can be densely echogenic (*Khan et al., 2007*).

Bladder tumours appear on ultrasound as echogenic lesions. The bladder wall has a more Intense echo pattern than tumour tissue, thus permitting distinction of early superficial lesions from those invading the deep layers of the bladder wall. However, tumours involving the superficial muscle can not be distinguished accurately from tumours involving the deep muscle (*Dershow and Scher, 1987*).

Ultrasonography is inaccurate for diagnosing early TCC, and it is useful in the diagnosis of obstructive uropathy. Ureteric lesions are particularly difficult to visualize unless they cause hydronephrosis and hydroureter. The other limitation of ultrasonography is that it is inaccurate in the staging of bladder TCC, particularly Ta and T1 tumors, and also in detecting pelvic lymph-node involvement (*Khan et al., 2007*).

Transurethral ultrasonography is the most valuable in determining the stage of tumour confined to the bladder wall. Also, it is of value in detecting tumour in a diverticulum and monitoring the distensibility of the bladder wall and transurethral resection of disease (*Koraitim et al., 1995*).



Color Doppler US detects ureteral jets and with unilateral ureteral obstruction, Doppler US reveals asymmetry to these ureteral jets. The presence of normal ureteral jets excludes significant obstruction (*Skucas 2006*).

3D US is a promising, alternative noninvasive technique for use in the detection of bladder tumors and its localization and perivesical spreads. The location, size, and morphology of the tumors shown on 3D US images were in good agreement with the findings of conventional cystoscopy (*Kocakoc et al. , 2007*).

#### **4-Magnetic Resonance imaging (MRI):**

Although several recent studies have shown MRI to be more accurate than CT in staging bladder neoplasms, most of the improvements are result from the increased detection of superficial or small bladder neoplasms on dynamic Gd-enhanced MR images information readily obtainable through cystoscopy (*Saito et al., 2000*).

MRI has the advantage of high intrinsic soft-tissue contrast, its direct multiplanar capability, and the availability of nontoxic renally excreted contrast agents. MRI appears to be at least as useful as CT in the evaluation of perivesical fat involvement, and it may be superior to CT in the detection of invasion of the adjacent organs. However, MRI cannot depict superficial invasion of the upper urinary tract TCC wall (*Khan et al., 2007*).

MRI is expensive and has limited availability. False-positive diagnosis has been reported. In staging bladder TCC, tumor extension is overstaged according to the

TNM classification in 7.5% of patients and understaged in 32.5% of patients (*Khan et al., 2007*).

The multiplanar and soft tissue characterization capabilities of MRI make it a valuable tool to image the urinary bladder. In addition to different imaging planes, recent advances of MRI such as fast imaging, pelvic phased array coil and dynamic Gd-enhanced technique improve the imaging quality and diagnostic accuracy for staging urinary bladder carcinoma (*Tsuda et al., 2000*).

Initial results with MR-lymphography show a promising sensitivity (85%) in the detection of nodal metastases of bladder cancer (*Pieterman et al., 2000*).

MR urogram is used to assess the multifocal carcinoma in the urinary bladder, ureters and renal pelvis (*Barentsz, 2002*).

### **5-Scintigraphy:**

Although nuclear medicine such as ilio-pelvic lymphoscintigraphy generally lack the resolution needed for localized staging of bladder cancer, bone scans have been used routinely in some institutions to evaluate bladder tumour patients for disseminated disease prior to cystectomy. Recent data would suggest, however, that in the presence of a normal history (no bony pain) and physical examination as well as normal serum alkaline phosphatase, routine pre-operative bone scanning is unnecessary (*Scattoni et al., 1996*).

Some workers have advocated the use of renal nuclear medicine studies in the follow up of patients with bladder cancers as an adjunct to routine cystoscopy to rule



out upper tract obstruction in high-risk cases. However, it would seem more prudent to follow these patients with intravenous urography and/or retrograde pyelography to exclude additional urothelial tumours, which develop in 5 % of upper collecting systems of patients with bladder carcinoma. Provided that the uretero-ileostomies are refluxing anastomoses, periodic loopograms should also be performed in patients with cystectomy for the same reason (*Oliff et al., 1989*).

### **6-Angiography:**

Because 90% of all bladder tumours have striking neovascularity, it is not surprising that angiography at one time was used in evaluation of patient with bladder cancer. However, since the advent of Ultrasound, CT and MRI there seem to be little reason to persist in using invasive angiographic procedures in evaluation of bladder carcinoma. Nevertheless, angiographic therapeutic embolization is occasionally the treatment of potentially life-threatening bladder haemorrhage from these very vascular tumours (*Wolf et al., 1995*).

Angiography has no role in the diagnosis of TCC, but it may have a role in preoperative planning, particularly when neoplasm sparing surgery is being considered. However, here also, CT angiography (CTA) and magnetic resonance angiography (MRA) are challenging the catheter studies. (*Khan et al., 2007*)

### **7-Lymphangiography:**

Studies correlating lymphangiography with pathologically determined stage have shown that approximately 25% of patients with B lesions, 30% of patients with C lesions and 65% of patients with D lesions will have positive

lymphangiograms. Therefore, bilateral pedal lymphangiography continues to be popular in some institutions because CT and MR imaging cannot exclude tumour involvement in normal sized nodes. Despite of the previously mentioned, there are false-negative and false-positive results. Lymphangiography can direct percutaneous lymph node biopsy (accuracy up to 95%), determine the response (or lack of response) to therapy and detect disease relapse because contrast remains in the lymph nodes for several months facilitating their follow up evaluation with plain radiographs (*Lerner et al., 1993*).

#### ***8-PET, SPECT, and Radioimmunosintigraphy:***

Conventional positron emission tomography (PET) is unsuitable for imaging bladder tumors because of its high urinary excretion. However, it is 67% sensitive, 86% specific and 80% accurate in detecting pathologic lymph nodes in patients with bladder cancer, which exceeds both CT and MRI (*Hain and Maisey 2003*).

#### ***9-Computed Tomography:***

Computed tomography was first introduced 30 years ago (Housefield 1973) and has since become an integral part of clinical practice. Because of rapid advances in technology few clinicians are aware of the scope and limitations of different types of scanners. This view describes the three main types of computed tomographic scanner that are used in routine clinical practice and discuss their use in the investigation of a wide range of different conditions. It also flags up differing views on the relative



merits of computed tomography versus magnetic resonance imaging (*Garvey and Hanlon, 2002*).

Computed tomography has low sensitivity for detection of small bladder lesions. For computed tomography to detect small bladder lesions optimal imaging conditions including adequate bladder distension and thin slice scanning must be satisfied. Therefore, negative findings on computed tomography warrant the performance of conventional cystoscopy in patients with hematuria (*Kim et al., 2002*).

Traditionally, a radiologist would look at the scanned images slice by slice. By mentally reconstructing the sampled information into a three-dimensional representation, he would judge on the health of the patient. This procedure requires the radiologist to have well-founded experience as well as a highly sophisticated understanding of human anatomy. To create a complete mental image of the patient structures, the radiologist has to take all available slices into account. It is obvious, that looking at hundreds of slices is way too time-consuming for a single patient (*König and Gröller, 2001*).

#### **Types and practical importance of computed tomographic scanners:**

##### **1-Conventional computed tomographic scanners:**

CT historically has had limited spatial and contrast resolution. Bladder tumours are too small to be seen, and their unenhanced attenuation is too close to that of normal bladder wall (*MacVicar 2000*).

Conventional scanners have some limitations. The scan time is slow and scans are

prone to artifact caused by movement or breathing. Scanners have a poor ability to reformat in different planes, studies of dynamic contrast are impossible and small lesions between slices may be missed. Often a conventional scanner is retained alongside a new scanner. Conventional scanners still have a role mainly in non-contrast examinations that do not require fast scanning for optimal vascular enhancement (*Garvey and Hanlon, 2002*).

### **2-Spiral (helical) computed tomographic scanners:**

The development of spiral CT scanning technology has been of great benefit in imaging. Spiral scanning involves continuous rotation of the x-ray tube and smooth passage of the patient through the scanner aperture. This enable the whole thorax (for example) to be covered rapidly within the time of a single breath-hold. Breathing artifact and misregistration of adjacent slices, a common problem with conventional single section CT are abolished. The speed of scanning also means that intravenous contrast agents can be deployed very accurately to maximize their effectiveness (*Whitehouse and Wright, 2003*)

Helical CT scanning is faster than the conventional technique and provides more information in the cranio-caudal axis. It yields continuous data with less respiratory or bowel motion misregistration. Helical CT scanning permits continuous imaging as the radiographic tube rotates around the moving patient, whereas conventional CT scanning is limited to a series of 360-degree slices through the stationary patient. A conventional CT scan can be conceptualized as a stack of slices, whereas a helical scan is a continuous helix (*Wood and Razavi, 2002*).

The aim of helical (spiral) CT is to obtain meaningful CT data as the patient

moves through a rotating continuous fan-beam exposure. Thus, a block of data in the form of a “corkscrew” or “helix” is obtained. If the table movement occurs at such a speed that during one revolution of the tube, the patient is moved by a distance equal to the slice thickness, a complete volume of tissue is examined, hence the term “spiral volumetric data” used (Grainger et al., 2001).

The selection of scan parameters in spiral CT is very similar to that in conventional CT scan. However, the only additional parameter to be selected in spiral CT is the “table feed” distance, which is the distance in millimeters covered by the table per one gantry rotation (360 degree). In currently, available helical CT scanners, the gantry rotation period is 1 second per single 360 degree. Thus, the value of table feed corresponds directly to the “table speed”.

**Table speed required scans length/scan duration (tolerable breath hold)**

The scan “pitch” used in some machines, is defined as the ratio of the table speed to collimator width multiplied by the gantry rotation period.

**Pitch table speed/ collimator Width x gantry rotation period**

An increase in helical pitch above 1:1 will increase scan coverage along the Z axis (the body’s longitudinal direction) at the expense of resolution (Rubin and Silverman, 1995).

Spiral scanning has several advantages. The scan time is much shorter than that of conventional computed tomography. Closely spaced scans are readily obtained, allowing good quality reconstruction in different planes. Lesions can be evaluated during different phases of contrast enhancement. Computed tomographic



angiography is possible, and the likelihood that a small lesion may be overlooked is less/smaller. Spiral tomography is a powerful diagnostic tool (*Garvey and Hanlon, 2002*).

Spiral CT was performed in each patient to obtain a total volumetric acquisition of the bladder to avoid the possibility of missing small infiltrating lesions (*Caterino et al., 2001*).

All spiral CT applications rely heavily on having a cooperative patient who will manage to keep perfectly still during the whole CT exposure. Any movement in the middle of a spiral exposure will negate many of the advantages (*Grainger et al., 2001*).

The first production spiral CT models had several technical limitations due to the limited tube anode heat capacity thus resulting in rather “noisy” images, limited volume coverage and prolonged x-ray tube cooling time delays. Furthermore, computer systems were unable to process the large amount of data coming from the detector arrays, which resulted in delays of image production and prolonged post processing times (*Grainger et al., 2001*).

Most of those problems have now been overcome by the production of high heat capacity x-ray tubes as well as rapid advances in computer hardware and software design enabling raw data handling with relative ease with online reconstruction of images. Moreover, computer workstations offer additional software manipulation tools for data visualization and analysis. These include multiplanar reconstruction capabilities, 3D reconstruction tools and most recently perspective internal rendering (e.g. virtual endoscopy) (*Grainger et al., 2001*).

.....  
**3-Multislice computed tomography:**

A recent refinement of spiral scanning is to replace the single bank of x-ray detectors with multiple rows of detectors, allowing several interlaced data helices to be acquired simultaneously. Multidetector or multislice CT allows larger volumes to be scanned with thinner sections and yet shorter scan times. The speed of scanning makes multislice CT well suited to the demonstration of vasculature and permits a shorter contrast medium injection, thus reducing contrast usage. The data sets produced are well suited to image post-processing, for example multiplanar reformat (MPR) in various planes, surface-rendered and maximum intensity projection (MIP) reconstruction, volume-rendered images and virtual endoscopy views (*Whitehouse and Wright, 2003*).

Multislice scanners generate an increased amount of data compared with single slice scanners, and in practice the throughput of patient is limited by the time taken to image and reconstruct these data. Computed tomography is generally superior to magnetic resonance imaging for the hollow viscera. Spiral scanning has enabled the development of computed tomographic fluoroscopy, providing real time imaging for intervention procedures guided by computed tomography. Most units that perform magnetic resonance imaging report a failure rate of 3-6% as a result of patients' claustrophobia or inability to keep still during the long scanning times, particularly in young or elderly patients. Multislice computed tomography, with its speed and capability of multiplanar reformats, can be substituted for magnetic resonance imaging in several clinical situations (*Garvey and Hanlon, 2002*).

With multidetector CT (MDCT) the entire abdomen and pelvis can be scanned with thin collimation. This technique results in high resolution images in the Z-axis

and the ability to obtain images in any plane. Increased spatial resolution may increase the ability to detect small bladder tumours (*MacVicar 2000*).

### **Role of computed tomography in bladder carcinoma**

CT is the imaging modality of choice for the workup of patients presenting with hematuria. It also indicated in patients with high-grade bladder cancer raising suspicion for muscle invasion. Routine contrast enhanced CT examinations are useful for detecting metastasis, but they may be inadequate for detecting and staging local urothelial lesions. In the setting of hematuria, CT urography (CTU) can be used as a one-stop-shop examination to evaluate the entire urinary system and diagnose possible causes of hematuria, including lithiasis, other benign etiologies, renal parynchmal lesions, and urothelial neoplasms, thus eliminating the need for additional imaging. (*Kawamoto et al., 2006*).

In the presence of urothelial tumour, the detailed evaluation of the entire urinary system provided by CTU is essential, as patients with urothelial tumour may have multifocal disease. In terms of cancer staging , CTU can detect direct perirenal, periureteral, and extravesical tumour spread, as well as lymphadenopathy and distant metastases. Compared with traditional excretory urography, CTU requires a shorter examination time and has greater accuracy for detecting urothelial lesions (*Caouli et al. 2005*). CTU also allows more detailed evaluation of the renal parynchma and perirenal tissues and permits better evaluation of obstructed collecting systems than does excretory urography (*Browne et al., 2005*).

Therefore, for evaluating urinary tract neoplasms and the work-up for hematuria, CTU is the imaging modality of choice for patients who can tolerate iodinated



intravenous contrast. The advantages of CTU are made possible by multidetector helical CT with volumetric acquisition of high-resolution images and allows multiplanar reconstruction (Zhang et al., 2007).

The commonly recognized presentations of TCC (transitional cell carcinoma) on CT scans include the following: irregular filling defects of the pelvicalyceal system and ureters, which tend to be associated with obstruction and dilatation of the ureter and pelvis proximal to the lesion; ureteral wall thickening; frondlike growth projecting into the bladder from a fixed mural site; and surface calcification of bladder TCC. On non-enhanced CT scans, the TCC is hypoattenuating or isoattenuating relative to the normal renal parenchyma, and it is hyperattenuating relative to urine. TCCs demonstrate mild-to-moderate enhancement after the administration of contrast material, and they become hypoattenuating relative to opacified urine (Khan et al., 2007).

Helical CT scan shows the blurred boundary between extravescical tumor and the bladder wall and a lack of fat space. Local bladder wall thickening combined with nodular or cauliflower-like mass protruding into the bladder is observed (Wang et al., 2004).

On CT examinations, bladder cancer may manifest various pattern of tumour growth along the bladder wall, including papillary, sessile, infiltrating, mixed, or flat intraepithelial growth (Tekes et al., 2005).

Focal, nodular soft tissue tumour or focal assymmetric bladder wall thickening may be evident. Occasionally, more superficial papillary tumours may project within the lumen of the bladder, with a narrow pedunculation arising from the bladder wall.

Retraction of the bladder wall may be present. Urothelial carcinomas have been shown to demonstrate increased vascularity on more angiographic studies, and, more recently, on contrast-enhanced CT (*Kim et al., 2004*).

When a neoplasm causes diffuse thickening of the bladder wall, it can be confused with cystitis, although the thickening is usually more uniform in the latter entity. Similarly, inflammatory (pseudotumour) of the bladder may present as a polypoid mass or focal wall thickening and therefore be indistinguishable from a bladder neoplasm on CT scans (*Gugliada et al., 1991*).

For local staging of bladder cancer, perivesical fat infiltration suggests transmural extension, or T3 disease. Recent TURBT, however, frequently causes linear or focal enhancement along the bladder mucosa or bladder wall, and at times bladder wall thickening, perivesical fat stranding, or fibrosis, thus limiting the specificity of CT. The reported accuracy in local staging of bladder cancer varies widely. Overall accuracy for local bladder cancer staging in the literature is near 60%, with a tendency to overstage (*Hall and MacVicar 2001*).

Accurate diagnosis of microscopic perivesical invasion (T3a disease) is particularly difficult. Various techniques have been investigated to improve local staging. In a cohort of 65 patients with staging grouped at less than or equal to T1, T2-T3a, T3b, or T4 disease, an accuracy of 91% was achieved by distending the bladder with contrast, and an accuracy of approximately 95% was achieved when the bladder was insufflated with air (*Caterino et al., 2001*).

More recently, sensitivity and specificity for perivesical invasion by CT, when performed 7 or more days after TURBT, were calculated at 92% and 98%,

---

respectively. But these decreased to 89% and 95%, respectively, in a larger number of patients without a delay between TURBT and CT (*Kim et al., 2004*).

According to Kim and colleagues, overall accuracy of 83% was achieved by CT for diagnosis of perivesical invasion (*Kim et al., 1994*).

For lymph node evaluation, the accuracy of CT ranges from 73% to 92%, with a tendency to understage nodal involvement, particularly when based on criteria for short axis nodal enlargement of near 1 cm (*Hall & MacVicar 2001*).

Currently, diagnosis of nodal metastases with CTU is based on anatomic size criteria; CTU has limited ability to detect normal-sized lymph nodes that harbor low-volume metastatic disease, or to differentiate lymph nodes enlarged by a benign process from those enlarged by metastatic involvement (*Deserno et al., 2004*).

Even subcentimeter perivesical nodes, particularly those that are rounded and avidly enhancing, may be noteworthy in patients with underlying bladder tumor, although they may be reactive. (*Hricak 2006*).

Nodes smaller than 1 cm in size usually are considered to be normal unless they are within the expected course of lymphatic spread. In these cases, CT-guided needle aspiration of the suspicious node is often performed, and the aspirate sent for cytologic examination. In the lymphatic spread from bladder cancer, the medial (obturator) and the middle groups of the external iliac nodes are often affected first, followed by the internal iliac and the common iliac nodes. Obturator nodal metastases are best seen on slices obtained 1 to 3 cm superior to the acetabulum (*Vinnicombe et al., 1995*).



Discovery and investigation of functional biologic targeted imaging markers likely will be a focus of future translational research to improve sensitivity and specificity in the staging of genitourinary tumors (*Hricak 2006*).

Distant metastasis tends to occur late in the clinical course of bladder cancer and especially at the time of recurrence, with bones, lungs, brain, and liver being the most common sites (*MacVicar 2000*).

Both conventional abdominal/pelvic CT and CTU, which may be combined with chest CT if needed, can be performed to detect distant metastases. CT also may suggest adjacent visceral invasion, although MR is superior because of better soft tissue contrast (*Zhang et al., 2007*).

One important consideration in performing CTU is radiation exposure, which is increased because of multiphase, thin-section imaging. One recent study calculated the radiation risk for standard three-phase CTU without adjustment of tube current factors and exposure technique for patient size to be approximately 1.5 times that of conventional excretory urography using standard threephase CTU imaging without routine adjustment of tube current factors and exposure technique for patient size (*Nawfel et al., 2004*).

Other studies have confirmed an approximate 50% to 80% radiation exposure increase with helical multiphasic CTU compared with conventional excretory urography (*Browne et al., 2005*).

This is an important consideration, particularly in young adult populations, given that overall cumulative lifetime exposure could be increased substantially in the setting of repeat surveillance examinations in a patient who has known underlying

pathology. Adjustment of tube current (tube potential, tube current–time product), scan pitch or length, and basing technique factors on patient size have been advocated as techniques to reduce overall exposure (*Nawfel et al., 2004*).

The density of a bladder neoplasm is similar to that of normal bladder wall on non-contrast scans but is higher than that of normal bladder wall immediately after bolus injection of iodinated contrast material. Calcification within the tumour may be seen on rare occasions. In one study, calcifications in transitional cell carcinomas were mostly on the surface of the tumour and nodular in appearance, whereas calcifications in mucous adenocarcinoma tend to be fine, punctate and scattered throughout the mass (*Moon et al., 1992*).

### **Post processing techniques:**

Helical CT, with high scanning speed, can provide high quality multiple-phase dynamic axial images, multiplanar reformation (MPR) and three-dimensional (3D) reconstruction images. It has been widely used in clinical applications with encouraging results (*Wang et al., 2004*).

#### **1. Multiplanar reformations (MPR):**

The stack of overlapping axial slices can be reconstructed along any desired plane by using a multiplanar reformation algorithm. The resulting multiplanar reformatted images are excellent for displaying anatomic relationships that vary along any single arbitrary direction (*Rubin and Silverman, 1995*).

Multiplanar views allow imaging of the curved bladder wall in such a way that cross-sectional images can be obtained perpendicular to the wall (*MacVicar*

2000).

## 2. Volume rendering technique (VRT):

The recent introduction of fast computer graphic workstations has enabled volume rendering tools to be developed that can be applied to helical CT data sets. A histogram of the pixel values in the volume is analyzed and the tissues are then assigned color, transparency and refractive index values depending on the information desired from the data set (*Rubin and Silverman, 1995*).

### • Virtual endoscopy:

Recently, three-dimensional computer-rendering techniques with rapid image acquisition have led to the development of virtual-reality imaging. With commercially available software, virtual reality imaging allows interactive intraluminal navigation through any hollow viscus, simulating conventional cystoscopy. This technique of virtual endoscopy has been applied to many organs, including the colon, bronchus, stomach, and bladder (*Arslan et al., 2006*).

The urinary bladder is a good candidate for virtual cystoscopy because of its simple luminal morphology, its relatively small volume, and the absence of involuntary peristalsis. Therefore, a virtual cystoscopic rendering of the bladder takes a short time to navigate and does not require great skill on the part of the operator (*Arslan et al., 2006*).

Virtual endoscopy is a recently developed noninvasive method to detect tumors protruding from the walls of hollow organs. A promising advantage of this imaging modality is that views not possible in conventional endoscopic examination can be



created. The volumetric data obtained with helical CT or MR imaging are computer-rendered to generate three-dimensional images, and with commercially available software, intraluminal navigation through any hollow viscus is possible (*Arslan et al., 2006*).

Several factors have contributed to virtual endoscopy accelerated growth: introduction of multislice CT (MSCT), development of powerful computers, and the commercial availability of software. Multislice CT is emerging as a preferred virtual endoscopy scanning method because of its incredible short scan time (often less than 30 seconds) and potential for reduced radiation (*Vining, 2002*).

There are two main techniques for the reconstruction of virtual image. One of them is volume rendering and the other is surface-rendering algorithm. Of the different three-dimensional rendering techniques available, the perspective volume rendering provides more information because the entire data set is incorporated (*Arslan et al., 2006*).

A high “visual gradient” is required between the visceral lumen and wall structures to allow differentiation of these structures, depending on the selection of a suitable threshold value (*Merkle et al., 1998*).

The chief requirement to create an adequate endoscopic view is a sufficient attenuation difference (image contrast) between the voxels to be viewed and those comprising the viewpoint. In the urinary bladder, distension with air, and potentially with iodinated contrast, can be used to achieve such image contrast (*Fishman and Jeffrey, 1998*).

These examinations were saved in cine-loop mode and viewed from the

workstation monitor for interpretation (*Hussain et al., 1997*).

As a minimally invasive procedure, virtual CT cystoscopy provides many advantages as compared to conventional cystoscopy. The virtual CT cystoscopy images could be stored in file and the lesion could be compared in follow up period with based images. The size of a tumor is measured objectively. Access to the anterior bladder wall or the lumen of a diverticulum is not restricted in virtual cystoscopy because various software reconstruction tools can be used and the tumor can be easily detected (*Prando 2002*).

Patients with a severe urethral stricture or marked prostatic hypertrophy, who may be poor candidates for conventional cystoscopy, can safely undergo virtual CT cystoscopy. It is also indicated for patients who are at risk of complications such as hemorrhage, perforation, infection, or pain, and for the examination of young patients (*Arslan et al., 2006*).

It was very difficult to differentiate the polyp without setting the threshold density value. This also showed us that axial images and virtual cystoscopy images should be evaluated together (*Arslan et al., 2006*).

### **Technique of virtual cystoscopy by helical CT:**

- **Preparation:**

Careful preparation of the patient is of particular importance:

- **Bowel preparation:**

*Sutton et al. in 2003*, used 40 ml of a water soluble iodine-base contrast diluted to 1

liter with fruit squash taken orally half an hour prior to the scan. A further 1 liter of dilute oral contrast is taken 4 hours before the scan to image the large bowel and rectum. Alternatively, the same contrast can be administered immediately before the scan as an enema.

Virtual cystoscopy may be performed in several ways, including instilling gas and/or iodinated contrast material into the bladder prior to CT scanning (*Vining, 2002*).

#### **A- Virtual cystoscopy of the air-filled bladder:**

This method assures about 1000 HU of difference between the wall and the lumen, and also provides an optimal distension of the bladder. The sensitivity and specificity with this technique are 94–97% and 98–100%, respectively (*Scardapane et al., 2007*).

In air VC the bladder can be expanded to almost the maximum capacity, whereas in IVU VC the bladder expansion depends on the maximum desire to void of each patient, i.e. in IVU VC the bladder may not be expanded to its maximum capacity, in which case folds on the bladder wall may obscure small tumours (*Kawai 2004*).

The air virtual cystoscopy technique consists of three general steps:

##### **1. Patient Preparation:**

VC with multislice CT began by placing a 12 F Foley catheter into the bladder to drain residual urine. The bladder was then insufflated with 300–500 ml of carbon



dioxide or air through the Foley catheter, according to the patient's tolerance, and was followed by helical CT. (*Kawai et al., 2004*).

## 2. Data Acquisition:

After a scout view is obtained with the patient in the supine position to locate the bladder and confirm its adequate distension, single breath-hold helical CT is performed, with 3 mm collimation (section thickness), pitch of 1:1, 110 - 120 KVP, 70- 230 mA. Images are reconstructed at 1-1.5 mm intervals by using the minimal field of view (*Song et al., 2001*).

The patient is then turned to the prone position, Additional bladder distension with approximately 100 ml of CO<sub>2</sub> is necessary in about half of the patients, since repositioning may lead to leakage of some of the insufflated gas from the bladder. Adequate bladder distension is required for optimal evaluation; imaging in both positions is necessary for visualization of the entire mucosal surface without obscuration caused by residual urine and helical CT of the bladder is repeated with use of the same parameters after a repeat scout view is obtained. (*Song et al., 2001*).

**Kawai et al., in 2004** used a helical CT scanner, which has 16 rows of detectors and better information processing capabilities than the original multislice CT devices. CT used 0.75-mm collimation, a pitch of 6. Slices for transverse-image diagnosis, The scan conditions were 12 kV, 240–260 mA and 0.8 s/rotation, Slices for reconstructing three dimensional images were 1.25-mm wide with a slice interval of 0.8 mm.

The data is downloaded to an independent workstation equipped with software for interactive intraluminal navigation (*Song et al., 2001*).

### 3. Postprocessing:

There are two main techniques for the reconstruction of virtual image. One of them is volume rendering and the other is surface-rendering algorithm. Of the different three-dimensional rendering techniques available, the perspective volume rendering provides more information because the entire data set is incorporated (Arslan et al., 2006).

The data are reviewed on a 3D computer workstation using a combination of 2D and 3D imaging techniques including virtual cystoscopy (Mang et al., 2003).

The first step towards surface rendering is segmentation. For the virtual endoscopic presentation, thresholding may be applied where a voxel is classified based on the signal intensity of the original data. For example, for CT voxels with a Hounsfield number equal to 200 are considered bone, while those below 400 are considered air (Jolesz et al., 2007).

A sense of depth, distance, and motion can be achieved by also using a perspective algorithm (perspective volume rendering). This algorithm is a computer graphics technique that causes the object to grow larger as the observer approaches. When combined with real-time viewing (5-30 frames per second), use of this technique conveys the effect of traveling through the bladder lumen in vivo (Fenlon et al., 1997).

#### **B- Virtual cystoscopy of the contrast material-filled bladder:**

Opacification of the bladder by iodinate urine in the late excretory phase, achieving sensitivity and specificity rates ranging between 90–95% and 85–87%, respectively (Scardapane et al., 2007)

**Fishman and Jeffrey in 1998** used a contrast-enhanced study with intravenous administration of 100 ml of Omnipaque-350 injected at a rate 2cc/sec with a scan delay of 50 seconds. The scanned area started from the mid-symphysis pubis to the diaphragm in a caudo-cranial direction (to ensure coverage of pelvic organs during peak vascular opacification which is critical for differentiating iliac blood vessels from lymph nodes) with a slice thickness and interval of 3-5 mm, and a pitch of 1.6. After

A scout view was obtained to locate the bladder and confirm its adequate distension, single breath-hold helical CT was performed with a scan length of 20-25 sec, collimation (slice thickness) of 3 mm, table speed of 3-5 mm/sec, a pitch of 1:1 and a 512 x 512 matrix. CT exposure factors varied between 110-120 KVP, 120-220 MA.

**Merkle et al. in 1998** examined 12 patients using a different technique where CT scanning of the pelvis was performed in three phases: (a) unenhanced scan with an adequately full bladder, (b) in the arterial phase during intravenous injection of contrast medium (150 ml Solutrast 300), with a flow rate of 3ml/s and a delay of 50 seconds and (c) after a delay of 30 min.

During the delay period, patients were instructed to move about to avoid possible sedimentation of the contrast medium in the bladder. Bed ridden patients, on the other hand, were moved several times from a right to left lateral position at the end of the delay period. Datasets from the three examination phases were processed and compared with the findings of fibre-optic cystoscopy and pathology. They reached results that the delayed study phase was the optimal phase for virtual cystoscopy.

Based on the unenhanced helical CT examination, virtual cystoscopy was possible in only one of the 12 patients since the difference in CT-measured attenuation between



the vesical mucosa and urine was in most cases insufficient to obtain a continuous network structure based on a single threshold value. Intravenous contrast medium increased the CT attenuation of the mucosa, resulting in a sufficiently high degree of contrast in some cases, because non-tumorous portions of vesical mucosa show no more than minor enhancement. Furthermore, "hole artifacts" frequently occur because the bladder wall is often very thin. The best "visual gradients" are obtained by waiting for the renal elimination of injected contrast medium. With this technique it was possible to generate a virtual cystoscopy in real-time (10 images per second) and delineate the intravesical tumour in less than 1 hour. The data processing resulted in a 3D representation of the bladder surface which could be examined interactively using the computer mouse for guidance of the endoscope (Merkle et al., 1998).

**Nambirajan et al., in 2004** used the following method: Patients had helical CT of the abdomen and pelvis with a slice thickness of 5 mm, after an intravenous injection with 100 ml of Iohexol 300 at 3 ml/s. This was followed by a delayed scan, 60 min after injection with contrast medium. During the delay, patients were instructed to move around, with the intention of avoiding sedimentation of contrast medium in the bladder. If the patient could not hold urine for this duration they were instructed to void but not to empty the bladder completely. The delayed images were obtained as a single breath-hold helical scan, using 120 kV, 250 mA, 3 mm collimation and a pitch of 1 (the ratio of table speed or subject movement to collimation or section thickness).

Images were reconstructed at 1-mm intervals. These delayed images were used to reconstruct the VC images; the data were downloaded to an independent workstation equipped with software for interactive intraluminal navigation. The threshold was

optimized for each case to obtain complete visualization of the bladder wall with no artifacts (Nambirajan et al.,2004).

Kim et al in 2005 used a contrast-enhanced study with intravenous administration of ultravest 300 or iopamiro 300 into an antecubital vein by a power injector at a dose of 2 ml/kg of body weight at a rate of 3 ml/sec to a maximum of 160 ml with a scan delay of 100-120 seconds & delayed scanning dedicated for bladder evaluation. The CT scanning covering the entire urinary tract through covering the abdomen and pelvis, After the first two scans were obtained, the delayed CT were performed when the patient felt a desire to void ( 90 – 140 min. after IV injection of contrast material), Then the patient was asked to alternately take a supine and prone positions four times to obtain adequate mixing of contrast material with urine in the bladder, thereafter CT scans were obtained with the patient in a supine position.

Immediately after completing this CT examination, the technicians in the CT room decided whether the contrast material and urine were adequately mixed in the bladder. Adequate mixing was indicated when high attenuation filled the entire bladder lumen homogeneously and there was no fluid-fluid level caused by unopacified urine. Scanning parameters for this examination included a beam pitch of 0.75, a detector array of 4 x 1.25 mm, a table speed of 15 mm per rotation, a reconstruction interval of 1 mm, an X-ray tube voltage of 120 kVp, and a tube current of 210-240 mA. The scanning covered the entire area of the urinary bladder.

The CT data were transferred to a workstation for reconstructing virtual cystoscopy and multiplanar reconstruction images

To systemically indicate the location of bladder lesion, we identified areas of the

bladder wall by evenly dividing the bladder wall into six sites, including anterior, posterior, superior, inferior, right, and left sites. The presence of a bladder lesion (positive finding) was indicated when either a surface irregularity or a polypoid lesion was noted. In addition, color change of the bladder mucosa on cystoscopic findings or focal wall thickening on multiplanar reconstruction or source CT images was regarded as a positive finding.

**Zhang et al., in 2007** performed CT urography (CTU) without oral contrast, using combined intravenous nonionic iodinated contrast (150 ml at 2.5 ml/s in a patient with normal renal function) and saline bolusing (400 cc). Thin-section precontrast, postcontrast, and delayed excretory phase images are obtained.

Postcontrast images typically are performed during the renal parenchymal phase (approximately 90 seconds after initiation of the intravenous contrast injection), and they cover the entire abdomen and pelvis. These images are helpful in the identification of enhancing urothelial lesions.

The excretory phase images (typically achieved with a scan delay of 10 minutes or more) provide substantial additional information, both in confirming enhancing lesions as true lesions and not pseudolesions related to focal opacified urine arising from a ureteral jet within the bladder lumen, and in demonstrating discrete filling defects caused by tumor not evident on earlier scans. If the urinary tract is not well distended and opacified with contrast throughout its entire course, then additional delayed images may be acquired targeting the nonopacified portion up to two times,

Images are transferred to a workstation for three-dimensional post-processing. Different image postprocessing algorithms either volume rendering of entire data set, or



reconstruct IVP-like projectional images are available for CTU to provide three-dimensional visualization of the urinary tract. The major role of postprocessed images is to provide a general overview of the anatomy and accentuate the areas of abnormality.

**C- Virtual cystoscopy of combined air distention with intravenous contrast injection :**

Coupled pneumo-CT cystoscopy with I.V. administration of contrast medium. With this protocol we always achieved optimal bladder distension, an adequate depiction and enhancement of bladder lesions. Furthermore, I.V. injection of contrast medium permitted visualization of the tumor extending into the terminal ureter, which appeared dilated in unenhanced scans. The presence of contrast enhancement was a very sensitive index for malignancies (*Scardapane et al., 2007*).

**Wang et al., in 2004** used the following method: Prior to the scan, adequate filling of the bladder with CO<sub>2</sub> or air was required. The precontrast helical CT scanning of pelvis was carried out, with collimation being 10.0 mm and pitch 1.0. After precontrast scanning, all patients received 80-100 ml contrast medium administered by a power injector at a rate of 2.0-2.5 ml/s. The scanning at arterial, venous, equilibrium and excretory phases were conducted, with collimation being 310-5.0 mm, pitch 1.0-1.5 and the delay time 20-25 seconds, 30 seconds, 60 seconds and 30 minutes respectively.

The images were reconstructed at a 1.0-2.0 mm interval using standard algorithm. The reconstructed images of excretory phase were transferred to an Advantage Windows 3.1 workstation, and the following images of the bladder were processed: (1) MPR: the coronal, sagittal and curved MPR images were done in all cases; (2) 3D reconstruction:

the shaded surface display (SSD) and RaySum 3D reconstruction were acquired; and (3) CT virtual cystoscopy (CTVC): using Navigator smooth virtual endoscopy software, CTVC images were obtained, and pseudocolor was added to simulate the normal tissue color in vivo. The processing time was 30-40 minutes.

*Arslan et al., in 2006* started virtual cystoscopic examinations with obtaining adequate filling of the bladder with approximately 250-450 ml of air was required. At the same time, IV 100 ml contrast medium was administered in all patients by a power injector at a rate of 2.0-2.5 ml/s for possible extravesical invasion of the tumor or some other pathology in supine position.

Helical CT was performed with 4 channel CT scanner in single breath hold, with 1 mm collimation, 1 mm reconstruction interval and 3 mm thickness. Other scanning parameters were as follows: 1 mm reconstruction interval, mAs 153, and 120 kV, feed/rotation 5 mm. The scanning time was only 8-12 second.

The patients were then turned to the prone position, and CT of the bladder was repeated with use of the same parameters after a repeated scout view was obtained. Additional bladder distention with approximately 80-120 ml of air was necessary in some of the patients, since repositioning led to leakage of some of the insufflated gas from the bladder.

The data were downloaded to an independent workstation equipped with software for interactive intraluminal navigation. Using multiplanar reformation from source images, a central observation point was defined in the middle of the lumen of the bladder. The camera for virtual cystoscopy was placed in the center of the bladder lumen

and thereafter was advanced to each quadrant in turn. When a possible abnormality was discovered, it was fully evaluated from various angles.

*Scardapane et al., in 2007* used this method: Just before the CT exam a 12-F urinary catheter was positioned and the residual urine was accurately drained. Then the bladder was distended with 200–350 cm<sup>3</sup> of room air according to patient tolerance. Pelvic unenhanced scans were acquired in supine position using a multislice scanner and the following protocol: thickness 2.5mm×4 mm, image index 0.6 m, pitch 1.25 and tube rotation time 0.75 s. If the urinary air–fluid level was visible in unenhanced images, the bladder was deflated to eliminate the residual urine, and re-distended just before uroangiographic contrast injection.

Enhanced abdomino-pelvic scans were obtained with the same scan parameters; 120–130 ml of nonionic uroangiographic contrast medium were administered intravenously using a power injector at a rate of 3.5–4 ml/s and a 40 s scan delay. A final scan was obtained in the pyelographic phase, after 7–10 min delay, for upper urinary tract visualization.

Finally, all the volumetric datasets were transferred to a workstation, where Multi Planar Reformatting (MPR) and virtual cystoscopy images were obtained.

#### **D- Virtual cystoscopy with color mapping of bladder wall thickness:**

*Schreyer et al., in 2000* used no oral or intravenous contrast agent prior to scan. Then a 12 French Foley catheter is placed in the bladder, all urine drained and the bladder is insufflated with approximately 300 cc room air or to tolerance. Three cc radio-opaque contrast medium is instilled through the Foley catheter to make urine produced during the scan discernible from the bladder wall. Using a scanner,



applying 280 mA with 120 KVp and the smallest field of view to fit, the images are acquired with 3 mm collimation and a pitch of 1.0. Reconstruction is performed at 3 mm increments. The data are transferred to a workstation. To improve the computation performance the slice resolution is reduced from 512 X 512 to a 256 X 256 pixel matrix. The next step is the segmentation of axial images, which is mandatory for surface reconstruction and thickness determination.

Thickness is defined as the shortest distance between a voxel on the inner wall to any voxel on the outer wall. To compute the wall thickness algorithm first identifies the contour for each wall by traversing the boundary of the segmentation independently on each slice. Once the thickness has been identified for each voxel on the bladder walls, the thickness values are stored in the updated contour files (*Schreyer et al., 2000*).

Using this technique a quantitative thickness value for each matched set of contour points is calculated with minimal artifact formation. By setting a color scale for the thickness information we can visualize the surface model with different colors representing different wall thickness. The scale width is restricted from 0 mm to 15 mm thickness represented by colors from red to blue. The color mapped three-dimensional model of the bladder including the urethra and ureters is imported into a virtual endoscopy program. In a reference window the camera position is represented by a pointer in the cross-sectional slice. A realtime free flight through three-dimensional reconstructed urinary bladder is feasible using three different mouse buttons for rotating the virtual camera, moving forward and backward and moving the position of the object (*Schreyer et al., 2000*).

**Fielding et al., in 2002** use this technique after voiding a 12 Fr balloon catheter was inserted into the bladder of each patient. The balloon was inflated with 5 cc saline. Residual urine was withdrawn. There were 2 cc diatrizoate meglumine and diatrizoate sodium instilled into the bladder to opacify incoming urine. With a standard barium enema, hand pump air was insufflated into the bladder to tolerance. Helical CT of the bladder was then obtained with the patient in the supine position. With a 120 kV. field of view to encompass the greater trochanter and maximum ma, axial images 3 mm. in thickness were obtained and reconstructed at 1.5 mm. increments. There were 3-D models of the bladder constructed with segmentation and advanced image processing techniques, Basically, the inner and outer surfaces of the bladder were manually outlined on each axial image. With these images an algorithm consisting of triangle decimation and marching cubes was used to generate 3-D renderings. The catheter, urethra and urethral orifice were identified as separate objects. Color mapping of wall thickness was performed with a computer algorithm, Bladder wall thickness was assigned a color according to a fixed and validated mm. scale, ranging from red (1 mm.) to purple (10 or greater). The color mapped renderings were then imported into an experimental virtual endoscopy program (Slicer), which allowed the viewing of inner and outer bladder surfaces. The analysis of 3-D renderings produced a blue or purple color indicating a region of wall thickness greater than 5 mm.

When 3-D renderings and axial source images were reviewed side by side, in many cases interpretation was revised usually because adjacent structures, such as the bowel or uterus, abutted the bladder making the exterior surface difficult to identify. This combined examination improved sensitivity and specificity for the tumors.

Average review time for 3-D renderings was 8 minutes for the examination of a positive case and 6 for negative.

**Jaume et al., in 2003** based this technique on comparison with a normal thickness atlas by using the following method consisting on five steps:

***A. Image Acquisition:***

A 12-French Foley catheter was inserted into the bladder, the residual urine drained, and the bladder insufflated with approximately 300 cc room air or to tolerance. The balloon of the catheter was inflated with 5 cc saline. To make urine produced during the scan discernible from the bladder wall, two cubic centimeters diatrizoate meglumine and diatrizoate sodium were instilled through the Foley catheter into the bladder. A 3-D CT image of the bladder was then obtained with the patient in the supine position. The resolution of the 3-D image was cubic millimeters.

***B. Segmentation Method:***

To segment the bladder wall, manually outlined the outer boundary of the bladder wall. the contrast in CT scans between wall tissue and other tissues is much smaller in comparison to air and tissue contrast which allows for automated segmentation of the inner boundary of the bladder wall. Therefore, a simple thresholding would not represent the bladder wall correctly. Thus, using a manual segmentation for the outer boundary of the bladder wall.

The appearance of the surface is coarse, but its accuracy is below the voxel size. Extracting the iso-surface from the CT scan without segmentation would create a



smoother surface. However, noise in the CT scan would create many handles, and the surface of the bladder would not be correctly defined.

***C. Thickness Estimation:***

To estimate the bladder wall thickness, computing for every vertex of the inner mesh its distance to the closest vertex of the outer mesh. The mesh discretization resulted in mesh vertices being separated by distances similar to the bladder wall thickness.

Thin regions of the bladder wall are color-coded in blue, while thick regions are color-coded in red.

***D. Atlas Construction:***

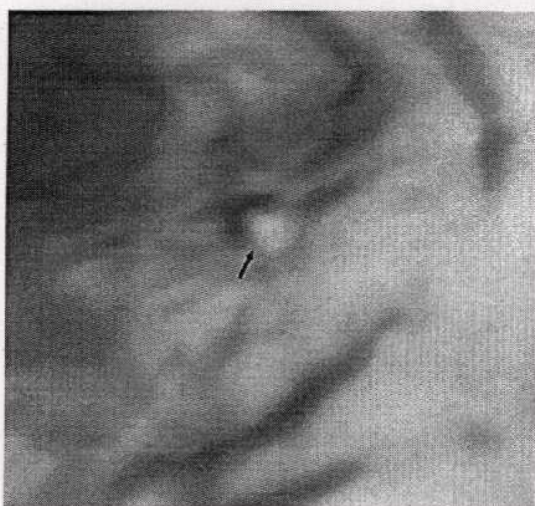
Bladder tumors are characterized by a thickening of the bladder wall. However, the thickness distribution varies over the bladder surface. Comparing the thick regions with a normal thickness map (*atlas*) to distinguish pathological thickness from normal thickness; The thickness variation is either larger at the top or at the bottom of the bladder.

***E. Measurement of Abnormality:***

Z score used to compare the bladder wall thickness to the normal thickness in the atlas. The Z score for a thickness value is the ratio without units characterizes the abnormality of the thickness.

Demonstration of bladder carcinoma:

I. Air distension virtual cystoscopy:

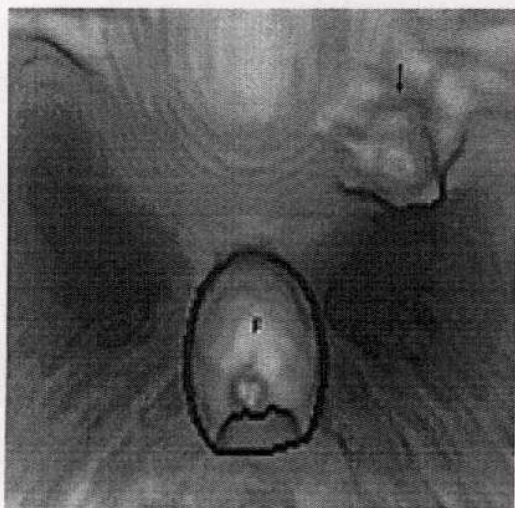


A

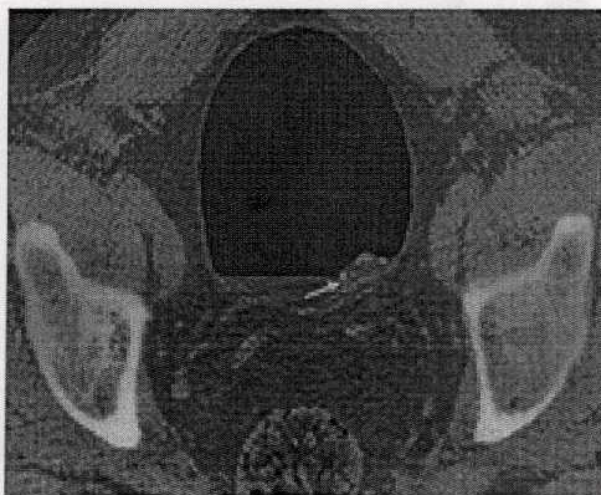


B

(Fig. 24 ) (A) Virtual cystoscopic image demonstrates a 4-mm polypoid lesion (arrow), a proved papillary transitional cell carcinoma, in the bladder neck. (B) The lesion was not seen on the transverse CT image. (Song et al., 2001).



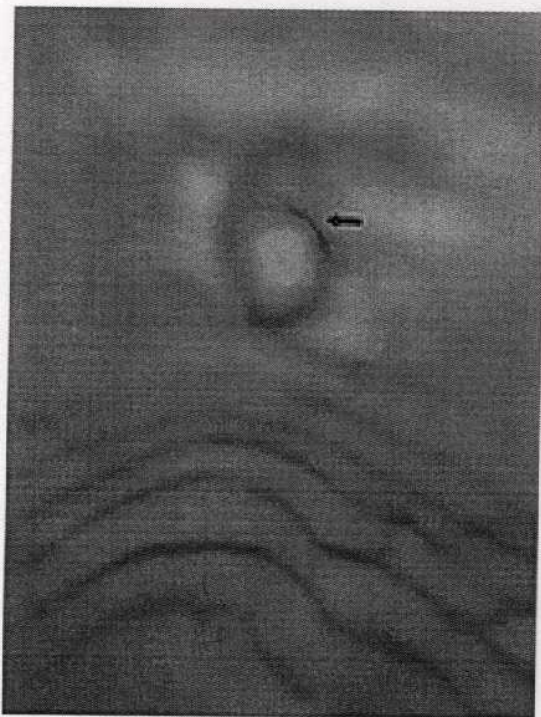
A



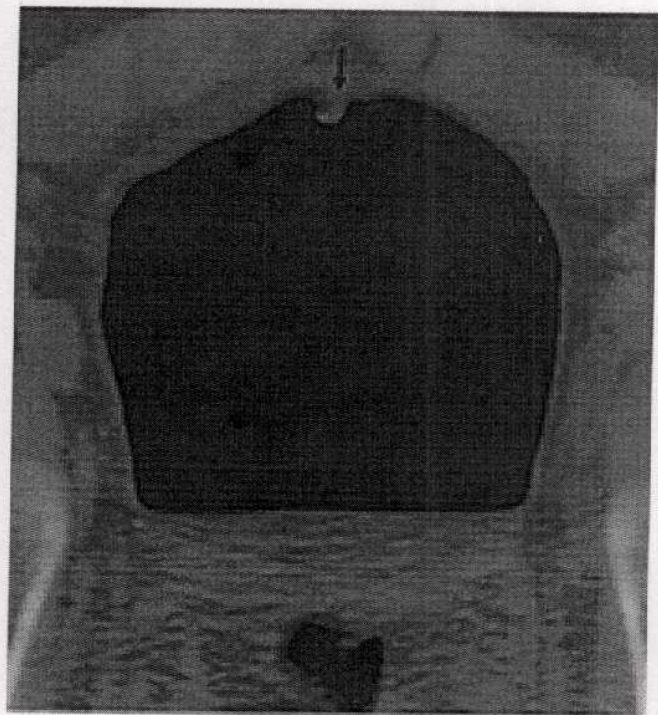
B

(Fig. 25) (A) Virtual cystoscopic and (B) transverse CT images demonstrate a soft-tissue mass (arrow), a low-grade papillary carcinoma, with punctate calcifications arising from the left trigone. F = Foley catheter balloon (not depicted in B because the catheter is at a lower level) (Song et al., 2001).





A



B



C

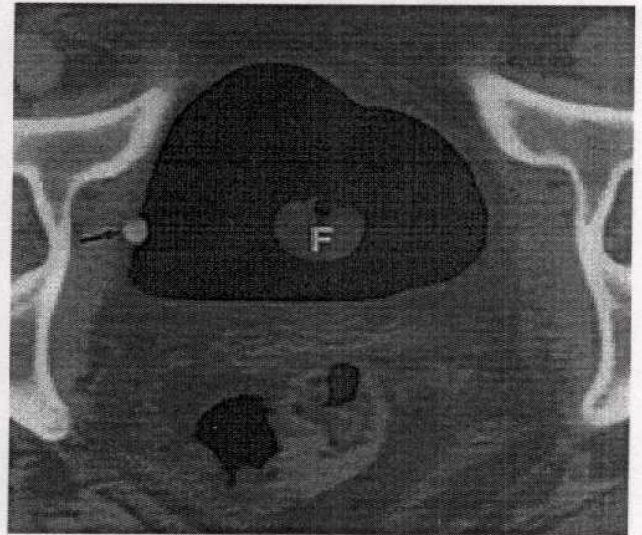
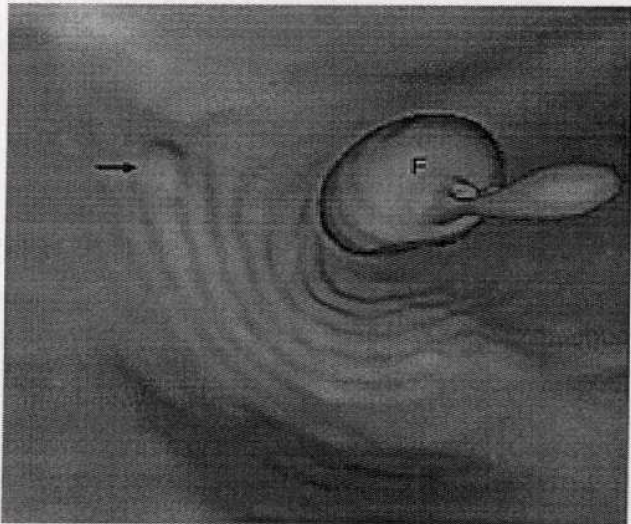
(Fig. 26 ) (A) Virtual cystoscopic and (B) transverse CT images demonstrate a calcified polypoid lesion (arrow) arising from the anterior wall of the bladder. Note the lobular morphologic appearance visible only in a. (C) Conventional cystoscopic image depicts a solid tumor (arrow), a high-grade transitional cell carcinoma with sarcomatoid features, with diffuse dystrophic calcification (Song et al., 2001).

The number, location, morphologic features, and size of lesions are evaluated on transverse and virtual images obtained with the patients in both the supine and prone positions. Each lesion is characterized as a focal polypoid lesion, a sessile mass, or



.....

wall thickening. A discrete lesion is considered polypoid if it is taller than it is wide, while a sessile mass is defined as a lesion that is wider at the base. A lesion is characterized as wall thickening when there is elevation of the bladder wall without a discrete mass. Masses may have a smooth or irregular surface (Song et al., 2001).



A

B

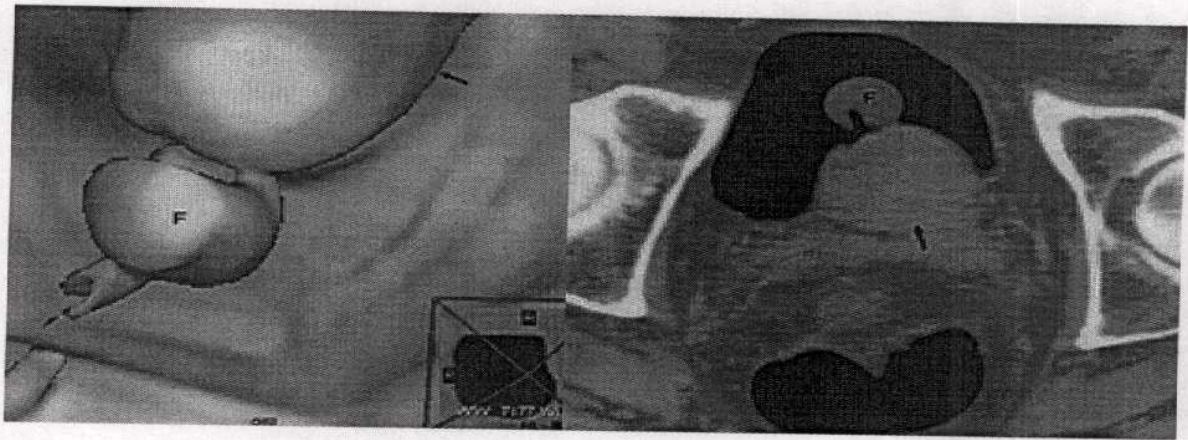
(Fig. 27) (A) Virtual cystoscopic image shows a pseudolesion that mimics a polypoid lesion (arrow). (B) Transverse CT view depicts the corresponding lesion as a calcified phlebolith (arrow). F = Foley catheter balloon (Song et al., 2001).

Patients with a severe ureteral stricture or marked prostatic hypertrophy, who may be poor candidates for conventional cystoscopy, can safely undergo CT cystoscopy, since a small ureteral catheter can be used to instill air into the bladder (Song et al., 2001).

In a trabeculated bladder, masses are reported if a local contour abnormality is identified that is out of proportion to the degree of adjacent trabeculation. The degree of bladder trabeculation and the presence of bladder diverticula are noted. Note is made of whether a mass appears to be intrinsic to the bladder or extrinsic. The degree of bladder distension, adequacy of drainage of urine, and presence of imaging



artifacts is also recorded (Fenlon et al., 1997).



A

B

(Fig. 28) (A) Virtual cystoscopic and (B) transverse CT images demonstrate the enlarged median lobe of the prostate gland (arrow) protruding into the bladder. F = Foley catheter balloon (Song et al., 2001).

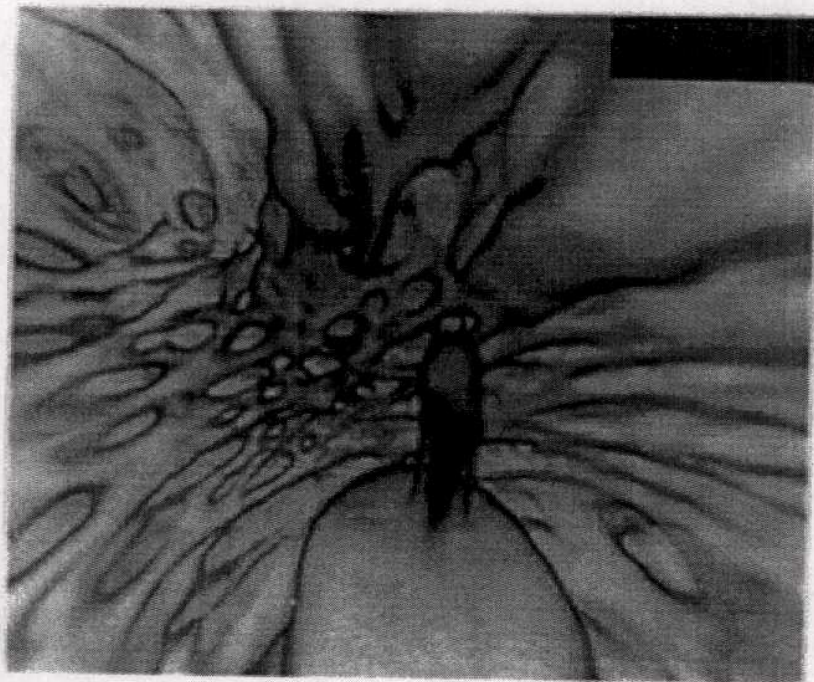


(Fig. 29) Bladder trabeculation. Virtual cystoscopy image shows a heavily trabeculated bladder in a patient with bladder outflow obstruction. A Foley catheter is shown in the foreground (Fenlon et al., 1997).



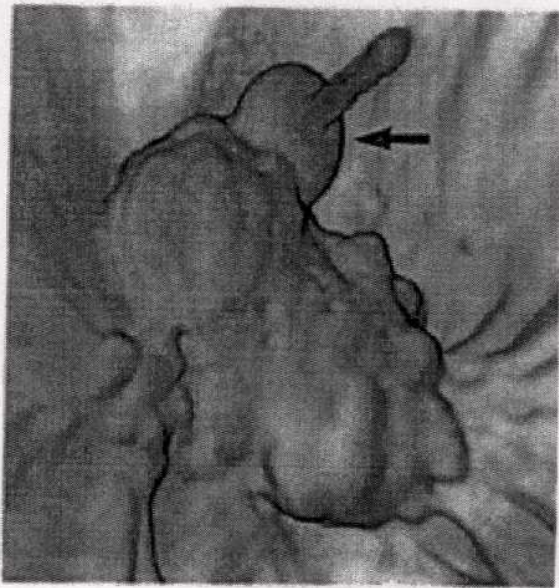


Fig. 30

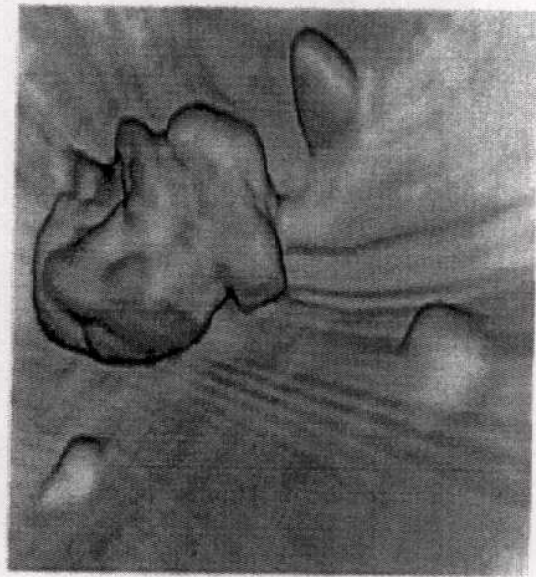


Fig. 31

*Figures 30, 31. (30) Bladder carcinoma. An 8-cm (maximum dimension) sessile mass arising at the bladder neck is shown at virtual cystoscopy. A 12-F Foley catheter is present adjacent to the mass (arrow). (31) Bladder carcinoma. A 4-cm sessile mass and three adjacent polyps smaller than 1 cm are shown at virtual cystoscopy (Fenlon et al., 1997).*

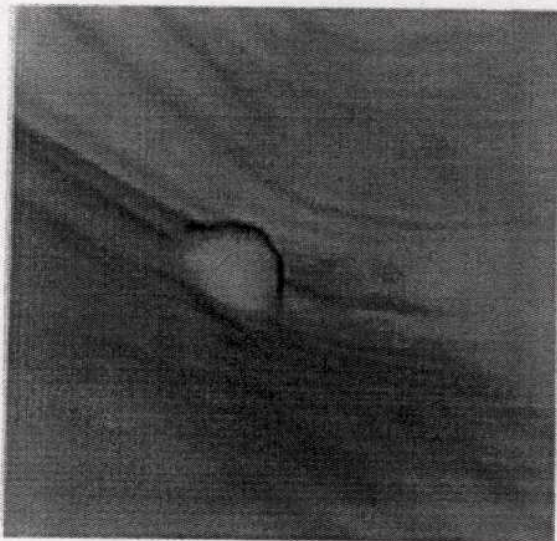


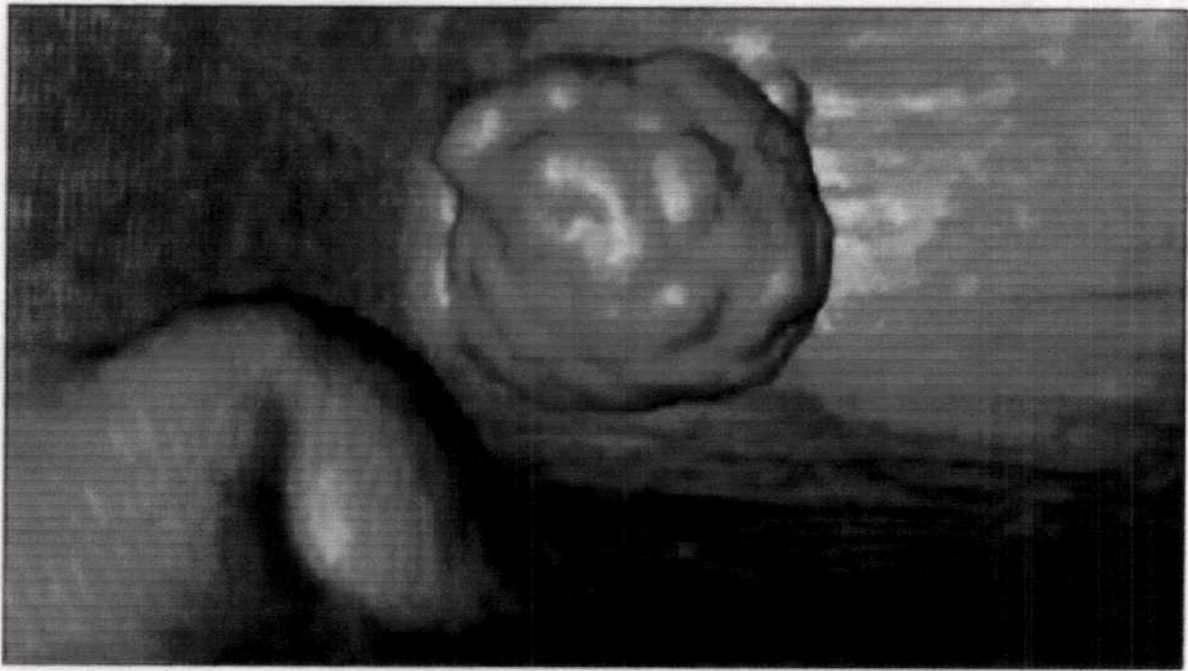
Fig. 32



Fig.33

*Figures 32,33. (32) Recurrent bladder carcinoma. A 3-mm (maximum dimension) bladder mass, the smallest found in our study, is shown at virtual cystoscopy. (33) Chronic mucosal ulceration. A magnified view of a virtual cystoscopy image shows focal mucosal nodularity. At conventional cystoscopy, a corresponding area of subtle mucosal granularity was identified that was a result of long-term bladder catheterization. (Fenlon et al., 1997).*





(Fig.34)-Virtual renderings of urinary bladder. 67-year-old man with bladder mass. Perspective volume-rendered image from data set of CT scan through gas-filled urinary bladder, from reference point within its right lateral portion, shows polypoid tumor mass and its irregular surface. Prostatic impression and urethral origin are seen at bladder base. (Quoted from Fielding et al., 1999).

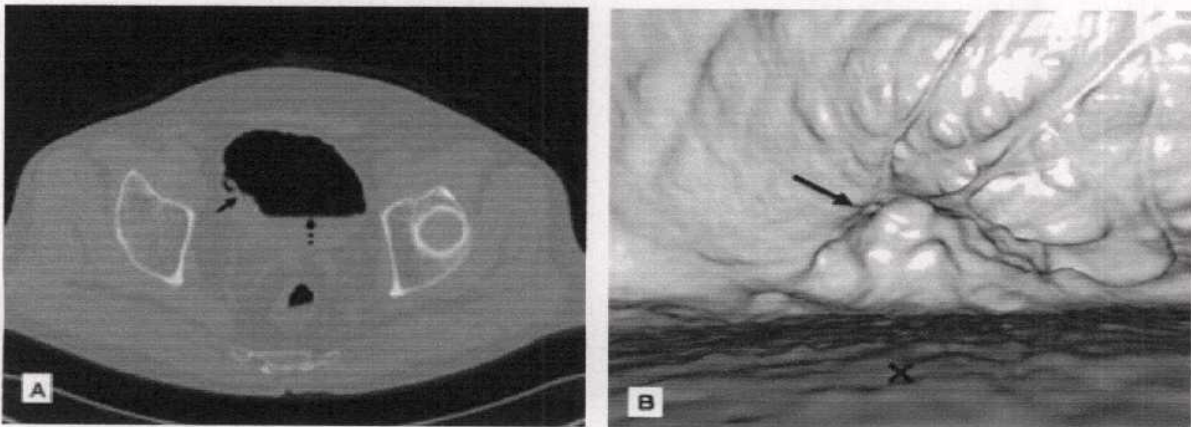


FIG. 35. (A) Reconstructed two-dimensional CT (transverse image) from air VC. The bladder lumen is filled with air. A bladder tumour with a large radius is present on the right lateral bladder wall (arrow). The water surface appears at the base of the bladder (dotted arrow), and bladder tumour under the water surface cannot be detected. (B): Air VC images of a bladder tumour with a large radius (arrow). Trabeculations around the tumour are also well indicated, as is the water surface (asterisk). However, structures under the water surface cannot be detected. (Kawai et al., 2004).



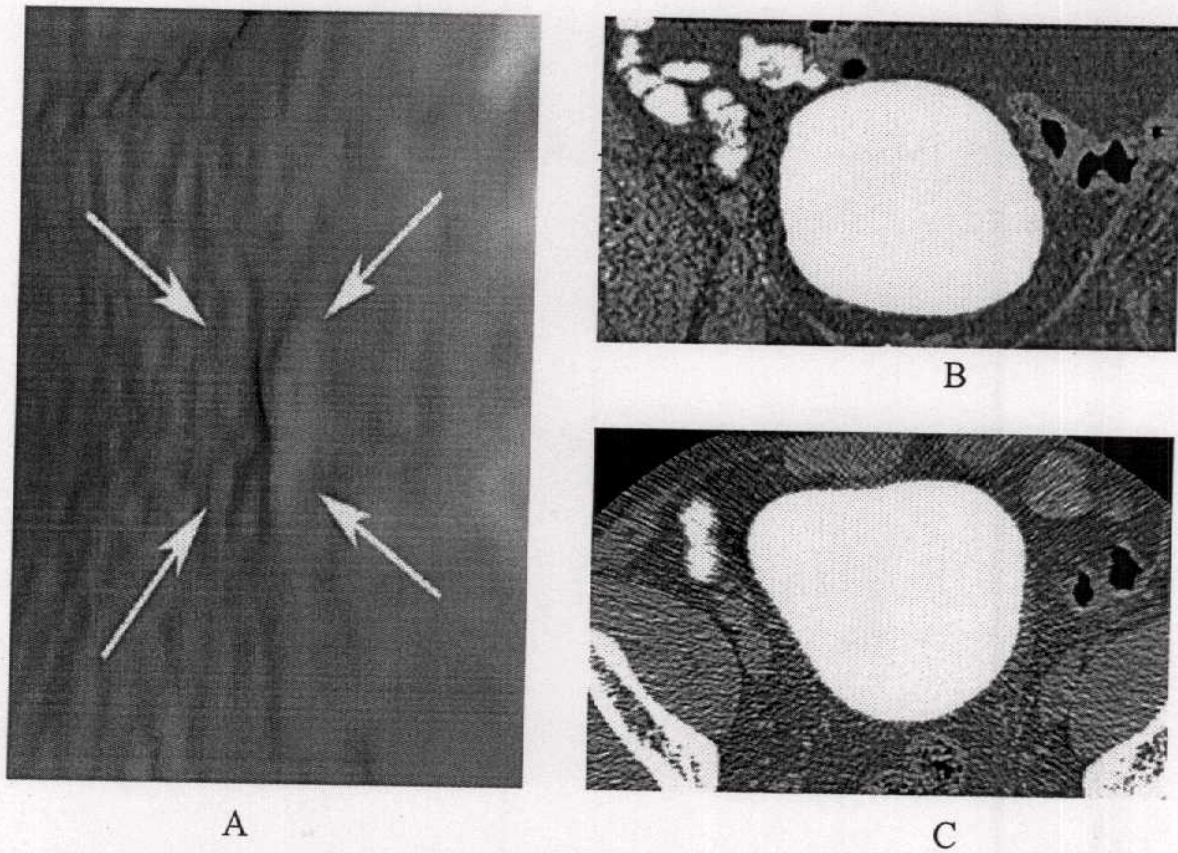
II. Contrast material filled bladder virtual cystoscopy:



FIG. 36. (A) Cystogram of a patient who had IVU VC; there is a filling defect on the left lateral wall (arrow). (B) Conventional cystoscopic findings of a bladder tumour, a papillary pedunculated tumour of 10 mm. (C) IVU VC image of a bladder tumour; this virtual viewpoint is from the bladder top to the bladder base. There is a mass with a rough surface on the right lateral wall (arrow); it is not completely pedunculated, but there is a small pedunculated lesion (double arrow). Mucosal upheaval caused by prostatic hypertrophy and the inner urethral orifice are clear (dotted arrow). These images cannot be reconstructed by air VC with the patient supine. (D) An image of the same mass as in (C) observed from just above it, and with a similar appearance. (Kawai et al., 2004).



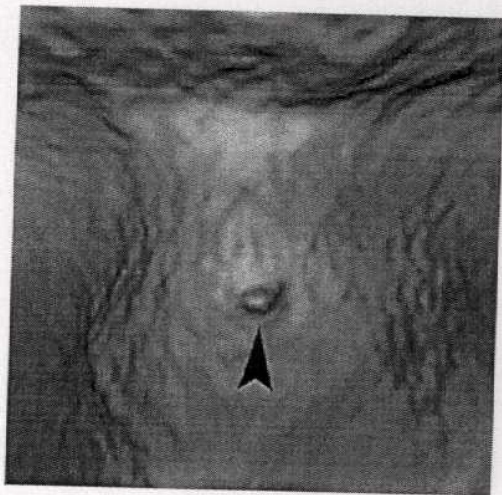
Virtual cystoscopy is superior to multiplanar reconstruction and source CT images for lesion detection in the contrast material-filled bladder. Given the merits of this advanced technology, virtual cystoscopy may contribute to initial screening for patients with hematuria and more accurate patient selection for invasive cystoscopy (*Kim et al., 2005*).



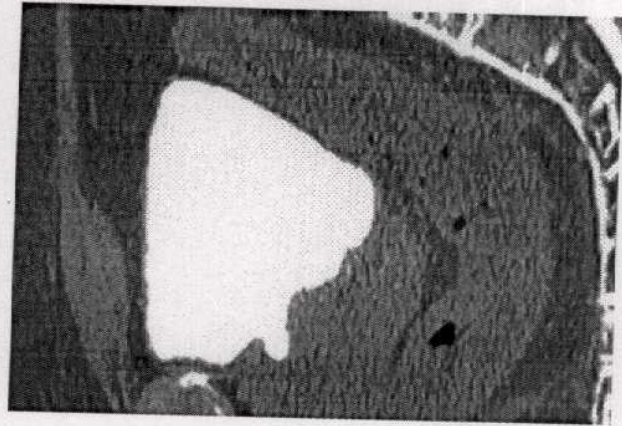
(Fig. 37) - 67-year-old man with transitional cell carcinoma at right site of bladder. (arrows, A) virtual cystoscopy image obtained toward right wall of bladder, (B) coronal reformatted image (C) transverse CT image showed no lesion. (*Kim et al., 2005*).

The sensitivity of lesion detection by bladder site and the accuracy for determining the presence or absence of a lesion at each site were significantly greater in virtual cystoscopy than in multiplanar reconstruction and source CT images (*Kim et al., 2005*).

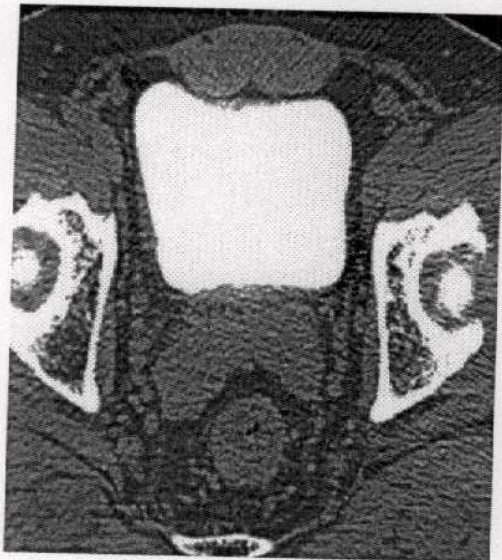




(A)



(B)



(C)

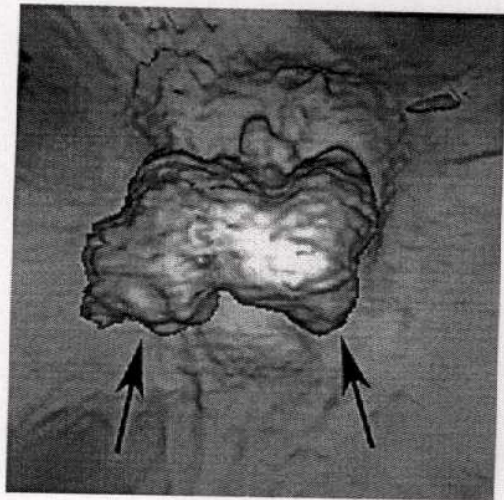
(Fig. 38 )- 60-year-old man with transitional cell carcinoma at anterior site of bladder.

A-C, Virtual cystoscopy image obtained toward anterior wall of bladder (A) shows polypoid lesion (arrowhead, A) that was identified by both first and second observers.

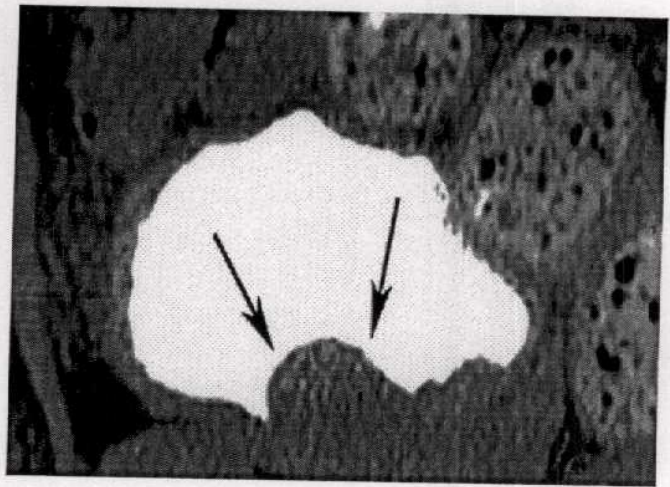
However, this lesion was not detected on sagittal reformatted image (B) or transverse CT image (C) (Kim et al., 2005).

The dynamic contrast-enhanced axial images could provide excellent intramural and extravesical information, MPR could directly demonstrate the origin and extravesical invasions of the tumours and their relation to the ureter. 3D and CTVC images were useful for displaying the surface morphology of the tumour and the relationship between the tumour and the ureteric orifices, whereas CTVC could depict the tumours smaller than 5 mm were not seen on the axial images (Wang et al., 2004).

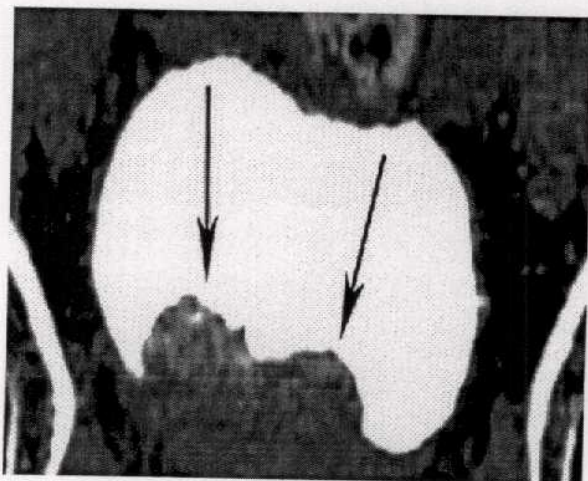




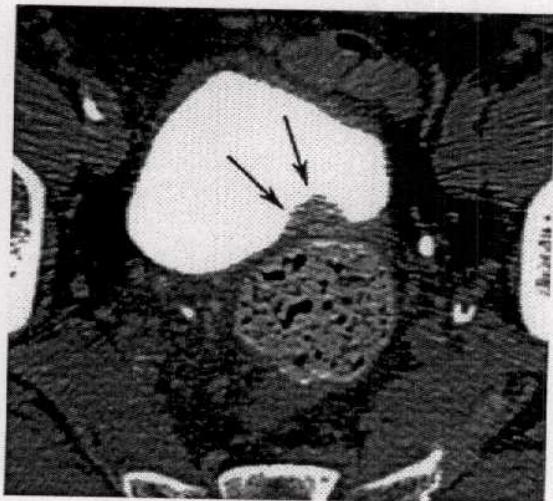
(A)



(B)



(C)



(D)

(Fig. 39) 70-year-old man with transitional cell carcinoma at inferior site of bladder.

A–D, Virtual cystoscopy image obtained toward inferior wall of bladder (A) shows polypoid mass (arrows). This lesion (arrows) is also identified on sagittal (B) and coronal (C) reformatted images and transverse CT image (D) (Kim et al., 2005).

Before undergoing virtual cystoscopy, all patients asked to alternate taking supine and prone positions four times so that the contrast material and urine in the bladder could be adequately mixed suboptimal images were caused by inadequate mixing of contrast material and urine, which resulted in artifacts on virtual images and fluid—fluid levels on source images (Kim et al., 2002).



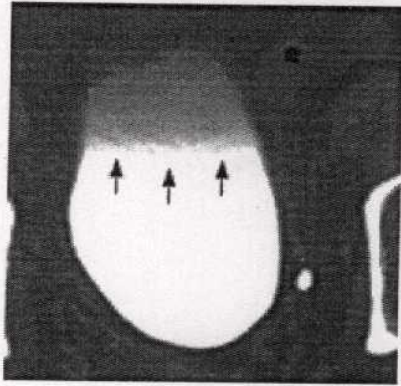


(Fig. 40) Virtual images of 54-year-old woman who presented with gross hematuria are of suboptimal quality because of inadequate mixing of contrast material and urine. Fluid—fluid level (arrows) is visible on multidetector helical CT source image (Kim et al., 2002).

The excretory phase images provide substantial additional information, both in confirming enhancing lesions as true lesions and not pseudolesions related to focal opacified urine arising from a ureteral jet within the bladder lumen, and in demonstrating discrete filling defects caused by tumor not evident on earlier scans. If the urinary tract is not well distended and opacified with contrast throughout its entire course, additional delayed images acquired targeting the nonopacified portion up to two times. Putting the patient in the prone position, applying abdominal compression, or both, may help distend the urinary collecting system (Zhang et al., 2007).

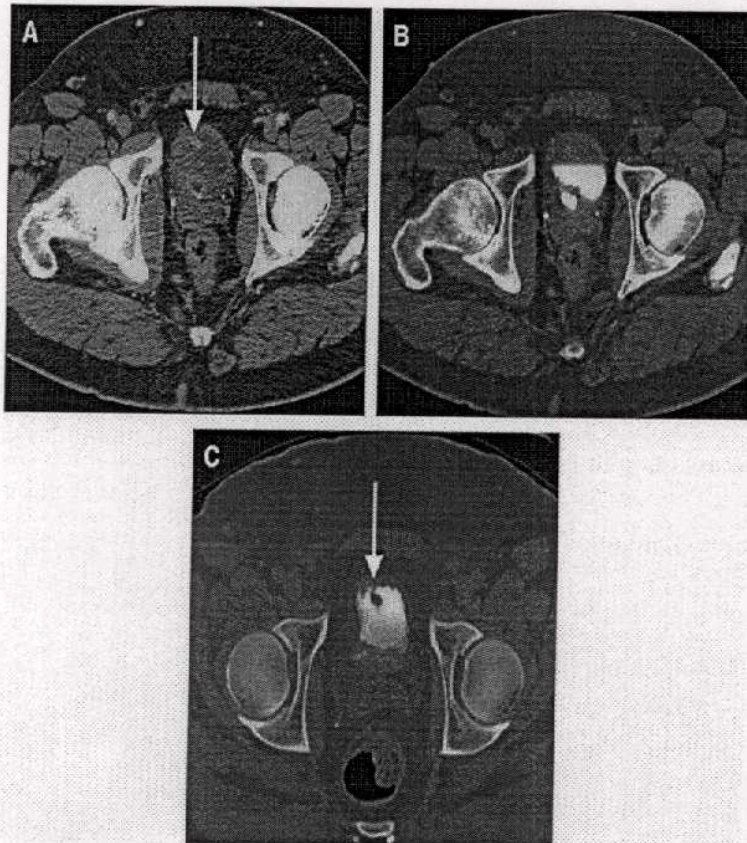


(Fig.41) 77-year-old man who has TCC of the bladder.

(A) Parenchymal phase CTU image demonstrates a 5-mm enhancing papillary lesion (arrow) arising from the anterior bladder wall.

(B) Excretory phase images do not readily demonstrate the lesion, as the non-dependent portion of the urine in the bladder is not opacified with contrast.

(C). Repeat excretory phase image in the prone position demonstrates the pedunculated tumor as a discrete filling defect (arrow). (Zhang et al., 2007).



In the setting of frank hydronephrosis, the patient may be allowed to return to the CT department 30 or 60 minutes later for delayed imaging. The excretory phase images are reconstructed further into thin overlapping sections, which then are transferred to a workstation for three-dimensional post-processing (Fig. 42) (Zhang et al., 2007).

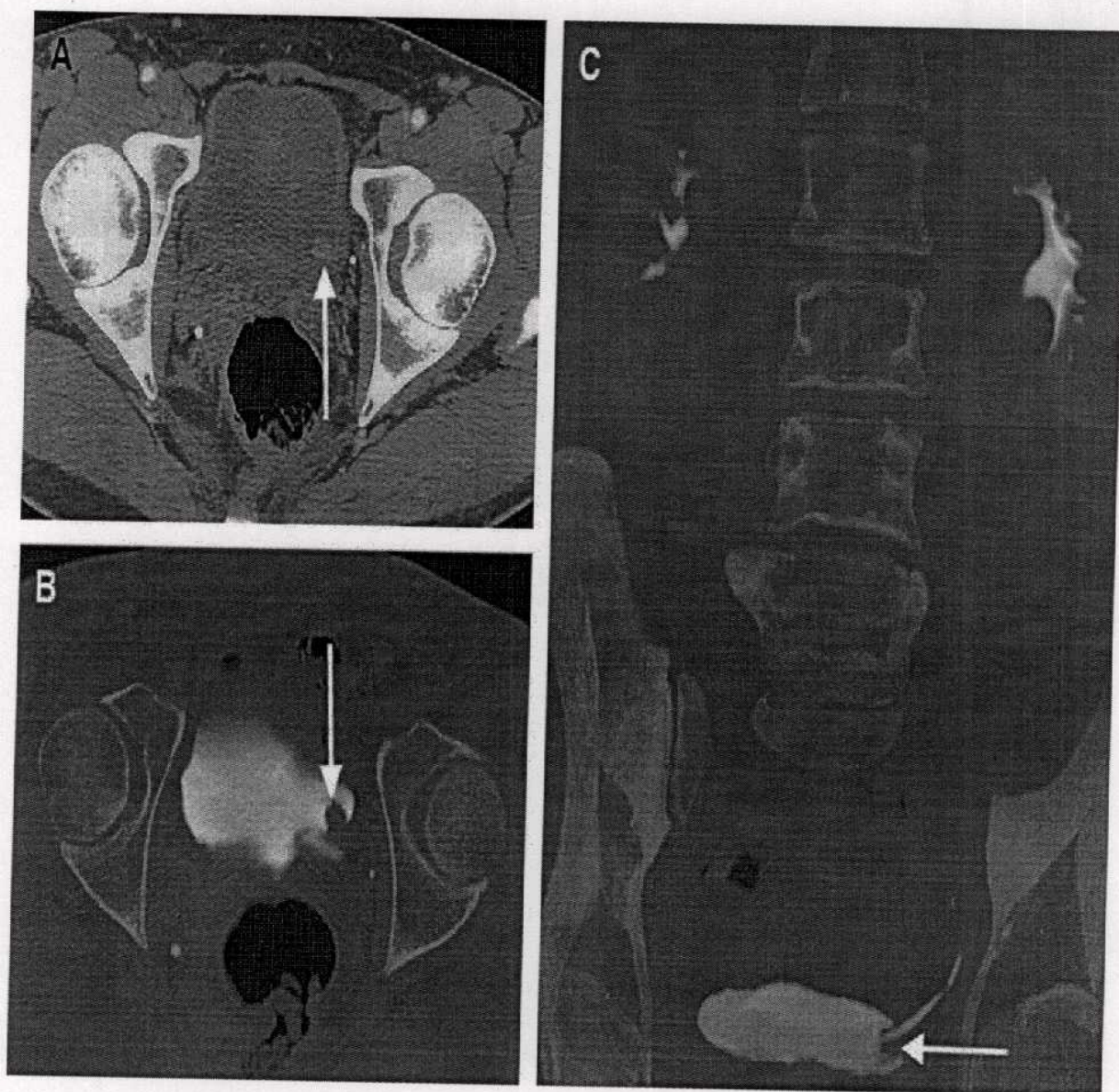


(Fig.42) 72-year-old man who has bladder cancer. (A) Early parenchymal phase CTU image demonstrates a bladder mass (arrow) with avid enhancement. (B) Excretory phase CTU image demonstrates the lesion as a papillary, nodular filling defect (arrow) in the opacified bladder adjacent to the left ureterovesicular junction (UVJ). (C) Coronal thin MIP image from excretory phase CTU images demonstrates the mass as a filling defect (arrow) adjacent to the left UVJ. (Zhang et al., 2007).



For local staging of bladder cancer, perivesical fat infiltration suggests transmural extension, or T3 disease (Fig. 43) (Zhang et al., 2007).

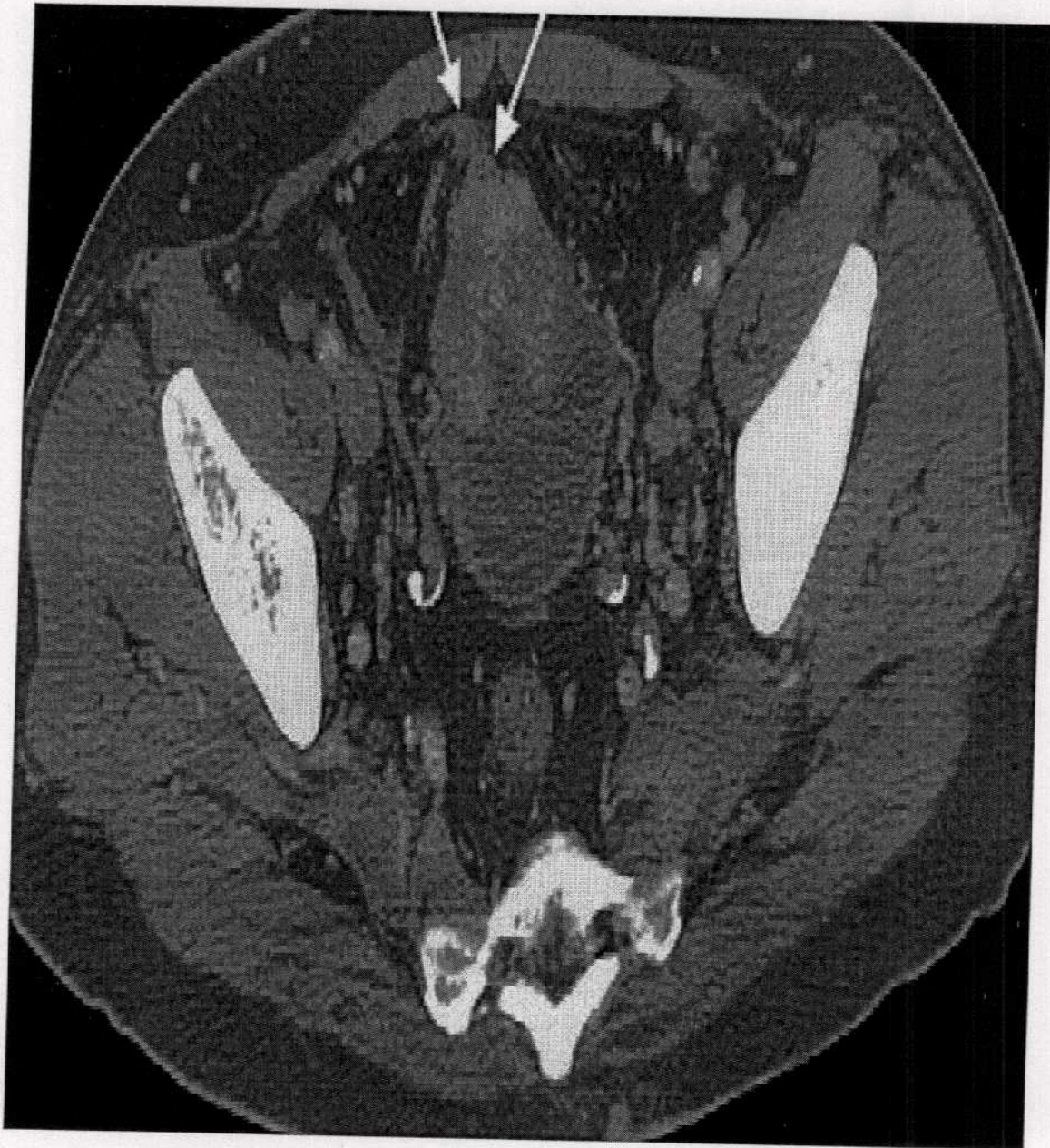


(Fig.43) 67-year-old man who has metastatic bladder cancer. Contrast-enhanced CT image demonstrates a large enhancing mass in the anterior bladder wall (long arrow). The mass has grown through the bladder wall with anterior perivesical soft tissue (short arrow) indicative of perivesical invasion (Zhang et al., 2007).



### III. Coupled air distension and contrast injection virtual cystoscopy:

Virtual cystoscopy is based on creating a high contrast between the bladder wall and the lumen. Some authors waited for opacification of the bladder by iodinate urine in the late excretory phase, achieving sensitivity and specificity rates ranging between 90–95% and 85–87%, respectively. In most cases CT cystoscopy is achieved by administering room air through a urinary catheter. This method assures about 1000HU of difference between the wall and the lumen, and also provides an optimal distension of the bladder. The sensitivity and specificity with this technique are 94–97% and 98–100%, respectively (Scardapane et al., 2007).

Coupled pneumo-CT cystoscopy with I.V. administration of contrast medium. To always achieve optimal bladder distension, an adequate depiction and enhancement of bladder lesions. Furthermore, I.V. injection of contrast medium permits visualization of the tumor extending into the terminal ureter, which appears dilated in unenhanced scans. The presence of contrast enhancement is a very sensitive index for malignancies (Scardapane et al., 2007).

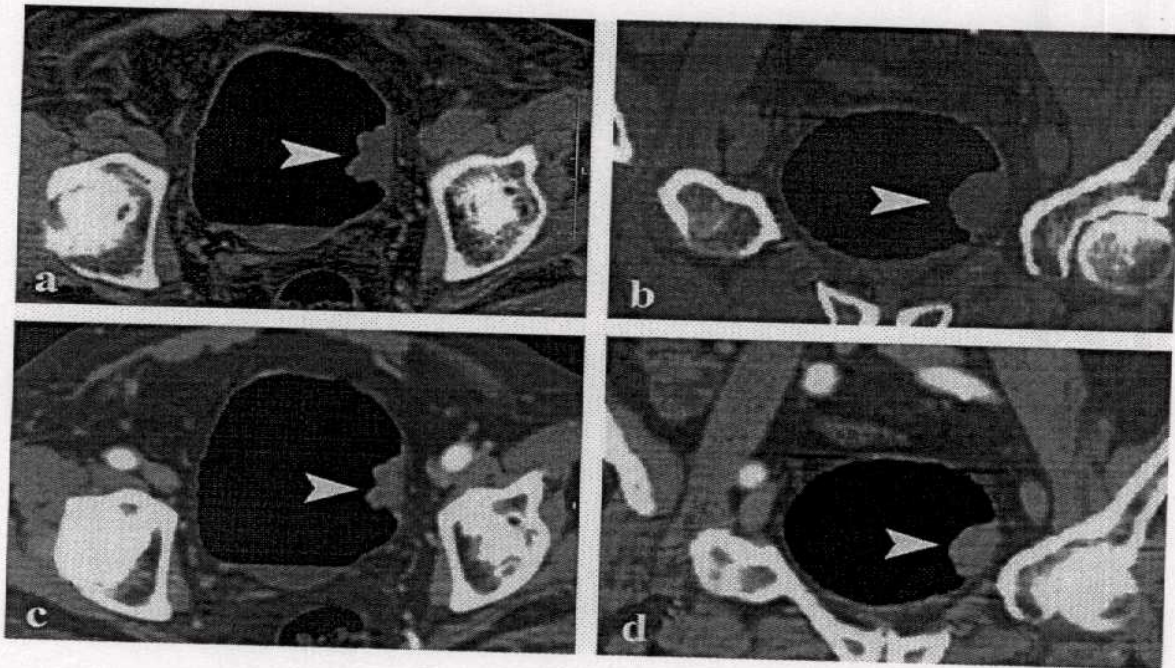


(Fig. 44) Urinary bladder cancer. (a, b) Unenhanced CT (c, d) Enhanced CT with air distension of the urinary bladder. The axial (a, c) and coronal reconstructions (b, d) show an enhanced papillary lesion of the left wall (arrowhead). (Scardapane et al. 2007).



Contrast injection was also useful to obtain a late urographic scan that revealed a synchronous upper lesion that was not recognizable in previous phases (Scardapane et al., 2007).

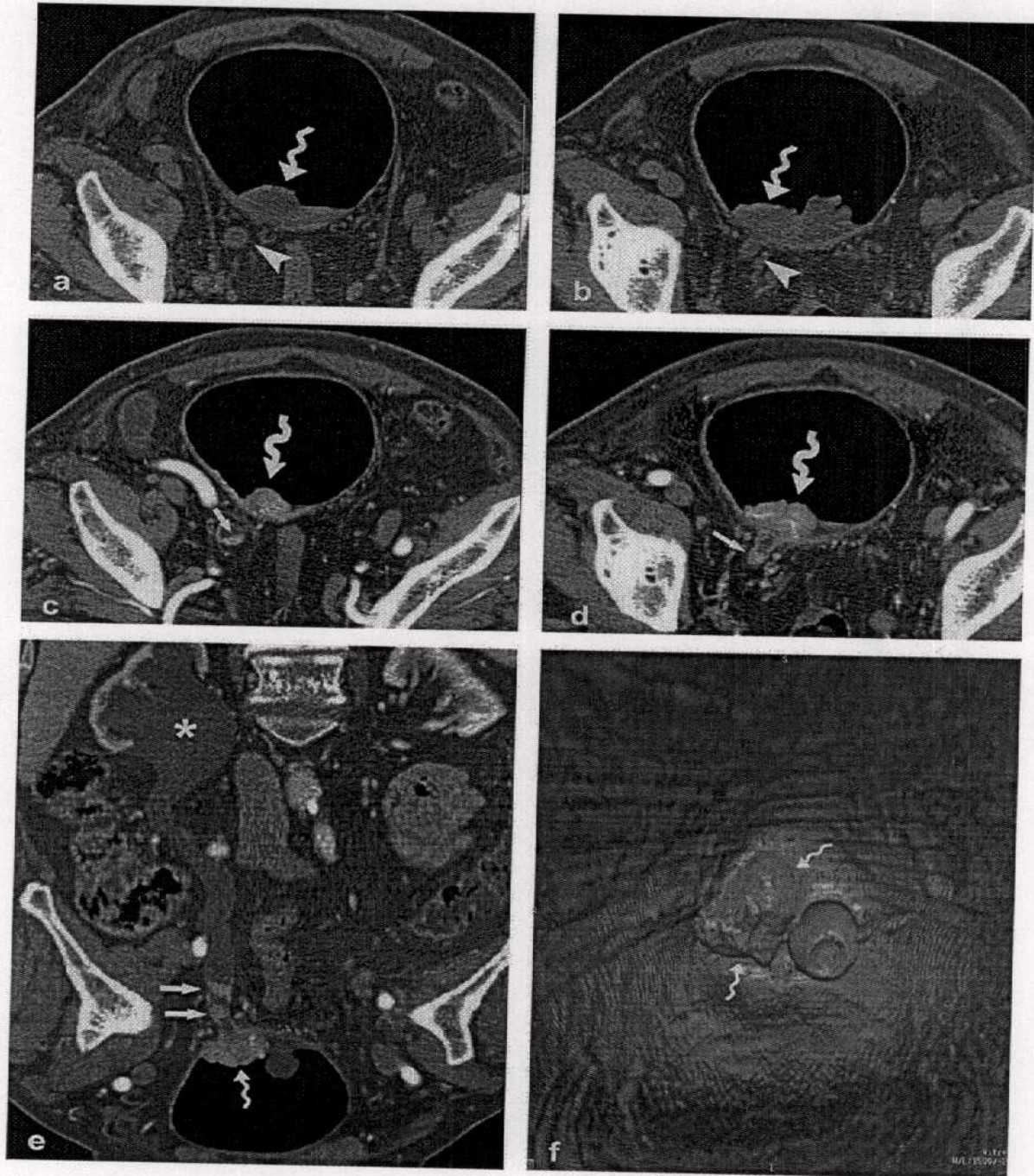


(Fig. 45) Bladder cancer extending to the distal ureter. Unenhanced CT scans (a,b) demonstrate a papillary lesion of the right trigonum (spiral arrow) with distal ureter distension (arrowhead). Enhanced CT scan (c, d) and curved MPR reconstructions (e) confirm a bladder papillary lesion (spiral arrow) and show enhanced tissue extending into the distal ureter (arrows). (f) Virtual endoscopic aspect of the lesion (spiral arrows) (Scardapane et al. 2007).



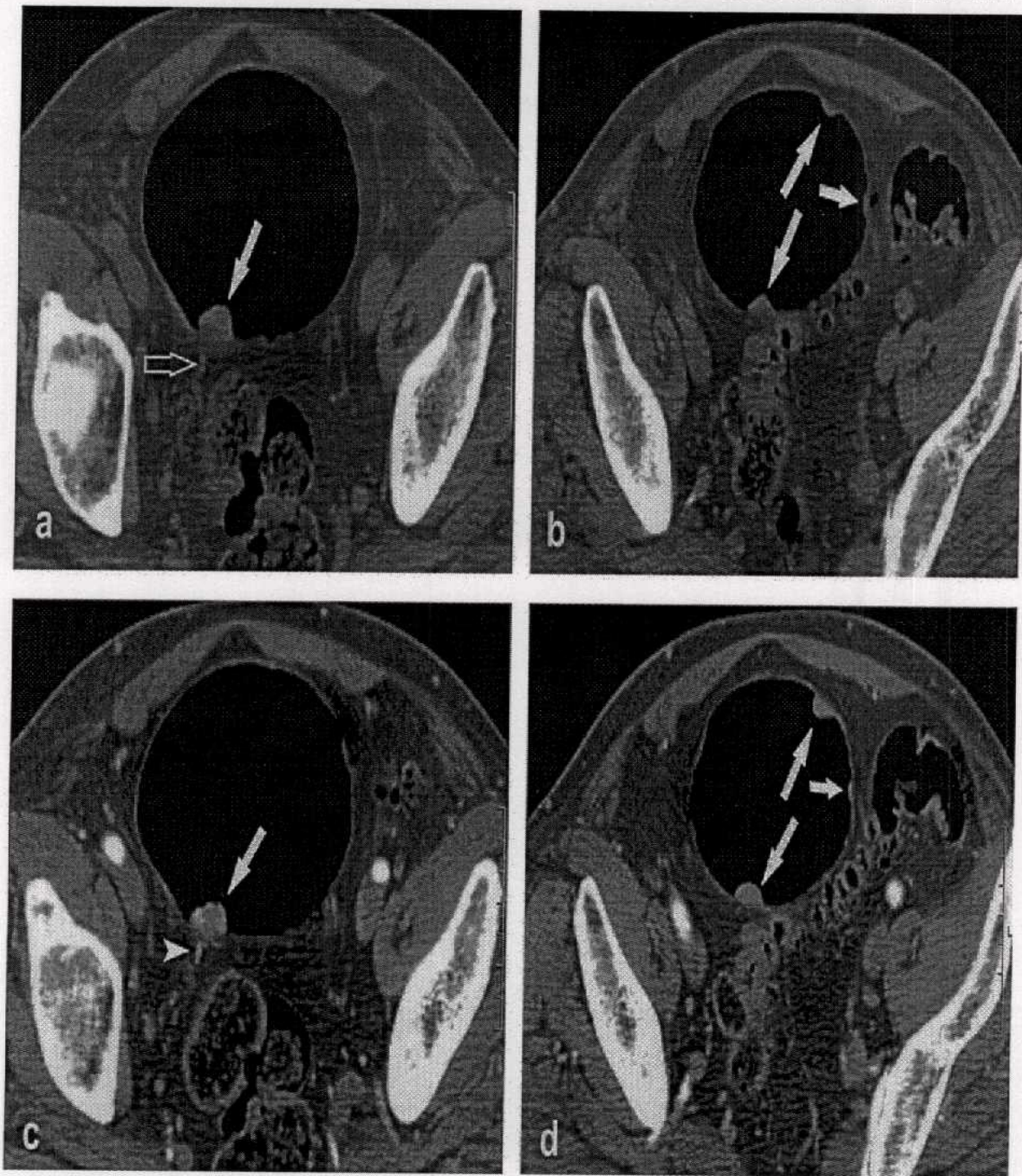


(Fig.46) Multiple papillary bladder lesions. Unenhanced (a, b) and Enhanced CT (c, d) scans show multiple hypervascular papillary lesions (arrows). Perivesical stranding was suspected on unenhanced scan (empty arrow in 'a'); while a vessel feeding a lesion was recognized after contrast injection (arrowhead in 'c'). Noninvasive Bladder Cancer was diagnosed with TURB) ( Scardapane et al. 2007).



All tumors described by the virtual cystoscopy with nearly similar findings in size localization and surface of the tumor except one lesion, which was smaller than 5 mm 90% of the tumors were diagnosed by virtual cystoscopy as compared to conventional cystoscopy (*Arslan et al., 2006*).

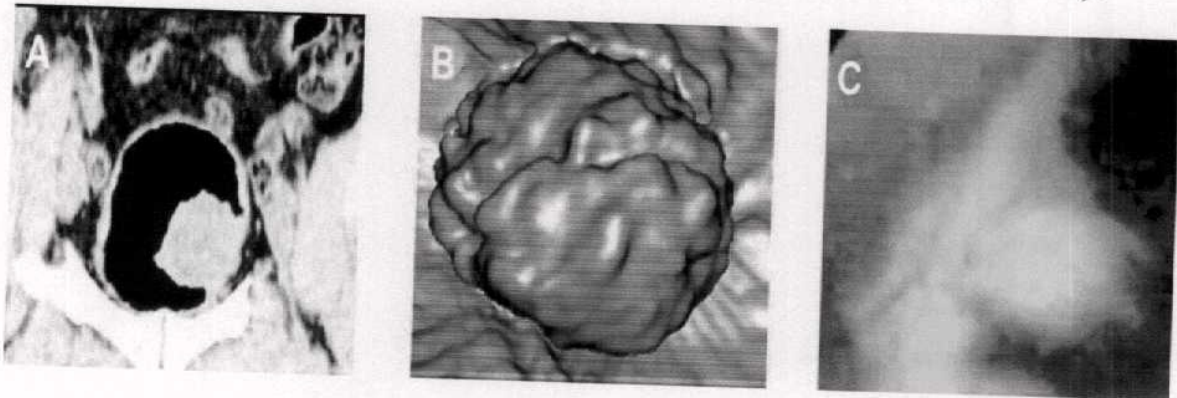


(*Figure 47*) – 50-year-old man with transitional cell carcinoma obtained in area toward left wall shows polypoid lesion. *A*) Coronal multiplanar reconstruction section. *B*) Virtual CT cystoscopy appearance. *C*) Conventional cystoscopy. Vegetative surface of the tumor was clearly identified in virtual CT cystoscopy. Surrounding mucosal surface appears normal both of the conventional and virtual CT cystoscopy (*Arslan et al., 2006*).

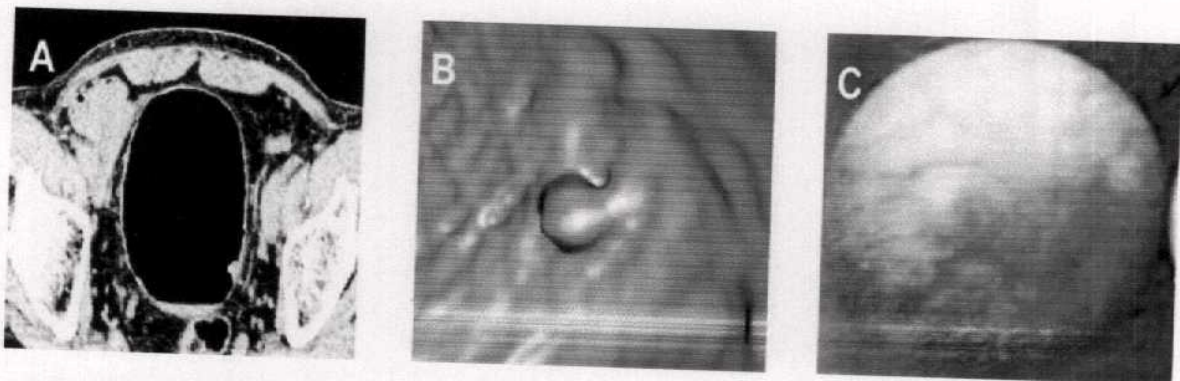


(*Figure 48*) – 60 year-old man with primary urinary bladder cancer. *A*) Transverse section. *B*) Virtual CT cystoscopy appearance. *C*) Conventional cystoscopy. Virtual CT cystoscopic image focused on polyp with 12 mm located near left urethral orifice. Internal urethral orifice can be identified only polyp with 12mm located near left urethral orifice. Internal urethral orifice can be identified in lower midportion (*Arslan et al., 2006*).

Mucosal thickness and trabeculations seen in the virtual CT cystoscopy and the appearance was similar in both conventional and virtual modalities (*Arslan et al., 2006*).



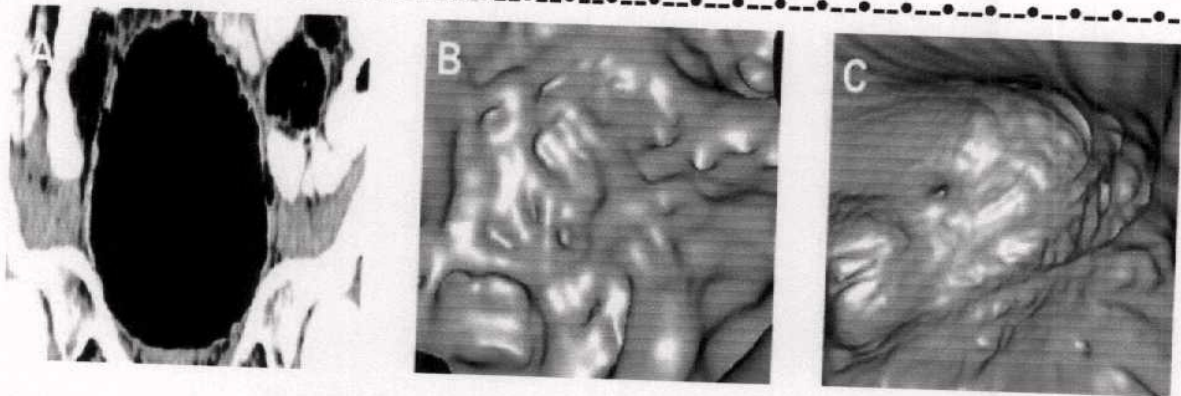


(Figure 49) – 71 year-old man with trabeculation because of the prostate hypertrophy. A) Coronal multiplanar reconstruction image. B) Magnified virtual CT cystoscopy appearance. C) General trabecular appearance of mucosal surface in virtual CT cystoscopy. Virtual CT cystoscopy shows mucosal thickness and trabeculation similar with the conventional cystoscopy (Arslan et al., 2006).

virtual CT cystoscopies were superior to conventional cystoscopy in demonstration of the interior of the diverticula; the interior of the diverticula could not be evaluated by conventional cystoscopy. but lumens were easily detected by virtual cystoscopy (Arslan et al., 2006).

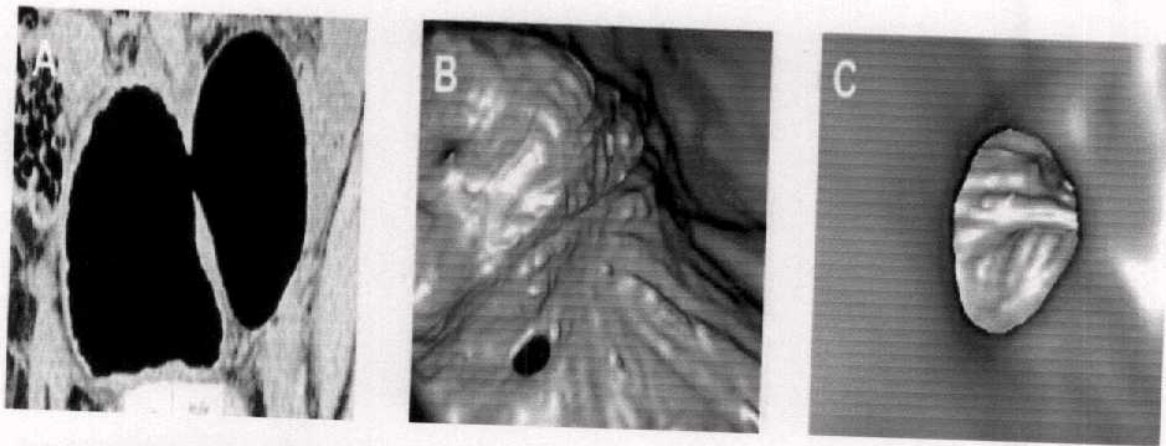


(Figure 50) – 45 year-old men with virtual CT cystoscopic images of bladder wall diverticulum. A) Sagittal multiplanar reconstruction image. B) Virtual CT cystoscopy appearance of the neck of the diverticulum. C) Interior appearance of the diverticulum. Diverticulum could be evaluated both of the multiplanar reconstruction images and virtual CT cystoscopy, but could not in the conventional cystoscopy. (Arslan et al., 2006).

The combination of axial, MPR, 3D and CTVC images with helical CT can provide comprehensive information on bladder tumour (Wang et al., 2004).



**IV. Virtual cystoscopy with color mapping of bladder wall thickness:**

Virtual cystoscopy with color mapping showed the relationship of the tumors to the ureters and urethra (Fig. 51). Color scale from red to blue representing 0 mm to 15 mm thickness proved to be very useful. Using this color range even subtle thickness changes appeared very clearly. Subtle thickening of the left lateral bladder wall was identified using conventional and color mapped virtual cystoscopy (Fig. 52) (Schreyer et al., 2000).

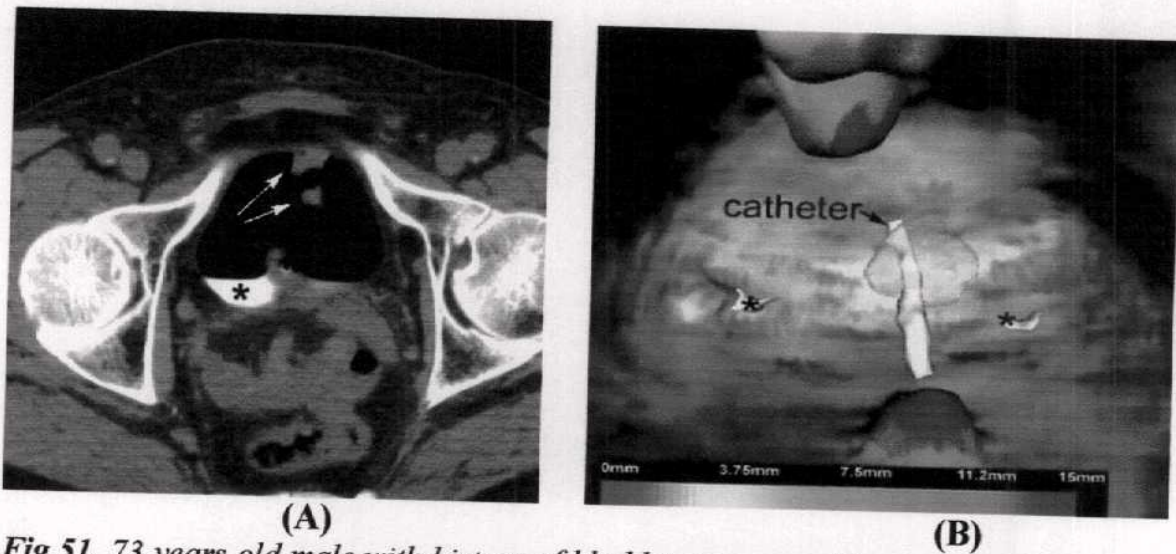


**Fig.51.** 73 years old male with history of bladder cancer and hematuria (A) Axial CT image shows polypoid mass arising from the anterior surface of bladder wall (arrows). Contrast enhanced urine (\*) pools adjacent to the catheter.(B)Color mapped virtual endoscopy view of the same bladder. Superior-inferior view showing the catheter with balloon, the ureters (\*) and the green to blue color mapped masses. (Schreyer et al., 2000).

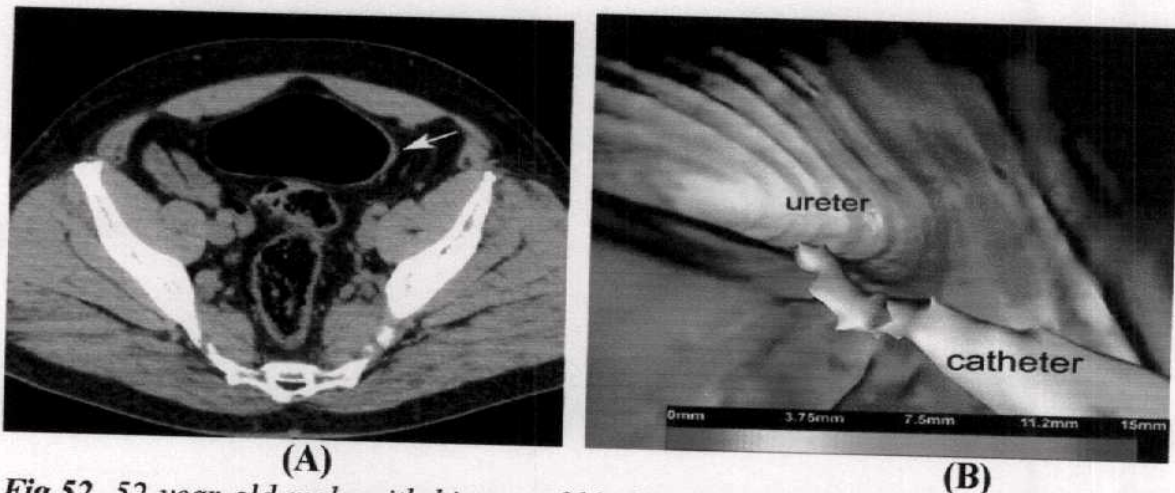


**Fig.52.** 52 year old male with history of bladder cancer. (A) Axial CT image shows subtle thickening of the left bladder wall (arrow). (B) Color mapped virtual endoscopy. Inferior-superior view with catheter and left ureter as landmarks. Green color mapping of the left bladder wall, indicating thickening (Schreyer et al., 2000).



Color mapping of bladder wall thickness assigned a color according to a fixed and validated mm. scale, ranging from red (1 mm.) to purple (10 or greater). The color mapped renderings which allowed the viewing of inner and outer bladder surfaces. The analysis of 3-D renderings produced a blue or purple color indicating a region of wall thickness greater than 5 mm.

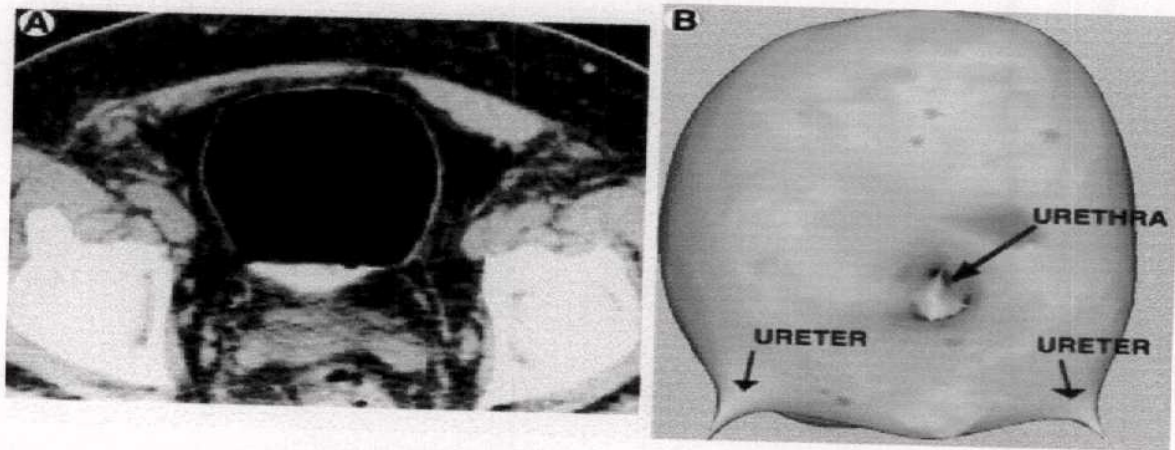


**Fig. 53.** 67-Year-old man with microscopic hematuria and normal conventional cystoscopic examination. **A**, axial CT of air distended bladder indicates no area of wall thickening or mass. **B**, 3-D rendering of external bladder surface with color wall thickness mapping and patient in lithotomy position. No suspicious blue or purple thickened area is identified. Entirety of wall is less than 5 mm. thick (Fielding et al., 2002).

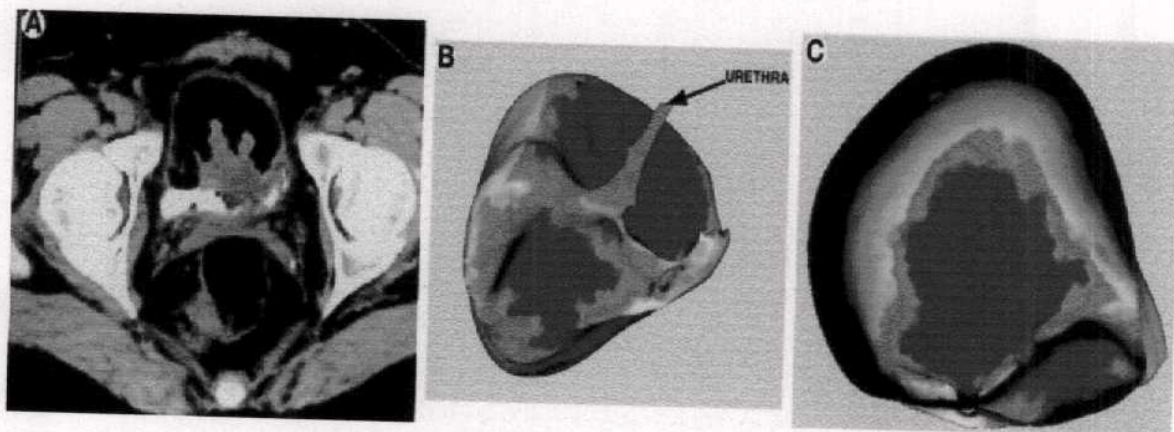


**Fig. 54.** Woman with microscopic hematuria and large mass at bladder base identified and biopsied during conventional cystoscopy. **A**, axial CT of air distended bladder shows large frond-like mass occurring from bladder base and posterior wall. **B and C**, 3-D rendering of bladder with color mapping of wall thickness. **B**, lithotomy view of external surface indicates large area of abnormal thickening (greater than 1 cm.) demarcated by blue and purple. **C**, view of bladder base from above with dome removed confirms location and irregularity of surface (Fielding et al., 2002).



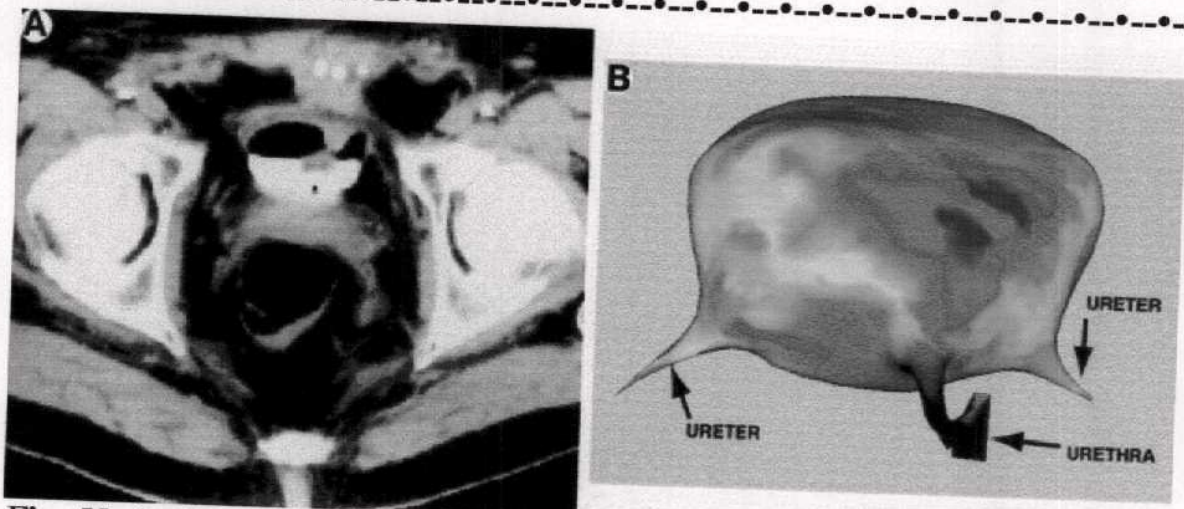


**Fig. 55.** Asymptomatic 60-year-old man with history of transitional cell carcinoma and anterior wall polyp identified on conventional cystoscopy. **A**, axial CT of inferior portion of bladder shows small soft tissue mass occurring from anterior surface and abutting catheter. Adjacent to this focal mass was 2 cm. region of diffuse wall thickening, possibly due to prior therapy. **B**, 3-D rendering of bladder with color mapping of wall thickness. Lithotomy view of external surface indicates bilobed region of wall thickening demarcated by blue and purple. Polyp cannot be distinguished from adjacent thickening. Biopsy showed recurrent superficial transitional cell carcinoma (Fielding et al., 2002).

Tumors create a thickening of the bladder wall, Positive Z scores characterize thickness larger than the average. The larger the Z score, the more atypically thick the bladder wall. (Fig. 57) (Jaume et al., 2003).

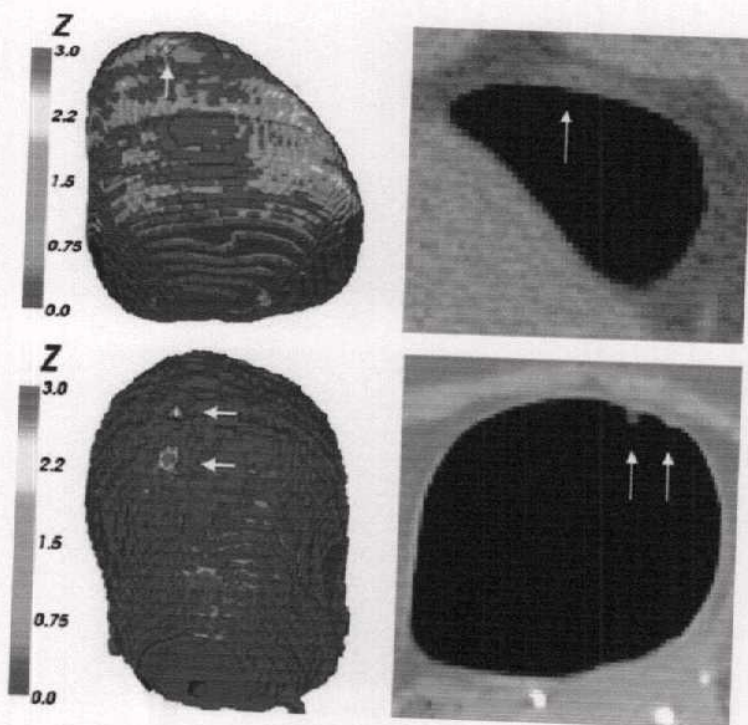


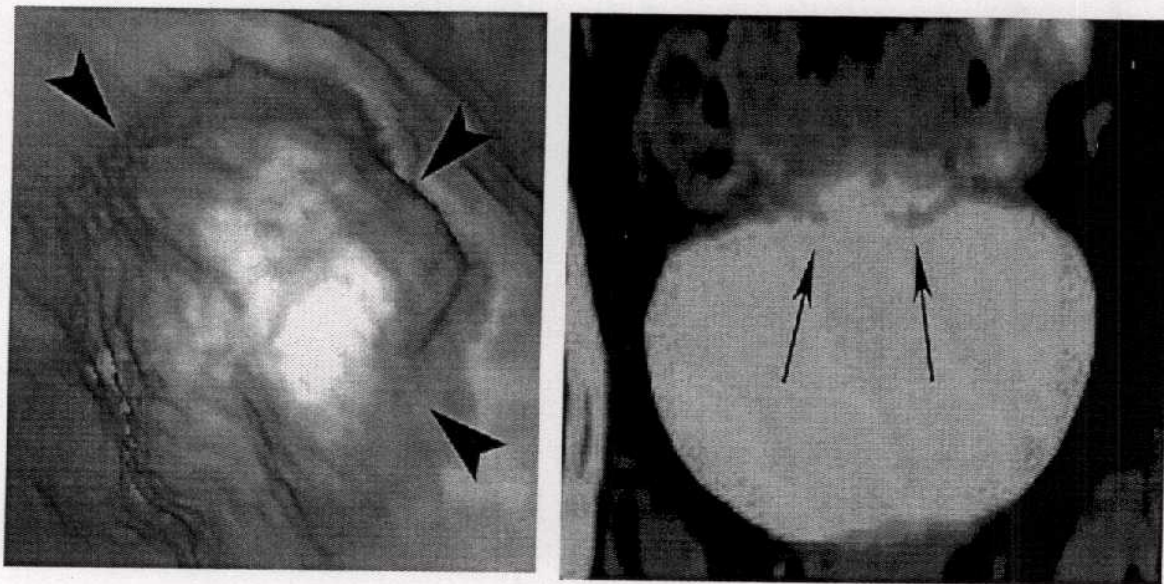
**Fig. 56.** Relative thickness difference between the patient bladder and the atlas, measured by the Z score, indicates the region of abnormal thickness. (top left) Z score for one patient. (top right) Zoom in the CT scan for this patient. Similarly, the bottom row shows Z score and CT scan for a second patient. At the top of the first bladder, the Z score reveals a region of abnormal thickness (red). At the center of the second bladder, the Z score reveals two spots of abnormal thickness (red). (Jaume et al., 2003).



**Pitfalls:**

Image artifacts and certain interpretive pitfalls encountered. Stair-step artifact, which appears as a series of concentric rings, was most obvious at the bladder dome. This artifact, which is a function of the scanning parameters selected, can be minimized by reformatting the data with a minimal 50% overlap between sections (*Fenlon et al., 1997*).

Partial-volume effects may render the bladder wall relatively translucent and result in “shine through” from adjacent, gas-distended loops of small and large bowel (**Fig.57**) (*Fenlon et al., 1997*).



(A)

(B)

(Fig. 57) 48-year-old man with normal bladder in conventional cystoscopic examination.

A and B, noted polypoid mass (arrowheads, A) on virtual cystoscopic image (A) obtained toward superior wall of bladder. However, on both reformatted image (B) and transverse CT image (not shown), both observers interpreted that bladder was normal. Coronal reformatted image (B) shows indentation of bladder dome by small bowel (arrows, B), which is suggested to cause false-positive lesion on virtual cystoscopy (*Kim et al., 2005*).



The presence of residual intravesical urine may obscure lesions in the dependent bladder, although this problem is easily overcome with use of both supine and prone or prone-oblique patient positioning during acquisitions.

Although acquisition times are short (approximately 15 seconds), motion artifacts can occur and can degrade image quality. In one of our patients in whom a median lobe of prostate was misinterpreted as an intrinsic bladder lesion, considerable **ring artifact** occurred due to patient movement (tremor secondary to Parkinson disease) and resulted in substantial image degradation (*Fenlon et al., 1997*).

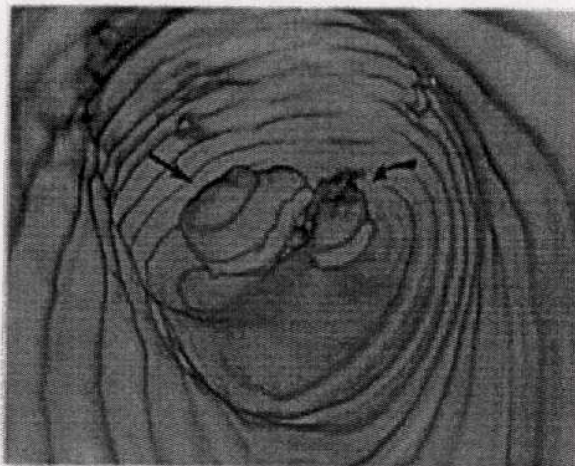


*Figure 58 . Motion artifact. This virtual cystoscopy image is degraded by ring artifact secondary to patient motion in a patient with a prominent median lobe of the prostate (straight arrow) that was misinterpreted as an intrinsic bladder tumor. Note artifactual distortion of the adjacent Foley catheter balloon (curved arrow) (Fenlon et al., 1997).*

### Treatment planning

Non-muscle invasive tumors (also referred to as superficial tumors) include noninvasive carcinomas (Ta), carcinoma in situ (Tis), and tumors invading the lamina propria (T1). The standard treatment for noninvasive bladder cancer is transurethral resection with fulguration, which can be repeated when necessary. Depending on the depth of invasion and histologic grade, intravesical medication such as BCG may be used to reduce the chances of recurrence or prevent progression to a higher grade or stage. Patients who have extensive multifocal recurrent disease or other unfavorable prognostic features may require more aggressive forms of definitive treatment such as radical cystectomy (*Amling et al., 1994*).

Imaging rarely changes clinical management in this group of patients. For muscle-invasive bladder cancer, additional workup procedures including a CT or MR imaging examination of the abdomen and pelvis are needed for accurate staging. For stage T2 and T3 disease, and selected T4a disease without nodal metastasis, radical cystectomy is considered standard treatment. It involves removal of the bladder, perivesical tissues, prostate, and seminal vesicles in men and the uterus, fallopian tubes, ovaries, anterior vaginal wall, and urethra in women and may or may not be accompanied by pelvic lymph node dissection (*Richie 1992*).

There is evidence that neoadjuvant therapy before cystectomy may improve survival of patients with muscle-invasive bladder cancer (*Grossman et al., 2003*).

The prognosis is poor for patients with stage IV bladder carcinoma (defined by the presence of pelvic or abdominal wall invasion, or nodal or distant metastasis). The potential for cure in stage IV disease is restricted to patients with involvement of pelvic organs by direct extension or small volume metastases to regional lymph nodes (*Vieweg et al., 2003*).

Radical cystectomy with or without preoperative irradiation or chemotherapy may be considered in these patients if no nodal disease is identified on imaging. If enlarged lymph nodes are documented by imaging, a biopsy may be needed for a



definitive confirmation before chemotherapy or radiation therapy is initiated. Findings suspicious for distant metastases on imaging also typically need to be confirmed by biopsy. If confirmed, these patients generally are treated with systemic chemotherapy (*Zhang et al., 2006*).

### ***Orthotopic Bladder Reconstruction***

Orthotopic bladder reconstruction is performed for muscle invasive bladder cancer, provided the prostate and urethra are not involved. After cystectomy either a colon segment or, more often, an ileum is used as a bladder substitute and anastomosed to the urethra. This procedure is an alternative to a cutaneous urinary diversion. Two currently used procedures are the Hautmann and Studer modifications. These neoleal bladder replacements use an ileal segment and provide an antireflux mechanism (*Skucas 2006*).

The Hautmann ileal neobladder consists of a detubularized, low-pressure, high-capacity reservoir constructed from ileum, without valves, and anastomosed to the urethra. Urodynamic imaging shows this neobladder to have a capacity similar to that of a normal bladder, a pressure of <30cm water, and no reflux. Initially the prostatic urethra was resected to establish a safe resection margin, and this operation was performed only in men. Currently, however, both a radical cystectomy and a bladder necksparing cystectomy, together with an orthotopic ileal neobladder anastomosed to the proximal urethra, are also performed in women (*Hautmann et al., 2000*); the position of the urethral resection line does affect the incontinence rate and the need for intermittent catheterization. Continence is achieved by most men and women (*Skucas 2006*).

Neobladder-related complications include abscess, urinary leakage or fistula, ureteral and urethroileal stenosis, and venous thrombosis. An occasional patient develops calculi. Fistulas are mostly a complication of combined irradiation and orthotopic bladder replacement (*Skucas 2006*).

Postoperative surgical anatomy after orthotopic bladder reconstruction can be evaluated with 3D CT (virtual endoscopy); while such imaging is useful if reoperation is required, its need on a routine basis is not established (*Skucas 2006*).

---

### **Postoperative Complications**

Urinary tract damage occurring during various gynecologic laparoscopic procedures includes bladder perforation, ureteral injury, and bladder fistula. The prevalence of these complications after major laparoscopic gynecologic surgery is probably similar to that seen after standard surgery (*Skucas 2006*).

#### **Leak**

Anastomotic leakage is a recognized complication of urinary tract reconstructive surgery (**Fig. 59**). The most common site is at the urethroenteric anastomosis. A majority of leaks are extraperitoneal in location; it is the intraperitoneal pouch leaks that are more difficult to detect with imaging. A number of leaks are delayed (*Skucas 2006*).

Catheter drainage or stenting as appropriate is therapeutic for most leaks (*Skucas 2006*).

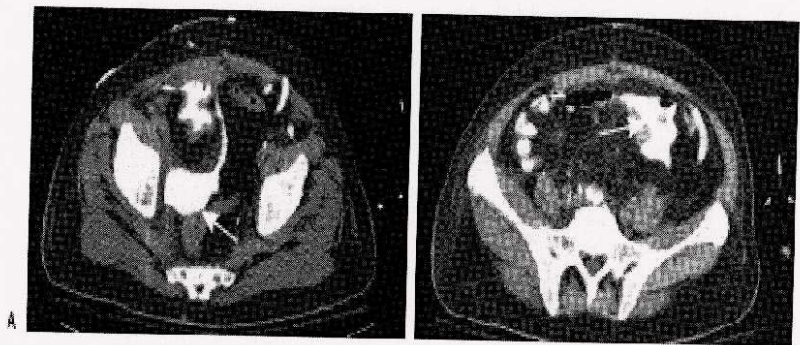


**Figure 59 .** Bladder leak after subtotal cystectomy and neobladder formation.  
**A:** CT cystogram identifies contrast in the bladder and extravasation posteriorly (arrow).  
**B:** Extravasation also extends to the left, adjacent to bowel (arrow).

*(Quoted from Titton et al., 2003).*



### **Stones/Stricture**

Patients with an enterocystoplasty or continent diversion are at risk for stone formation and ureterointestinal stricture. Patients with a continent diversion are more prone to developing stones than those with an augmentation or a substitution cystoplasty (*Skucas 2006*).

Surgical treatment of ureterointestinal strictures consists of open ureteral reimplantation. Percutaneous antegrade dilation is a viable alternative in some patients, but is plagued by a low success rate and recurrent restenosis (*Skucas 2006*).

Dilated ureters are common in patients with a neobladder, and it is difficult to differentiate between partial obstruction and dilation due to reflux and other causes. An IV urogram with furosemide is occasionally helpful in such a situation. Furosemide normally results in good contrast flow distally once renal pelvis are opacified; on the other hand, increased renal pelvis and caliceal dilation and the lack of contrast washout during such diuresis imply an obstruction (*Skucas 2006*).

### **Malignancy**

A low but increased risk of cancer exists after various uroenteric anastomoses, generally beginning a decade or more after surgery. These range from adenocarcinoma to transitional cell carcinoma and squamous cell carcinoma. A reasonable approach is to recommend routine annual surveillance beginning about 10 years after the initial surgery (*Skucas 2006*).

### **Other Complications**

An ileoileal intussusception is an uncommon complication of bladder augmentation. Computed tomography and MR should detect this complication (*Skucas 2006*).

An autostapler is often used when bowel is interposed in the urinary tract, with the metallic staples buried beneath the intestinal mucosa. A staple expressed

---



into the bladder lumen acts as a nidus for subsequent stone formation (Skucas 2006).

An occasional patient with portal hypertension develops massive bleeding from ileal conduit peristomal varices; such bleeding can be controlled with transjugular intrahepatic portosystemic shunt (TIPS) (Skucas 2006).

### Post-treatment imaging

Bladder cancer has a high tendency toward multifocality at presentation and recurrence after treatment (Lammle et al., 2002).

Imaging of bladder cancer after recent treatment is particularly challenging. Intravesical medication and transurethral resection or biopsy of the tumor often cause inflammation and edema, leading to avid mucosal and submucosal enhancement after administration of intravenous contrast (Fig. 60) (Tekes et al., 2005).

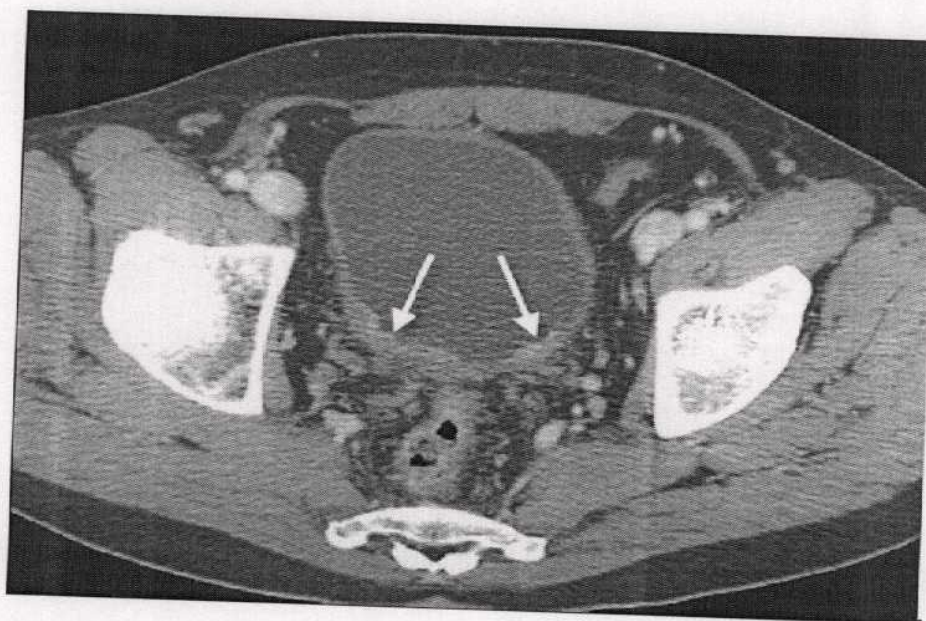


(Fig. 60) . 64-year-old man's status after recent transurethral resection of noninvasive bladder tumor. Contrast-enhanced CT image of the pelvis demonstrated posterior bladder wall thickening with superficial enhancement along the bladder mucosa (arrows), and the presence of perivesical inflammatory change.

(Quoted from Zhang et al., 2006)

---



Using CT or MR imaging, it is difficult to discriminate between recent post-treatment changes and tumor recurrence by signal characteristics alone, but the presence of a mass with signal characteristics typical of tumor may indicate the presence of tumor recurrence (*MacVicar 2000*).

Radiation and surgery also may cause prolonged nonspecific thickening of the bladder wall, and the rest of the urinary collecting system (*Fig. 61*) (*Zhang et al., 2006*).

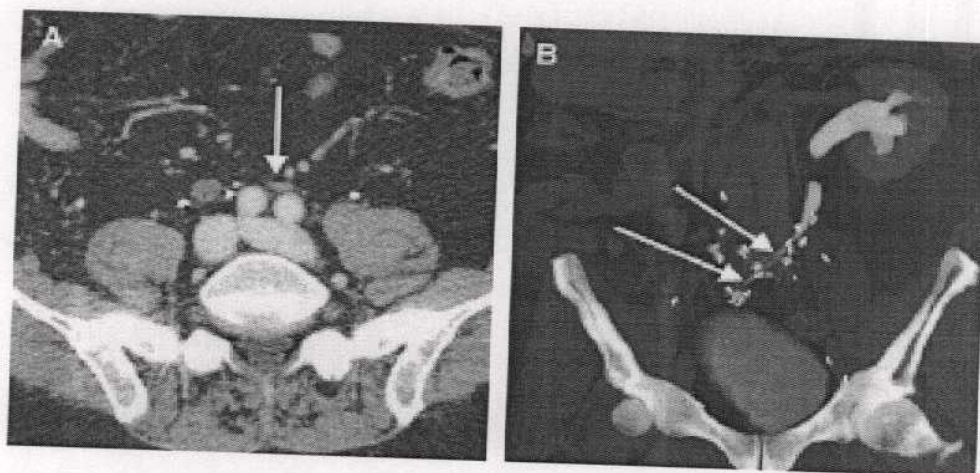


*(Fig. 61)* . 82-year-old man's status after cystectomy and ileal neobladder reconstruction for bladder cancer, presenting with negative urine cytology.  
*(A)* Axial parenchymal phase CTU image shows left ureteral narrowing with mild wall thickening at the level where the ureter crosses the abdominal midline (arrow) right ureteral stump.  
*(B)* A coronal thin MIP reconstructed from the excretory phase CTU images confirms the segmental narrowing of distal left ureter as shown on A (arrows). This finding was stable on multiple subsequent surveillance CTUs and considered most likely to be a postoperative change.

*(Quoted from Zhang et al., 2006)*

.....  
These changes are difficult to distinguish from tumor based on imaging. Interval changes over time on imaging, such as increased thickening or development of mass-like lesions may be helpful for diagnosing recurrence or progression of disease (*Zhang et al., 2006*).



CTU offers a comprehensive evaluation of the urinary system and has value in assessment for complications related to various treatments, from radiation therapy to intravesical therapy such as BCG administration and TURBT, to cystectomy and neobladder reconstruction. Cystitis, with resultant bladder wall thickening, may be seen after radiation therapy (*Zhang et al., 2006*).

After intravesical administration of BCG for treatment of superficial bladder cancer, some patients may develop a systemic reaction referred to as BCG granulomatosis, which may include fever and systemic symptoms, with masses involving urinary organs such as the kidneys, bladder, and prostate gland (**Figs. 62, 63, and 64**).

The renal masses tend to be hypoattenuating on CT examination, with less avid enhancement, which may or may not appear heterogeneous (**Fig. 63**). (*Soda et al., 1999*) and (*Tavolini et al., 2002*).

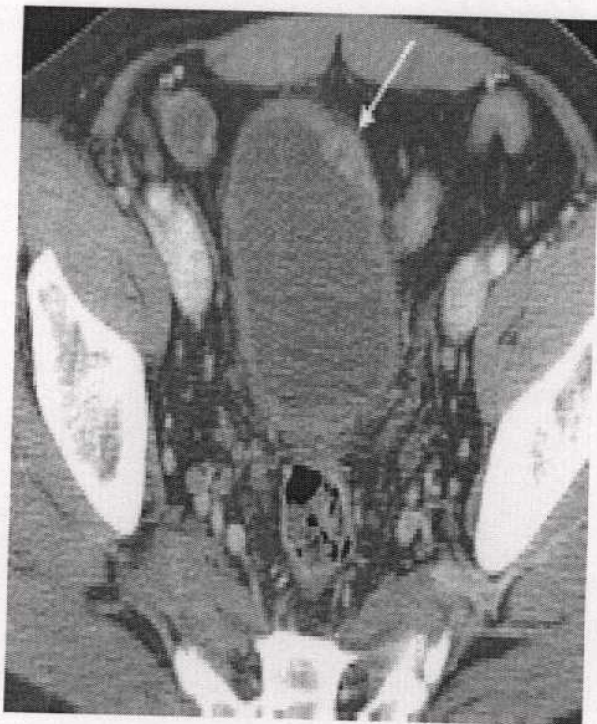


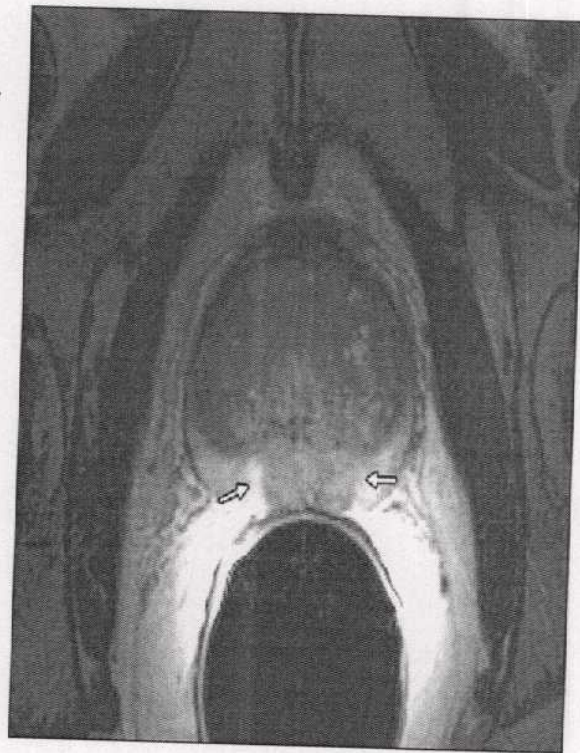
**(Fig.62)** . 64-year-old man's status after resection of stage T1 high-grade bladder TCC, presenting with chills, arthralgias, and myalgias after commencing second course of intravesical BCG treatment. Contrast-enhanced CT image of the pelvis demonstrated focal nodular thickening with enhancement of the left anterior bladder wall (arrow), which was new compared with prior examinations. After treatment with antituberculosis medications, this completely resolved. Subsequent biopsy showed only inflammatory cells. (*Zhang et al., 2006*).





**Fig. 63 .** 52-year-old man who has worsening fever, chills, and night sweats after intravesical BCG therapy for bladder cancer. Contrast-enhanced CT image of the abdomen demonstrated large hypoattenuating mass (\*) in the mid-portion of the left kidney. After several weeks of antituberculosis therapy, the lesion significantly decreased in size (not shown), and the patient's constitutional symptoms resolved. (Zhang et al., 2006).

**Fig. 64.** 67-year-old man's status after intravesical BCG treatment of bladder cancer, presenting with elevated prostate-specific antigen and palpable prostate nodule on digital rectal examination. Axial T2 weighted endorectal MR image of the prostate demonstrates a large nodule (arrows) at the base of the posterior peripheral zone with capsular bulging, corresponding to the nodule palpated on digital examination. Subsequent ultrasound-guided prostate biopsy confirmed granulomatous prostatitis (Zhang et al., 2006).



Similar to renal BCG granulomas, bladder lesions also appear expansile, and typically appear intramural in location. Bladder wall lesions may show avid enhancement (**Fig. 62**). BCG granulomas involving the prostate may mimic prostate cancer on both physical examination and blood biochemical tests (**Fig. 64**). These lesions may be difficult to differentiate from primary or metastatic urinary tumors. The awareness of this entity in the appropriate clinical setting is critical in making the diagnosis, and the patient should be treated medically with antimycobacterial therapy. Follow-up imaging to confirm response to therapy is important (*Zhang et al., 2006*).

Perforation of the bladder wall is one of the most common complications associated with transurethral resection of cancer (incidence 5%). It is associated with increased postoperative hemorrhage and infection (*Dick et al., 1980*).

Recognition of this complication is important for timely initiation of proper treatment. Complications related with various surgical techniques, such as cystectomy with orthotopic neobladder reconstruction, diversions with continent reservoirs, or other diversions, are well evaluated by CTU. Common complications include postoperative urinary leak, stricture with obstruction, extrinsic compression of the diverted ureter, and development of abscesses (*Sudakoff et al., 2005*).

It is challenging to find the appropriate method for long-term surveillance of bladder cancer. Because these patients have increased risk of cancer in the entire urothelial surface, they often require lifelong surveillance, which is essential to clinical management, as most recurrences are superficial and can be managed by endoscopic means. Cystoscopy with biopsy remains the gold standard for detecting bladder cancer recurrence, but it is invasive and expensive. In addition,



it cannot detect upper tract tumor. Urinary cytology is noninvasive and relatively inexpensive. It has been used routinely for tumor detection and long-term surveillance (*Wong-You-Cheong et al., 2006*). It has high specificity (>90%) but low sensitivity for low-grade tumors (<50%) (*Planz et al., 2000*).

Investigations are being performed to find new urinary markers to improve sensitivity while maintaining specificity in the detection of urinary tumors. Imaging is a routine part of surveillance in patients who have bladder cancer. The imaging modality of choice is CTU for the reasons discussed previously. With the advancement in MR technique and faster imaging acquisition, MR imaging of both bladder and the upper tract may be done in one comprehensive examination for patients in whom contrast-enhanced CT is contraindicated (*Zhang et al., 2006*).

Generally speaking, MR of the upper tract is hindered by its relatively low spatial resolution compared with CT, much longer examination time, and the need for additional injections (diuretics, saline bolus, or both) to distend the collecting system (*Zhang et al., 2006*).

MR imaging, however, is promising for predicting treatment response in patients with advanced bladder cancer early in the course of chemotherapy (*Barentsz et al., 1998*) and (*Barentsz et al., 1999*).

It has been shown that using changes in the time to the start of tumor or lymph node enhancement at fast dynamic contrast-enhanced MR imaging, the accuracy, sensitivity, and specificity in distinguishing responders from non-responders were 95%, 93%, and 100%, respectively, significantly higher than the values achieved using conventional tumor size parameters with conventional MR imaging (73%, 79%, and 63%, respectively) (*Barentsz et al., 1998*).

---

.....

The prognosis for any patient with progressive or recurrent invasive bladder cancer is generally poor, despite reports of relatively high rates of response, and occasional complete responses, to combination chemotherapy (*Harker et al., 1985*) and (*Sternberg et al., 1989*).



## Summary

Several imaging techniques are available for use in the detection of bladder pathology. US, urogram, CT, MRI and conventional cystoscopy could be used in the bladder disease (Arslan et al., 2006).

Conventional cystoscopy was accepted as a gold standard in bladder. However, there are several disadvantages of the conventional cystoscopy. It is often difficult to perform adequately when exploring the anterior bladder wall or a diverticulum cavity. Primary intra-diverticular carcinomas are rare, but diagnosis is often difficult with conventional method. There are some contraindications for the conventional cystoscopy such as bacteriuria, acute cystitis, urethritis, prostatitis, obstructive prostatic hypertrophy, and stricture or rupture of the urethra. Marked hematuria is another factor that limits the technical success of cystoscopy, thereby decreasing its reliability. On the other hand, cystoscopy is performed in general or local anesthesia and it is an invasive and uncomfortable procedure for patients, and complications such as infections, uretral or bladder perforation, scarring, and stricture of the urethra have been observed (Arslan et al., 2006).

As a minimally invasive procedure, virtual CT cystoscopy provides many advantages as compared to conventional cystoscopy. The virtual CT cystoscopy images could be stored in file and the lesion could be compared in follow up period with based images. The size of a tumor is measured objectively (Arslan et al., 2006).

Compared with standard cystoscopy, virtual cystoscopy offers a better visibility of the bladder neck. In a standard cystoscopic exam, the clinician may

miss tumors in the bladder neck due to the limited flexibility of the scope near the entrance (Jaume et al., 2003). Access to the anterior bladder wall or the lumen of a diverticulum is not restricted in virtual cystoscopy because various software reconstruction tools can be used and the tumor can be easily detected. Patients with a severe urethral stricture or marked prostatic hypertrophy, who may be poor candidates for conventional cystoscopy, can safely undergo virtual CT cystoscopy. It is also indicated for patients who are at risk of complications such as hemorrhage, perforation, infection, or pain (Arslan et al., 2006).

Virtual cystoscopy has advantages over multiplanar reconstruction and source CT images. First, virtual cystoscopy is dedicated for evaluating the mucosal surface of the bladder and therefore can detect superficial lesions missed by multiplanar reconstruction or source CT images. Second, virtual cystoscopy can allow the operator to navigate the mucosal surface in various projections. Third, interactive navigation is provided by virtual cystoscopy, and the operator can therefore make decisions more confidently (kim et al., 2005).

Virtual cystoscopy is based on creating a high contrast between the bladder wall and the lumen (Scardapane et al., 2007).

Techniques have been used to obtain the CT source data for reconstructed virtual cystoscopic images, scanning the bladder filled with either air and/or contrast material (Arslan et al., 2006).

Either air or I.V. contrast have some advantages and disadvantages when compared with one another (Arslan et al., 2006).

Virtual cystoscopy of the air-filled bladder is minimally invasive because catheterization is required to introduce air into the bladder (Arslan et al., 2006).



The drainage of residual urine, which could not be removed completely, and left a water surface at the base of the bladder. VC cannot be used to reconstruct images under this water surface. This problem can be overcome by using CT twice, while supine and then prone (*Kawai et al., 2004*). Supine and prone examination is another disadvantage of the air-filled bladder method. On the other hand, filling the bladder with IV contrast material has been easily achieved in many studies. In this method, there is no need for examination in prone and supine position. Therefore, this means lesser radiation and cost (*Arslan et al., 2006*).

In air VC the bladder can be expanded to almost the maximum capacity, whereas in IVU VC the bladder expansion depends on the maximum desire to void of each patient, i.e. in IVU VC the bladder may not be expanded to its maximum capacity, in which case folds on the bladder wall may obscure small tumours. This is one of the disadvantages (*Kawai et al., 2004*).

IVU VC has a specific disadvantage; images cannot be reconstructed in patients in whom IVU is contraindicated, e.g. allergic to the contrast medium and with renal dysfunction (*Kawai et al., 2004*). Waiting for bladder filling and inadequate distention is another disadvantage. In addition to these disadvantages, repeated patient positioning and scanning required more time for adequate mixing of urine and contrast (*Arslan et al., 2006*).

The advantages of IV VC include being a totally noninvasive screening test for haematuria, evaluating both upper and lower urinary tracts, replacing several with one test (*Nambirajan et al., 2004*). The presence of contrast enhancement is a very sensitive index for malignancies (*Scardapane et al., 2007*).

Image artifacts and certain interpretive pitfalls: (1) **Stair-step artifact**, which is a function of the scanning parameters selected, can be minimized by reformatting the data with a minimal 50% overlap between sections. (2) Partial-volume effects may render the bladder wall relatively translucent and result in “**shine through**” from adjacent, gas-distended loops of small and large bowel and combination of axial, MPR, CTVC images overcomes this problem. (3) The presence of **residual intravesical urine** may obscure lesions in the dependent bladder, although this problem is easily overcome with use of both supine and prone or prone-oblique patient positioning during acquisitions. Although acquisition times are short; a single breath hold (approximately 15 seconds), (4) **motion artifacts** can occur and can degrade image quality. due to patient movement (tremor secondary to Parkinson disease) and resulted in substantial image degradation giving ring artifact (*Fenlon et al., 1997*).

Virtual cystoscopy has several limitations. A major limitation is that it is unable to depict flat lesions, which appear as subtle mucosal color changes on conventional cystoscopy. However, various factors influence the detection of sessile lesions, including the method used to acquire the CT data, interactive navigational skill of the operator, attenuation coefficient ranges used for voxel categorization, and degree of bladder distention (*Arslan et al., 2006*).

For the detection of small or flat and sessile lesions color mapping contributes more comprehensive information, because it is not restricted to the surface and takes changes of the entire wall thickness into account. Other than in fiberoptic endoscopy it is not possible to see subtle color changes and flat tumors arising from mucosa. Virtual endoscopy can compensate for this lack of subtle high-resolution surface information by adding three-dimensional depth



information. This algorithm pursues the idea of higher integration of information content in voxel-based images (Schreyer et al., 2002).

Secondly, the differentiation between small tumors and inflammatory swelling of the mucosa could be difficult, especially in patients with unsatisfactory bladder filling. Inflammatory swelling of the mucosa thus could be misdiagnosed as a tumor, or small tumors could be missed on virtual cystoscopy. Insufficient distention of the bladder may also cause the mucosa to wrinkle. (Arslan et al., 2006).

Coupled pneumo-CT cystoscopy with I.V. administration of contrast medium. to achieve optimal bladder distension, an adequate depiction and enhancement of bladder lesions. Furthermore, I.V. injection of contrast medium permits visualization of the tumor extending into the terminal ureter, which appeared dilated in unenhanced scans (Scardapane et al., 2007).

Third, mucosal thickening secondary to fibrosis cannot be distinguished from a neoplasm. Of course, a similar problem on conventional cystoscopy because biopsy is often required to determine whether a bladder lesion is inflammatory, fibrotic, or neoplastic (Arslan et al., 2006).

A fourth disadvantage of virtual cystoscopy is that it lacks the ability to provide tissue for histologic evaluation, an ability that is possible on conventional cystoscopy and biopsy. Fifth, it is difficult to visualize the lumen of the urethra as is routinely done with conventional cystoscopy. However, it was reported that urethra could also be evaluated by virtual cystoscopy (Arslan et al., 2006).

**Conclusion:**

In conclusion, virtual CT cystoscopy is a promising technique for tumor and some other bladder lesions, such as diverticula. Virtual CT cystoscopy is likely superior to demonstrate the interior part of the diverticulum. Adequate bladder distention and analysis of virtual images are required for optimal evaluation. This minimally invasive method can be of value for screening, primary diagnosis and surveillance of bladder lesions. Virtual CT cystoscopy may be indicated as a clinical routine when conventional cystoscopy is contraindicated or restricted in feasibility and interpretation or there is risk of hemorrhage, perforation, or pain especially in young patients. In the future, it may be possible or even advantageous to incorporate into the imaging algorithm for evaluation of bladder lesion through continued development and advancement of hardware and software. (Arslan et al., 2006).

Importance of studying the urinary bladder with room air distension and I.V. contrast medium injection. This protocol easily achieves an optimal distension of the bladder, as well as visualizing the maximum difference of density between the walls and lumen and hence facilitating the interpretation of the images. In our opinion intravenous contrast administration is mandatory for a complete staging of bladder cancer. There are three main advantages of this procedure: firstly, it enables the most accurate parietal and perivesical staging achievable with CT, secondly, a complete thoracic and abdominal evaluation and finally, thanks to the excretory scans, the possibility of studying the upper urinary tract for synchronous lesions (Scardapane et al., 2007).

Virtual cystoscopy is superior to multiplanar reconstruction and source CT images for lesion detection in the contrast material-filled bladder. Given the



invasive cystoscopy (*Kim et al., 2005*). The combination of axial, MPR, 3D CTVC images with helical CT can provide comprehensive information on bladder tumour (*Wang et al., 2004*).

The replacement of invasive conventional cystoscopy by noninvasive VC with multislice CT as a preliminary examination will be beneficial to patients, and IVU VC will be more useful than air VC as it is not invasive. However, because of the clinical need for tumour biopsy and removal of foreign bodies, conventional cystoscopy will remain the most reliable final technique (*Kawai et al., 2004*).

Virtual cystoscopy reconstruction technique is particularly helpful to surgeons for rapid visualization of the CT dataset providing a complete map of the lesions (*Scardapane et al., 2007*).

Virtual cystoscopy can also be used to simulate endoscopic surgery before the actual performance; thus helping the surgeon plan the operative approach (*Wood and Razavi 2002*).

VR simulation offers exciting opportunities and may revolutionize endourologic training in the future. The URO-Trainer represents the latest generation of VR-based endoscopy simulators. Its instructional effectiveness and construct validity were demonstrated for cystoscopy and intravesical therapy (*Reich et al., 2006*).

References

- Amendola MA, Glaser GM & Grossman HB (1990):**  
Staging of bladder carcinoma: MRI-CT surgical correlation. *AJR*;146:1179-1183.
- Amling CL, Thrasher JB, Frazier HA, et al.(1994):**  
Radical cystectomy for stages Ta, Tis and T1 transitional cell carcinoma of the bladder. *J Urol*;151(1):31-5 [discussion 35-36].
- Arce S, Lopez R & Almageur M(1983):**  
HLA-antigens and transitional cell carcinoma. *Cancer*; 52:1273-1280.
- Arslan H, Ceylan K, Harman M, Yilmaz Y, Temizoz O, Can S(2006):**  
Virtual computed tomography cystoscopy in bladder pathologies. *International Braz J Urol*;32(2):147-154.
- Babaian RJ, Johnson DE & Liams L(1990):**  
Metastases from transitional cell carcinoma of the urinary bladder. *Urology*;26:142-150.
- Barentsz JO(2002):**  
Bladder cancer in Pollack HM & McCleannan BL(eds). *Clinical urography*. Philadelphia WB. P:1642-1668.
- Barentsz JO, Berger-Hartog O, Witjes JA, et al.(1998):**  
Evaluation of chemotherapy in advanced urinary bladder cancer with fast dynamic contrast-enhanced MR imaging. *Radiology*;207(3):791-7.
- Barentsz JO, Engelbrecht M, Jager GJ, et al.(1999):**  
Fast dynamic gadolinium-enhanced MR imaging of urinary bladder and prostate cancer. *J Magn Reson Imaging*;10(3):295-304.
- Barentz JO, Jager GJ, Vierzen PBJ & Witjes JA(1996):**  
Primary staging of urinary bladder carcinoma The role of MRI and a comparison with CT. *Eur. Radiology*;6:129-133.
- Beahrs OH, Henson DE, Hatter RV & Myers MH(1990):**  
Manual for staging of cancer;193-195.



- Bennett JK, Wheatly JK & Walton KN(1984):**  
10-year experience with adenocarcinoma of the bladder. J.Urology;  
131 :262-275.
- Blute MI, Engen DE & Traris WD(1989):**  
Primary signet ring cell adenocarcinoma of the bladder. J.Urology;  
141 :17-20.
- Bock CE, Bergman RA and Afifi AK(2007):**  
"Anatomy Atlases" A digital library of anatomy information. Present in  
[www.anatomyatlases.org/atlasofanatomy/plate36/html](http://www.anatomyatlases.org/atlasofanatomy/plate36/html). Visited 2007.
- Brick SH, Friedman AC & Pollacic HM(1988):**  
Urachal carcinoma. Radiology;169:377-382.
- Browne RF, Meehan CP, Colville J, et al.(2005):**  
Transitional cell carcinoma of the upper urinary tract: spectrum of  
imaging findings. Radiographics;25(6):1609-1627.
- Bullock N, Sibley G & Whitaker R(1990):**  
Urothelial tumours. Essential Urology;16:214-226.
- Caoli EM, Cohan RH, Inampudi P, et al.(2005):**  
MDCT urography of upper tract urothelial neoplasms. AJR;184(6):  
1873-1881.
- Caterino M, Giunta S, Finocchi V, Giglio L, Mainiero G, et al.(2001):**  
Primary cancer of the urinary bladder: CT evaluation of T parameter  
with different techniques. Abdom. Imaging, 26:433-438.
- Chan TY, Epstein JI(2001):**  
In situ adenocarcinoma of the bladder. Am J Surg Pathol;25:892 -899.
- Chen S, Hsu Y, Chen K, Luke S, Chang L(1996):**  
Urinary bladder endometriosis: a report of two cases. Chin Med J  
(Taipei); 58 :66-9.
- Choi H, Lamb S & Pintar K(1984):**  
Primary signet ring cell carcinoma of the urinary bladder. Cancer; 53:  
1989-1990.

- Cirillo RL, Lamki N, Coombs BD, Becker JA, Krasny RM and Lin EC(2007):**  
Schistosomiasis, bladder. Present in: [www.emedicine.com/radio/topic621.html](http://www.emedicine.com/radio/topic621.html).
- Clark SS, Marlet MM, Prudenico RF(1989):**  
Neurofibromatosis of the bladder in children, case report. *J.Urology*; 118:654.
- Connor JP & Olsson CA(1989):**  
Long term follow up in patients treated with chemotherapy for transitional cell carcinoma of urinary bladder. *Urology*; 34:353-363.
- Cotran RS, Kumar V, Collins T (1999):**  
Pathologic basis of disease. 6<sup>th</sup> ed., W.B. Saunders; 997-1010.
- Damjanov I& Linder J(1996):**  
Anderson's pathology. Tenth edition, Mosby-Year Book Inc. Chapter 66,P:2143-2165.
- Deklerk DP & Catalona WJ(1988):**  
Malignant pheochromocytoma of the bladder. *J Urology* ;113:864-870.
- Dershaw DD & Scher HI(1987):**  
Sonography in the evaluation of carcinoma of the bladder. *Urology*; 29:454-457.
- Deserno WM, Harisinghani MG, Taupitz M, et al.(2004):**  
Urinary bladder cancer: preoperative nodal staging with ferumoxtran-10-enhanced MR imaging. *Radiology*;233(2):449-456
- De Vita VT, Hellman S & Rosenberg SA (2001):**  
Cancer: Principles and practice of oncology. Sixth edition, Lippincott Williams & Wilkins. Chapter 3, section 3, P.1396-1418.
- Dick A, Barnes R, Hadley H, et al.(1980):**  
Complications of transurethral resection of bladder tumors: prevention, recognition and treatment. *J Urol*;124(6):810-1.
- Durkee C & Benson R(1980):**  
Bladder cancer following administration of cyclophosphamide. *Urology*; 16:145-160.

**Dyson M. (1999):**

Urinary bladder. In CD 'Gray's anatomy, 38th ed Churchill Livingstone 1999.

**El Bolkainy MN, Ghoneim M & Mokhtar NM(1981):**

Pathology of bladder cancer associated with Schistosomiasis:A computer analysis of 1095 cases. Med. J. Cairo Univ.;49:361-374.

**Elkin M (1980):**

Tumour of urinary bladder. In radiology of the urinary system, first edition, vol.1, chapter4, Boston: little, Brown and company;296-426.

**Fenlon HM, Bell TV, Ahari HK, Hussain H(1997):**

Virtual cystoscopy: Early clinical experience. Radiology; 205:272-275.

**Fielding JR, Hoyte LX, Okon SA, Schreyer A, Lee J, et al.(2002):**

Tumor detection by virtual cystoscopy with color mapping of bladder wall thickness. J. Urol.;167(2 Pt 1):559-562.

**Fielding JR, Silverman S, Rubin G.(1999):**

Helical CT of the Urinary Tract. AJR;172:1199-1206.

**Fishman EK & Jeffrey RB(1998):**

Spiral CT (principles, techniques and clinical application), Second edition, Lippincott-Raven. Chapter 3, P:35-52.

**Flamm J & Bucher A(1990):**

Recurrent superficial transitional cell carcinoma of the bladder. J.Urology; 144:260-268.

**Friedell GH, Soloway MS & HilgarAG(1986):**

Summary of workshop on carcinoma in situ of the bladder. J.Urology; 136:1047-1050.

**Friedman AC, Radecki PD, Toaff AS & Hilpert FL (1990):**

Clinical pelvic imaging: CT,US and MRI;346-380.

**Garvey CJ & Hanlon R(2002):**

Computed tomography in clinical practice. BMJ; 324:1077-1080.



- Gordon NS, Sinclair RA & Snow RM(1990):**  
Pelvic lipomatosis with cystitis cystica, cystitis glandularis and adenocarcinoma of the bladder. J.Urology; 60:229-236.
- Grainger RG, Allison DJ, Adam A & Dixon AK(2001):**  
Diagnostic radiology. Fourth edition, Churchill Livingstone. Vol. 1, section 1, chapter 4, P:81-99. Vol. 2, section 6, chapter 72, P:1615-1629, chapter 76, p:1718.
- Grossman HB, Natale RB, Tangen CM, et al.(2003):**  
Neoadjuvant chemotherapy plus cystectomy compared with cystectomy alone for locally advanced bladder cancer. N Engl J Med; 349(9):859-66.
- Gugliada K, Nardi PM, Borenstein MS & Torno RB(1991):**  
Inflammatory pseudosarcoma (Pseudotumor) of the bladder. Radiology; 179:66-68.
- Gupta S, Shah S, Motashaw ND, Shan N, Darshana V, Dave V(2001):**  
Case report: bladder wall endometrioma. Ind J Radiol Imag 2001; 11:1:23-24.
- Hahn D(1990):**  
Neoplasms of the urinary bladder. Clinical urology:1353-1380.
- Hain SF and Maisey MN(2003):**  
Positron emission tomography for urological tumours. BJU Int; 92(2): 159-164.
- Hall TB and MacVicar AD(2001):**  
Imaging of bladder cancer. Imaging;13(1):1-10.
- Hardeman SW, Perry A & Solaway MS(1990):**  
Transitional cell carcinoma of the prostate following intravesical therapy for transitional cell carcinoma of the bladder. J.Urology;140:189-295.
- Harker WG, Meyers FJ, Freiha FS, et al.(1985):**  
Cisplatin, methotrexate, and vinblastine (CMV): an effective chemotherapy regimen for metastatic transitional cell carcinoma of the urinary tract. A Northern California Oncology Group study. J Clin Oncol; 3(11):1463-70.

**Hautmann RE, de Petroni R, Kleinschmidt K, Gottfried HW, Gschwend JE.(2000):**

Orthotopic ileal neobladder in females: impact of the urethral resection line on functional results. *Int Urogynecol J Pelvic Floor Dysfunct*;11:224-229.

**Hoffman B, Masuda Y & Wynder EL(1989):**

A1-ha-naphthylamine and beta-naphthylamine in cigarette smoking. *Cancer*;46:120-129.

**Hricak H(2006):**

New horizons in genitourinary oncologic imaging. *Abdom Imaging*;31(2): 182-187.

**Hricak H and White S.(1999):**

Radiological evaluation of the urinary bladder and prostate. In CD 'Grainger and Allison's diagnostic radiology, 3<sup>RD</sup> ed., Churchill Livingstone 1999.

**Huang WL, Ro JY & Griguan DJ(1990):**

Postoperative spindle nodule of the prostate and bladder. *J. Urology*; 143:824-840.

**Husband JES, Olliff JFC, Williams MP et al.(1989):**

Bladder cancer staging with CT and MR imaging. *Radiology*;173:435-440.

**Hussain S, Loeffler JA, Babaian RK & Fenlon HM(1997):**

Thin section helical computed tomography of the bladder: Initial experience with virtual reality imaging. *Urology*;50:685-689.

**Jaume S, Ferrant M, Macq B, Hoyte L, Fielding JR, Schreyer A, Kikinis R, Warfield SK(2003):**

Tumor detection in the bladder wall with a measurement of abnormal thickness in CT scans. *IEEE Trans Biomed Eng.*;50(3):383-390.

**Jinzaki M, Tanimoto A, Shinmoto H, Horiguchi Y, Sato K, Kuribayashi S, Silverman SG(2007):**

Detection of Bladder Tumors with Dynamic Contrast-Enhanced MDCT. *AJR*; 188:913-918.

.....  
**Jolesz FA, Lorensen WE, Kikinis R, et al.(2007):**

Interactive Virtual Endoscopy. Present in: [www.spl.harvard.edu/pages/splpre2007/pages/papers/frank/virt/endoscopy/endoscopy.html](http://www.spl.harvard.edu/pages/splpre2007/pages/papers/frank/virt/endoscopy/endoscopy.html).

**Kabala JE, Robinson PJA, Whittlestone T, and Grier D. (2003a):**

The urogenital tract: anatomy and investigations. Textbook of radiology and imaging, 7<sup>th</sup>ed., Churchill Livingstone 2003a;885-928.

**Kabala JE, Sibley GN, Jenkins JPR, and Hulse P(2003b):**

The bladder and prostate. In textbook of radiology and imaging, 7<sup>th</sup> ed., Churchill Livingstone 2003b;989-1016.

**Kabalin JN, Freiha FS& Niebel JD(1990):**

Liomyoma of the bladder. Urology;35:210-217.

**Kakizoe T, Matsumoto K & Audoh M(1983):**

Adenocarcinoma of urachus. Urology;21:360-365.

**Kalble T, Tricher AR& Friedel P(1990):**

Risk of carcinoma and etiological factors for carcinogenesis. J.Urology; 144:1110-1120.

**Kantor AF, Hartge P & Hoover RN(1988):**

Epidemiological characteristics of squamous cell carcinomas of the bladder. Cancer; 48: 3853-3866.

**Kawai N, Mimura T, Nagata D, Tozawa K & Kohri K(2004):**

Intravenous urography-virtual cystoscopy is a better preliminary examination than air virtual cystoscopy. BJU International;94:832-836.

**Kawamoto S, Horton KM, Fishman EK(2006):**

Opacification of the collecting system and ureters on excretory-phase CT using oral water as contrast medium. AJR;186(1): 136-140.

**Kawashima A, Vrtiska TJ, LeRoy AJ, et al.(2004):**

CT urography. Radiographics;24(Suppl 1):S35-54.

**Kay R & Lattanzi C(1985):**

Nephrogenic adenoma in children. J.Urology;133:99-119.



- Kazam E.(1986):**  
Intraperitoneal paravesical spaces: CT delineation with US correlation.  
Radiology 159;311-3 17.
- Keep JC, Piehl M, Miller A, et al.(1989):**  
Invasive carcinomas of the urinary bladder. J.Urology;141 :33-50.
- Kent DL, Shacher R& Sox HC(1990):**  
Efficient scheduling of cystoscopies in monitoring for recurrent bladder cancer. Med. Decis. Making V. 9 :26-36
- Khan AN, Chandramohan H, Macdonald S, Krishna LR, et al.(2007):**  
Transitional cell carcinoma. present in:www.emedicine.com/radio/  
topic711.html.
- Kim B, Semelka R, Ascher SM., et al. (1994):**  
Bladder tumor staging: comparison of contrast-enhanced CT, T1-and T2-  
weighted MR imaging, dynamic gadolinium-enhanced imaging.  
Radiology; 193:239-245.
- Kim JC, Kim KH & Jung S(2003):**  
Small cell carcinoma of the urinary bladder: CT and MRI imaging  
findings. Korean J Radiol;4:130-135.
- Kim JK, Ahn JH, Park T, Ahn HJ, Kim CS & Cho K(2002):**  
Virtual cystoscopy of the contrast material filled bladder in patients with  
gross haematuria. AJR;179:763-768.
- Kim JK and Cho KS(2003):**  
CT urography and virtual endoscopy: promising imaging modalities for  
urinary tract evaluation. British Journal of Radiology;76, 199-209.
- Kim JK, Park SY, Ahn HJ, et al.(2004):**  
Bladder cancer: analysis of multidetector row helical CT enhancement  
pattern and accuracy in tumor detection and perivesical staging.  
Radiology;231(3):725-731.
- Kim JK, Park SY, Kim HS, Kim SH and Cho KS(2005):**  
Comparison of virtual cystoscopy, multiplanar reformation, and source  
CT images with contrast material-filled bladder for detecting lesions.  
AJR; 185:689-696.

- .....
- Kocakoc E, Kiris A, Orhan I, et al.(2007):**  
Detection of bladder tumour with 3D ultrasound and virtual cystoscopy.  
AJR; 188:A29-A32.
- Konig AH and Gröller E(2001):**  
3D medical visualization:breaking the limits of diagnostics and treatment.  
ERCIM News No.44, January 2001.
- Koraitim M, Baker K, Metwalli N, Zaky Y(1995):**  
Trans-urethral Ultrasonographic assessment of bladder carcinoma: Its  
value and limitation. J.Urology;154; 375-378.
- Kroft SH & Oyasu R(1994):**  
Urinary bladder cancer: mechanisms of development and progrssion  
Lab.Invest.;71 :158.
- Kundra V and Silverman PM(2003):**  
Imaging in the diagnosis, staging, and follow-up of cancer of the urinary  
bladder. AJR;180:1045-1054.
- Kunz E, Schauer A & Schmitt M(1983):**  
Histology and histopathogenesis of two different types of inverted  
papillomas. Cancer;51:348-359.
- Lämmle M, Beer A, Settles M, Hannig C, Schwaibold H& Drews C(2002):**  
Reliability of MR imaging-based virtual cystoscopy in the diagnosis of  
cancer of the urinary bladder. AJR;178:1483-1488.
- Lerner SP, Skinner DG& Leiskovsky G(1993):**  
The rationale for en block pelvic lymph node dissection for bladder  
cancer patient with lymph node metastases: long term results. J.Urology;  
149:758-765.
- Locke JL, Hill DE & Walzer Y(1985):**  
Incidence of squamous cell carcinoma in patients with long term catheter  
drainage. J.Urology;133:1034-1044.
- Lutzeyer W, Rubben H& Dahm H(1982):**  
Prognostic parameters in superficial bladder cancer. J.Urology;127:250-  
262.
- .....

- MacVicar AD.(2000):**  
Bladder cancer staging. BJU Int;86(Suppl 1):111-22.
- Malmstrom PU, Busch C & Nerlon BJ(1987):**  
Recurrence , progression and survival in bladder cancer.J.Urology;  
21 :185-190.
- Mang T, Happel B, Prokop M, Kramer G.(2003):**  
Virtual multidetector row CT cystoscopy in the detection of the urinary  
bladder lesions. 10th European Symposium on Urogenital Radiology S30.
- Merkle EM, Wunderlich A, Aschoff AJ, et al.(1998):**  
Virtual cystoscopy based on helical CT scan datasets: perspectives and  
limitations. Br J Radiol;71:262-267.
- Messing EM, Catalona W(1998):**  
Campbell's urology, 7th ed. Philadelphia: Saunders;2327-2410.
- Mohseni M, Nourbaksh A, Hatami Z(2005):**  
Association of smoking with high-grade transitional cell carcinoma of  
the urinary bladder. Archives of Iranian medicine, volume 8, number 4:  
286-289.
- Moeller TB and Reif E (2001):**  
Pocket atlas of sectional anatomy computed tomography and magnetic  
resonance imaging. Vol. 2:187.
- Montei JE(1990):**  
High stage bladder cancer: bladder preservation or reconstruction.  
Clin.J.Med.;57:280-290.
- Moon WK, Kim SH, Cho JM & Han MC(1992):**  
Calcified bladder tumors: CT features. Acta Radiology;33:440-443.
- Mostafa MH, Shweita SA & O'Conner PJ(1999):**  
Relationship between schistosomiasis and bladder cancer. Clin.Microbiol.  
Rev.; 12(1):97-111.
- Murphy WM(1997):**  
Urological pathology. Second edition. WB Saunders company. Chapter2  
:35-114.



- Nambirajan T, Sohaib SA, Muller-Pollard C, Reznek R & Chinegwundoh FI(2004):**  
Virtual cystoscopy from computed tomography: a pilot study. BJU international;94:828-831.
- Nawfel RD, Judy PF, Schleipman AR, et al.(2004):**  
Patient radiation dose at CT urography and conventional urography. Radiology;232(1):126-132.
- Net Image: Frontiers in bioscience(2007):**  
[www.bioscience.org/atlas/tumpath/kidurin/bladder/3/1.htm](http://www.bioscience.org/atlas/tumpath/kidurin/bladder/3/1.htm).(Visited 2007).
- Olliff JFC, Husband JES & Williams MP(1989):**  
Bladder cancer: staging with CT and MR imaging. Radiology;173:435-440.
- Olsen JH, Boice JD, Seersholm JR(1995):**  
Cancer in parents of children with cancer. New Engl.J.med;333;1594.
- Panebianco V, Laghi A, Sansoni I, Visconti S, Fazzini D, et al.(2003):**  
Virtual Cystoscopy: comparison between MR and CT protocols. 10th European Symposium on Urogenital Radiology S28.
- Pieterman RM, Van Putten JWG, Meuzelaar JJ et al.(2000):**  
Preoperative staging of non- small cell lung cancer with positron-emission tomography. N Engl. J. of Med.;vol.343:254-261.
- Piper JM, Tonascia J & Metnoski GM(1985):**  
Heavy phenacetin use and bladder cancer. Cancer; 34:359-362.
- Planz B, Synek C, Robben J, et al.(2000):**  
Diagnostic accuracy of DNA image cytometry and urinary cytology with cells from voided urine in the detection of bladder cancer. Urology;56(5):782-6.
- Prando A(2002):**  
CT-virtual endoscopy of the urinary tract. International Braz J Urol vol. 28 (4): 317-322.

- Prout GB, Griffin PP, Daly JJ & Heney NM(1983):**  
Carcinoma in situ of the urinary bladder with and without associated vesical neoplasms. *Cancer*; 52:524.
- Putman CE & Ravin CE (1994):**  
Textbook of diagnostic imaging ; 2011-2029.
- Reich O, Noll M, Gratzke C, Bachmann A, Waidelich R, Seitz M, et al.(2006):**  
High-level virtual reality simulator for endourologic procedures of lower urinary tract. *Urology*;67:1144-1148
- Richareds D and Jones S(1998):**  
The bladder and prostate. In Sutton D, Textbook of radiology and imaging. 6<sup>th</sup> British Library cataloging in publication data, Long man , Asia, Hong Kong Ltd., Sec.5.Chap.41:1167-1187.
- Richie JP(1992):**  
Surgery for invasive bladder cancer. *Hematol Oncol Clin North Am*;6(1):129-45.
- Riede UN and Werner M(2004):**  
Color Atlas of Pathology, Tumor Pathology. Chapter 22; 320-386.
- Risch HA, Burch JD, Miller AB, et al.(1997):**  
Dietary factors and the incidence of cancer in the urinary bladder. *Am J Epidemiol*; 127:1179-1185.
- Rosi F, Selli C, Carini M, et al.(1983):**  
Myxoid liposarcoma of the bladder. *J.Urology*; 130:560-577.
- Rubin GD & Silverman SG(1995):**  
Helical (spiral ) CT of the retroperitoneum. *Radiologic clinics of north America*.V.33:5.
- Ryan S and McNicholas M(1998) :**  
Anatomy for diagnostic radiology;232-234.
- Saito W, Amanuma M, Tanaka J et al.(2000) :**  
Histopathological analysis of bladder cancer stalk observed on MRI. *MRI*;18(4):411.

- Scardapane A, Pagliarulo V, Ianora AAS, Pagliarulo A, Angelelli G(2007):**  
Contrast-enhanced multislice pneumo-CT-cystography in the evaluation of urinary bladder neoplasms. *European Journal of Radiology* xxx (2007) xxx-xxx.
- Scattoni V, Da-Pozzo LF, Colombo R, Nava L, Regatti P, De et al.(1996):**  
Dynamic Gadolinium- enhanced Magnetic Resonance Imaging in staging of superficial bladder cancer. *J. Urology* ;155:1594-1599.
- Schreyer AG, Fielding JR, Warfield SK, Lee JH, Loughlin KR, et al.(2000):**  
Virtual CT cystoscopy: color mapping of bladder wall thickness. *Invest Radiol.*;35(5):331-4.
- Scout LM, McCarthy SM and Moss AA (1992):**  
Article-computed transaxial tomography, pelvis. Moss AA, ed, Philadelphia, PA:WB Saunders Co.
- Sella A, Dexeus FH & Chong C(1989):**  
Radiation therapy associated bladder tumours. *Urology*;33:185-190.
- Sen SE, Malek RS & Farrow GM(1985):**  
Sarcoma and carcinosarcoma of the bladder in adults. *J.Urology*;133:29-34.
- Sen S and Zincke H(1984):**  
Value of excretory in the diagnosis of bladder tumours. *Br J Urol.*; 56:499-501.
- Sharma P, Gnjjatic S, Jungbluth AA, Williamson B, Herr H, et al. (2003):**  
Frequency of NY-ESO-1 and LAGE-1 expression in bladder cancer and evidence of a new NY-ESO-1 T-cell epitope in a patient with bladder cancer. *Cancer immunity*, Vol. 3, p. 19.
- Silverberg E, Boring CC& Squires TS(1990):** *Cancer statistics*; 40:49.
- Silverman DT, Levin LI, Hoover S(1989):**  
Occupational risks of bladder cancer in the United States. *Cancer*; 46:1009-1019.
- Sinnatamby CS (1999):**  
Last's anatomy Regional and applied. Tenth edition, Churchill Livingstone Part 14, P:288-290.



- .....
- Skinner DG(1982):**  
Management of invasive bladder cancer. J.Urology;128:34-50.
- Skucas J(2006):**  
Advanced Imaging of the Abdomen. Springer-Verlag London.Ltd.  
Part II.sec.11;685-718.
- Smith FW(1988):**  
Magnetic resonance imaging of the pelvis. Radiology; 158:367-378.
- Smith H, Weaver G & Barenbruch O(1990):**  
Routine excretory urography in follow up of superficial transitional cell carcinoma of the bladder. J.Urology;34:193-203.
- Smith RC, Reinhold C& McCauley TR(1999):**  
Multicoil high resolution fast spin echo MR imaging of the female pelvis. Radiology;148:665-669.
- Sobin LH, Wittekind CH(2002):**  
TNM classification of malignant tumours, 6th ed. New York: Wiley-Liss.;199-202
- Soda T, Hori D, Onishi H, et al.(1999):**  
Granulomatous nephritis as a complication of intrarenal Bacille Calmette-Guerin therapy. Urology;53(6):1228.
- Song JH, Francis IR, Plait JF, et al.(2001):**  
Bladder tumor detection at virtual cystoscopy. Radiology;218:95-100.
- Sontag JM(1980):**  
Experimental identification of genitourinary carcinogens. Urol Clin North Am; 7:803.
- Spring DB, Deshon CE, Babu S (1983):**  
Sonographic appearance of fluid in the perivesical space. Radiology147: 205-206.
- Sternberg CN, Yagoda A, Scher HI, et al.(1989):**  
Methotrexate, vinblastine, doxorubicin, and cisplatin for advanced transitional cell carcinoma of the urothelium. Efficacy and patterns of response and relapse. Cancer;64(12):2448-58.
- .....

- Sudakoff GS, Guralnick M, Langenstroer P, et al.(2005):**  
CT urography of urinary diversions with enhanced CT digital radiography: preliminary experience. *AJR Am J Roentgenol*;184(1):131-8.
- Sutton D, Robinson PJA, Jenkins JPR et al.(2003):**  
Textbook of radiology and imaging. Seventh edition, Churchill Livingstone. Vol. 11, section 4, chapter 29:885-928, chapter 31:989-1016.
- Swanson DA, Liles A & Zagar GK(1990):**  
Pre-operative irradiation and radical cystectomy of squamous cell carcinoma of the bladder. *J.Urology*;143:37-42.
- Tanagho LA (1992):**  
Anatomy of the lower urinary tract. *Campbell's urology*;Vol.1; 40-47.
- Tavolini IM, Gardiman M, Benedetto G, et al.(2002):**  
Unmanageable fever and granulomatous renal mass after intracavitary upper urinary tract Bacillus Calmette-Guerin therapy. *J.Urol*;167(1) :244-5.
- Tekes A, Kamel IR, Chan TY, Schoenberg MP & Bluemke DA(2003):**  
MR imaging features of non-transitional cell carcinoma of the urinary bladder with pathologic correlation. *AJR*; 180:779-784.
- Tekes A, Kamel IR, Imam K, et al.(2005):**  
Dynamic MRI of bladder cancer: evaluation of staging accuracy. *AJR Am J Roentgenol*;184(1):121-7.
- Titton R, Gervais DA, Hahn PF, Harisinghani MG, Arellano RS, et al.(2003):**  
Urine leaks and urinomas: diagnosis and imaging-guided intervention. *RadioGraphics*;23:1133-1147.
- Tricker AR and Spiegelhalder B(1989):**  
Urinary excretion of nitrate, nitrite, n-nitroso compounds in Bilharzial bladder cancer patients. *Cancer*;10:547-559.
- Tsili Ch, Tsampoulas C, Vadivoulis T, Silakos A, et al.(2003):**  
Computed tomographic cystoscopy for the detection of urinary bladder neoplasms. 10th European Symposium on Urogenital S29.
- Tsuda K, Narumi U, Nakamura H et al.(2000):**  
Staging urinary bladder cancer with dynamic MRI. *Hinyokika Kyo*;46(11):835-859.

***Tsukamoto T & Lieber MM(1990):***

Sarcoma of the kidney, urinary bladder and prostate. *Cancer*;50:44-50.

***Van Der Werf-Messing BH(1984):***

Carcinoma of the urinary bladder. *Cancer*;44:1084-1090.

***Van Tilborg AA and Van Rhijn BW (2003):***

Bladder: urothelial carcinomas. Atlas genet cytogenet oncol haematol. Present in: <http://AtlasGeneticsOncology.org/Tumors/blad5001.html> (Visited 2007).

***Veličković L, Dimov D, Kutlešić C, Katić V, Tasić D, Marjanović G(1998):***

Premalignant lesions of urinary bladder mucosae. The scientific journal facta universitatis series: Medicine and Biology Vol.5, No 1, pp. 33-36.

***Vieweg J, Gschwend JE, Herr HW, et al.(1999):***

The impact of primary stage on survival in patients with lymph node positive bladder cancer. *J Urol*;161(1):72-6.

***Vining DJ(2002):***

The Virtual procedure. *The Journal of Imaging Technology Management*, May 2002.

***Vinnicombe SJ, Normal A, Nicolson V & Husband J(1995):***

Normal pelvic lymph nodes: Evaluation with CT after bipedal lymphangiography. *Radiology*;194:349-355.

***Walsh JW(1996):***

Computed tomography of the pelvis. In: *Computed tomography and magnetic resonance imaging of the whole body*. Haggag JR, Lanzieri CF, Sartoris DJ and Zerhoun EA (ed) Mosby St. Louis. Baltimore Berline Boston. Third edition. 1327-1349.

***Wang D, Zhang WS, Xiong MH, et al.(2004):***

Bladder tumors: dynamic contrast-enhanced axial imaging, multiplanar reformation, three-dimensional reconstruction and virtual cystostomy using helical CT. *Chin Med J*;117(1):62-66.

***Wayne State University.***

CT anatomy of the pelvis. Present in: [www.med.wayne.edu/diagRadiology/Anatomy\\_Modules/Pelvis/Pelvis.html](http://www.med.wayne.edu/diagRadiology/Anatomy_Modules/Pelvis/Pelvis.html). (Visited 2007).



- Weiss RM, George NJR, O'Reilly PH. (2001):**  
Comprehensive urology. Mosby 2001; 36:38.
- Whitehouse RW and Wright AR(2003):**  
CT scanning of the lungs. In Textbook of radiology and imaging. Sutton D, Robinson PJA, Jenkins JPR et al(eds). Seventh edition, Churchill Livingstone. Vol. 1,section 1,chapter 1 :30.
- Williams PL, Dyson M, Warwick R & Bannister LH (1995):**  
Gray's anatomy. Thirty-eighth edition, Churchill Livingstone Chapter 6:855, Chapter 8:1416.
- Wolf JS, Cher M & Era M(1995):**  
The use accuracy of cross-sectional imaging and fine needle aspiration cytology for detection of pelvic lymph nodes metastases. J.Urology; 153:993-999.
- Wood BJ, Razavi P(2002):**  
Virtual endoscopy: a promising new technology. Am Fam. Physician; 66:107-112.
- Young RH(1987):**  
Carcinosarcoma of the urinary bladder. Cancer;59:1333-1350.
- Zafar S, Jafri H, Shetty M, Choyke PL, Bluth EI, Bush WH, et al.(2005):**  
Panel on Urologic Imaging: Pretreatment staging of invasive bladder cancer. ACR, 1891 Preston White Drive, Reston, VA 20191-4397.
- Zhang J, Gerst S, Lefkowitz RA, Bach A(2007):**  
Imaging of Bladder Cancer. Radiol clin N Am 45:183-205.
- Zuk RJ, Baithum SI, Martin JE, Cox EL, Revell PA(1989):**  
The immunocytochemical demonstration of basement membrane deposition in transitional cell carcinoma of the bladder. Virchows Archiv [A] 1989; 414:447.

*Arabic*  
*Summary*

تتوافر الكثير من طرق التصوير الطبي لتشخيص أمراض المثانة البولية، كالموجات فوق الصوتية، الأشعة البصغرة على المسالك البولية، الأشعة المقطعية، الرنين المغناطيسي و المنظار التقليدي و على الرغم من اعتبار المنظار التقليدي الطريقة الذهبية لتشخيص أمراض المثانة البولية إلا أن له عيوباً. ففي الغالب تكون هناك صعوبة لرؤية الجدار الأمامي للمثانة و الجيب الداخلي للمثانة الذي قد يوجد به أورام.

و هناك الكثير من الموانع لإجراء المنظار التقليدي منها الالتهابات الحادة بالبروستاتا، مجرى البول و المثانة البولية، و أيضاً ضيق مجرى البول و تضخم البروستاتا، و لكونه وسيلة غير آمنة مع ضرورة استخدام التخدير الجزئي أو الكلي، غالباً ما تكون هناك مضاعفات بعد إجراءه مثل الالتهابات، انسداد مجرى البول و خرق المثانة أو مجرى البول.

أما المنظار التخيلي باعتباره وسيلة آمنة فله الكثير من المميزات بالمقارنة بالمنظار التقليدي. فصور المنظار التخيلي يمكن الاحتفاظ بها في ملفات و استخدامها لمتابعة المرض و القياس الدقيق لحجم الورم. و يقدم رؤية أفضل لعنق المثانة التي يصعب رؤيتها باستخدام المنظار التقليدي لعدم طواعيته في مدخل المثانة. كما أن الجدار الأمامي و الجيب الداخلي للمثانة يمكن رؤيتهما بسهولة و ذلك بفضل برامج إعادة الإنشاء بالحاسب الآلي و لذلك يمكن تشخيص الورم بسهولة. و ينصح بالمنظار التخيلي للمرضى الذين يعانون من ضيق مجرى البول و تضخم البروستاتا و من هم عرضة للمضاعفات مثل التزيف، الالتهابات، الألم أو خرق المثانة أو مجرى البول.

و المنظار التخيلي له مميزات تفوق صور الأشعة المقطعية الأصلية المستخدمة في بناءه و الصور المعاد بناؤها بطريقة ثنائية الأبعاد فهو أولاً : يقيم النسيج السطحي المبطن للمثانة و يمكن تشخيص مرض سطحي به لم يمكن تشخيصه باستخدام صور الأشعة المقطعية الأصلية و الصور المعاد بناؤها. ثانياً: المنظار التخيلي يمكن الطبيب من رؤية النسيج المبطن للمثانة من عدة اتجاهات. ثالثاً: يمكن للطبيب اتخاذ قرارات نتيجة الملاحظة داخل المثانة و التفاعل التخيلي.

و المنظار التخيلي مبني على خلق تباين كبير بين جدار المثانة و داخلها، و ذلك بأخذ صور الأشعة المقطعية بعد ملء المثانة بالهواء أو الصبغة أو كلاهما. و لكل من الطريقتين مزايا و عيوب، فاستخدام المسوا للء المثانة غير آمن نسبياً و ذلك لاستخدام قسطرة بولية لسحب البول من المثانة و ملؤها بالهواء. و في بعض الأحيان لا يتم سحب كمية البول الموجودة كلها مما يخلق وسط مائي بالمثانة لا يسمح ببناء الصورة التخيلية



و يمكن التغلب على ذلك بتصوير المريض مستلقيا على ظهره مرة و على بطنه مرة و ذلك يعد عيبا آخر لهذه الطريقة لا يحدث عند الحقن بالصبغة فيقل التعرض للأشعة و تقل التكلفة.

و على الوجه الآخر فإن ملء المثانة بالهواء يتيح تمدد جدار المثانة لأقصى حد بينما عند امتلائها بالصبغة سيعتمد تمدد الجدار على قدر امتلائها الذي تحدده رغبة المريض بالتبول و قدرته على الاحتمال مما يترك الفرصة لاختفاء ورم صغير بين تعرجات جدار المثانة الغير مشدود.

و طريقة استخدام الصبغة لها عيب خاص بها و ذلك لعدم إمكانية استخدامها في المرضى الذين يعانون من حساسية للصبغة أو خلل وظيفي بالكلى. و من عيوبها أيضا الانتظار حتى امتلاء المثانة و تغيير وضع المريض أكثر من مرة للتأكد من الاختلاط التام للصبغة مع البول. لكن على الوجه الآخر فإن هذه الطريقة آمنة تماما لاكتشاف أسباب البول الدموي و تقييم الجهاز البولي كله بدلا من استخدام أكثر من اختبار، كما أنها من أكثر الطرق حساسية لاكتشاف الأورام.

و للمنظار التخيلي عدة عيوب أولها عدم قدرته على تشخيص الأورام المستوية السطح و التي تظهر بالمنظار التقليدي كتغير في لون البطانة، أيضا هناك عوامل متنوعة تؤثر على تشخيص الأورام اللاعنقية من حيث نوع الطريقة المستخدمة، مهارة الطبيب، درجة التباين بين جدار المثانة و داخلها و درجة امتلاء المثانة. لكن بالنسبة لهذه الأورام التي يصعب تشخيصها بالمنظار التخيلي العادي فإن تقنية المنظار التخيلي باستخدام الألوان تعطي معلومات أكثر دقة لأنها ليست محدودة بالتغيرات السطحية فقط ولكن التغيرات في كل سمك جدار المثانة. و بخلاف المنظار التقليدي الذي يظهر الأورام المستوية و التغير في لون البطانة فإن المنظار التخيلي باستخدام الألوان يتخطى عدم دقة و وضوح الصورة بإضافة معلومة العمق في صورة ثلاثية الأبعاد.

ثاني هذه العيوب عدم قدرة المنظار التخيلي على التفريق بين الأورام الصغيرة و تضخم البطانة نتيجة الالتهابات خاصة عندما تكون المثانة غير ممتلئة تماما، و للتغلب على هذا العيب تتم مزاججة الطريقتين معا بملء المثانة بالهواء و حقن الصبغة معا.

ثالثا: عدم القدرة على التفريق بين سمك البطانة الناتج عن التليف و الناتج عن الأورام كما هو الحال عند استخدام المنظار التقليدي إلا أن الأخير يمكن أخذ عينه بواسطته.

رابعاً: لا يمكن فحص مجرى البول كما هو متاح بالمنظار التقليدي رغم أنه قد تم تسجيل هذه  
الإمكانية للمنظار التخليبي مؤخراً.

الاستنتاج :

إن المنظار التخليبي طريقة واعدة للاكتشاف المبكر، التشخيص و المتابعة لأورام المثانة البولية و  
بعض أمراضها الأخرى. و له الأفضلية فوق المنظار التقليدي في رؤية أجزاء صعبة الرؤية باستخدام الأخير أو  
عند وجود موانع لاستخدامه، لكن تظل ميزة اخذ عينات الأنسجة للمنظار التقليدي. و للحصول على  
أفضل النتائج للمنظار التخليبي يجب مناظرة جميع نتائج صور الأشعة المقطعية الصدرية، الصور الثنائية الأبعاد  
المعاد بناؤها و صور المنظار التخليبي معا. و تقنية المنظار التخليبي باستخدام الألوان تساعد على اكتشاف  
التغيرات الطفيفة في سمك جدار المثانة. و مستقبلاً سيتمكن المنظار التخليبي الجراحيون من التخطيط الدقيق لما  
يمكن إجراؤه أثناء الجراحة.

## تقييم دور المنظار التخيلي في تشخيص أورام المثانة البولية

رسالة مقدمة لاستكمال درجة الماجستير بالأشعة التشخيصية

من

الطبيب/ محمد جميل أنور قشطة  
بكالوريوس الطب و الجراحة

تحت إشراف

**أ.د / جنات علي مطاوع**

أستاذ الأشعة التشخيصية - قسم الأشعة  
كلية الطب - جامعة الأزهر

**أ.م / صلاح الدين محمد كريم**

أستاذ مساعد الأشعة التشخيصية - قسم الأشعة  
كلية الطب - جامعة الأزهر

**أ.م / محمد علي عبود**

أستاذ مساعد الأشعة التشخيصية - قسم الأشعة  
كلية الطب - جامعة الأزهر

قسم الأشعة التشخيصية  
كلية الطب - جامعة الأزهر

٢٠٠٧

02 5101293